Renewable and Sustainable Energy Reviews 16 (2012) 1999–2040

Contents lists available at SciVerse ScienceDirect

Renewable and Sustainable Energy Reviews

journal homepage: www.elsevier.com/locate/rser

Form-stable phase change materials for thermal energy storage

Murat M. Kenisarin [a,*], Kamola M. Kenisarina [b]

[a] Academasbob Scientific and Production Association, Uzbekistan Academy of Sciences, F. Khodjaev St, 28, 100125 Tashkent, Uzbekistan
[b] Institut für Thermische Energietechnik, Universität Kassel, Kurt-Wolters-Straße 3 D-34109 Kassel, Germany

ARTICLE INFO

Article history:
Received 13 May 2011
Accepted 5 January 2012
Available online 18 February 2012

Keywords:
Energy conservation
Thermal energy storage
Phase change materials
Form-stable latent heat storage
Solid–solid transition
Paraffins
Fatty acids
Perlite
Vermiculite
Thermophysical properties
High-density polyethylene

ABSTRACT

The present paper considers the state of investigations and developments in form-stable phase change materials for thermal energy storage. Paraffins, fatty acids and their blends, polyethylene glycol are widely used as latent heat storage component in developing form-stable materials while high-density polyethylene (HDPE), styrene–butadiene–styrene (SBS) triblock copolymer, Eudragit S, Eudragit E, poly (vynil chloride) (PVC), poly (vynil alcohol) (PVA) and polyurethane block copolymer serve as structure supporting component. A set of organic and metallo-organic materials with high transition heat in solid–solid state is considered as perspective for-stable materials to store thermal energy. Another perspective class of form-stable materials are the materials on the basis of such porous materials as expanded perlite and vermiculite impregnated with phase change heat storage materials. The technology of producing new form-stable ultrafine heat storage fibers is developed. It opens availability to produce the clothers with improved heat storage ability for extremely cold regions. The perspective fields of application of form-stable materials are discussed. The further directions of investigations and developments are considered.

Contents

1. Introduction

Continuous growth of level of greenhouse gases emissions into atmosphere and high cost of fossil fuel are the basic motive forces for more effective utilization of energy in all spheres of mankind activity. Commercial buildings and housing apartments are the most energy-intensive consumers. So, for example, 38.9% of all energy which has been consumed in the country [1] was used for heating, air-conditioning and illumination of buildings in the USA in 2005. The similar situation is observed in the European Union where buildings consume now 40% of all energy used in these countries [2]. These examples show us how important to use energy effectively in buildings.

Thermal energy storage (TES) is one of the most perspective methods of increasing efficiency in energy conservation and effective using available sources of heat. Thermal energy can be stored

* Corresponding author. Tel.: +998 71 263 8590.
E-mail address: kenisarin@mail.ru (M.M. Kenisarin).

1364-0321/$ – see front matter
doi:10.1016/j.rser.2012.01.015

Table 1
Examples of formulations used for tiles [41].

Tile number	Polymer	Phase change material	Polymer/PCM w/w ratio	Reinforcement
1	PVA	SA + LA 3:1 mixture	1/1.25	
2	VAc-VC	SA + LA 1:1 mixture	1/1.66	
3	PVC	SA + LA 3:1 mixture	1/1	
4	PVA + PVC 1:1 polyblend	SA + LA 3:1 mixture	1.25/1	
5	PVA + VAc-VC 8:10 polyblend	SA + 3:1 LA mixture	1/1.25	
6	PVA	SA + LA 1:3 mixture	1/1.2	
7	VAc-VC	SA + LA 1:3 mixture	1/2	
8	PVAc	SA + LA 1:3 mixture	1/1.8	5% cellulose fibers
9	PVAc	SA	1/1	5% glass fibers
10	PVC	SA	1/1	10% glass fibers
11	PVC	SA	1/1	
12	HDPE	Emery E-400	1/1	

by using sensible energy of solids or liquids, latent heat of phase change materials or chemical reaction of some chemicals. The main requirements and fields of applications of thermal energy storage system are generalized in Refs. [3–10]. Among TES methods, in many cases, latent heat (heat of fusion) storage (LHS) is more preferable [11–13]. LHS differs in high density of accumulated energy at constant temperature and narrow temperature region. At present time, a lot of solid–liquid phase change materials (PCM) have been studied and they are commercially produced for different purposes [14–40].

As known the materials with solid–liquid phase change along with indisputable advantages have set of shortages. The neccesity of macrocapsulation or microcapsulation, supercooling, instability of some salt hydrates, high volume change can be classified as disadvantages of such PCMs. For instance, macrocapsulation of PCMs can raise the cost of thermal energy products substantially in comparison with the bulk phase change material [16,26]. Studies of physical properties of solids in last 30–40 years showed that some of them have solid–solid transitions which accompany with high enthalpy of transition. Consequently, substances with high latent heat of solid–solid transition are attractive for using them as thermal storage materials. In addition to this, a wide class of form-stable phase change materials which are characterized by similar properties as the materials with solid–solid transitions has been offered. Since form-stable PCM have set of advantages in comparison with solid–liquid PCM, the aim of this work is to analyze the state of the art in developing the form-stable materials for thermal energy storage.

2. Form-stable materials on the basis of paraffin as latent heat storage material

Feldman et al. [41] investigated the possibility of developing the form-stable compositions on the basis of polymers and fatty acids. Poly(vinyl chloride) – PVC, poly(vinyl alcohol) – PVA, poly(vinyl acetate) – PVAc, vinyl acetate-vinyl chloride copolymer – VAc-VC and high-density polyethylene – HDPE were used as structure polymer materials. As phase change latent heat storage materials were used: lauric acids (LA); stearic acid (SA); pressed stearic acid – PSA (Emery 400). Emery 400 consists of 60% stearic acid, 30% palmitic acid and 10% of various fatty acids, depending on the batch. Bleached cellulosic fibers and glass fibers were used as reinforced agents and paraffin chloride and antimony trioxide were used as fire retardants. These materials (Table 1) were mixed in a blender and then were moulded into a tile form with dimension 200 × 200 × 20 mm. Generally, these tiles keep their shape and dimensions up to 37–43 °C, depending on the composition, without losing any fatty acids. Samples made of HDPE showed no deformation up to 51 °C. Test showed that the better mechanical properties were obtained with larger amount of long glass fibers (85–110 mm). The IR-Spectra and DSC results indicate interactions between the polymers and the phase change materials. Further investigations should be done to clarify the nature of the interactions in these systems.

Inaba and Tu [42] used paraffin and high-density polyethylene for developing a form-stable PCM. The paraffin used in this study mainly consists of pentacosane, $C_{25}H_{52}$ (solid-state transition temperature T_{tr} = 47 °C, melting point T_m = 54 °C). In order to reduce oozing rate of the paraffin from the shape-stabilized composition by a repetition of solidification and melting processes, low crystallinity and high viscosity a small amount of the resin such as ethylene-α olein was added to the paraffin. The test shape-stabilized paraffin is composed of the paraffin 74 mass% and HDPE 26 mass%. Table 2 gives the data measured by utilizing the differential scanning calorimeter, such as the latent heat including both of phase transition heat and phase change heat, phase transition temperature and melting point of the shape-stabilized paraffin and dispersed paraffin as a latent heat storage material, respectively. As indicated in Table 1, the latent heat of the shape-stabilized paraffin shows good agreement with the result obtained by multiplying the latent heat of the dispersed paraffin with its mass fraction in the dispersed paraffin. Furthermore, the transition temperature and melting point of the shape-stabilized paraffin coincide with those of the dispersed paraffin within a standard deviation of 2%.

Such thermophysical properties of the paraffin and the shape-stabilized PCM as the density (Fig. 1), specific heat (Fig. 2) and thermal conductivity (Fig. 3) are also measured with high accuracy in order to obtain a relationship between the thermophysical properties of the shape-stabilized paraffin and those of compositing materials. As shown in Fig. 1, as the temperature increases, the densities of both the shape-stabilized paraffin and the dispersed paraffin decrease. These decreasing rates of density with temperature differ in each range of solid, transitional and liquid phase. It is seen that the volume change in shape-stabilized composite at melting point is less than the volume change in pure paraffin. The specific capacities and thermal diffusivities of paraffin and composite PCM in solid and liquid states are very close each other.

Ye and Ge [43] evaluated several kinds of HDPEs and paraffins as candidate materials for polyethylene-paraffin compound (PPC) as a form-stable PCM. At first the two materials are melted and mixed together at a temperature higher than the melting point of the HDPE, then let the compound to cool down. The structure of

Table 2
Latent heat, transition temperature and melting point for the test sample.

Test sample	Heat of fusion (J/g)	Transition temperature (°C)	Melting point (°C)
Paraffin	164.0	35.3	54.1
Shape-stabilized PCM (with 74 wt.% paraffin)	121.0	37.5	54.1

Adapted from [42].

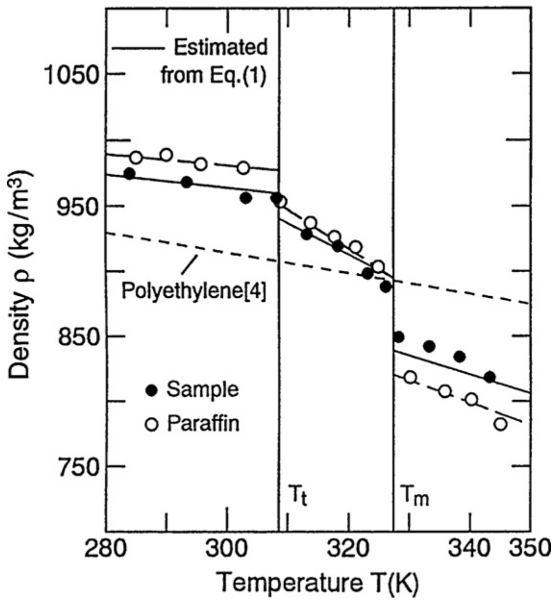


Fig. 1. Variation of density with temperature [42].

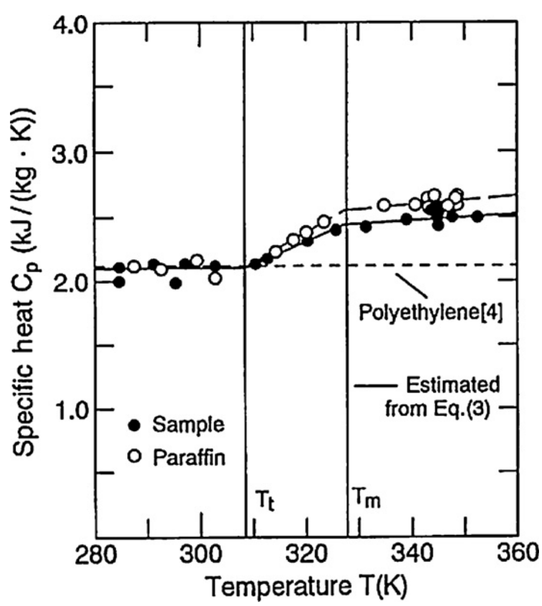


Fig. 2. Variation of specific heat with temperature [42].

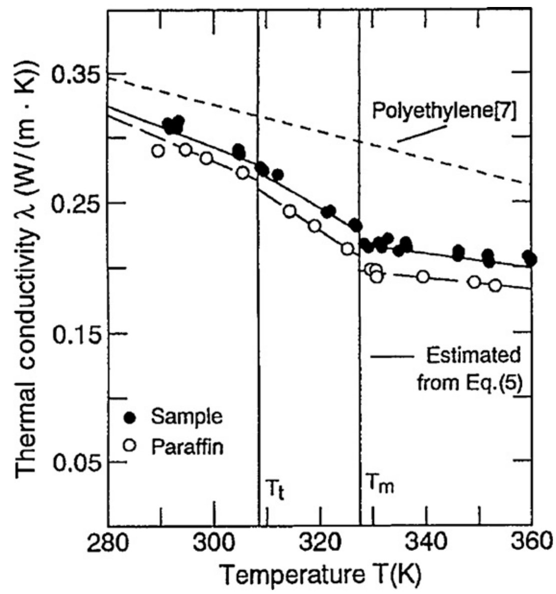


Fig. 3. Variation of thermal conductivity with temperature [42].

the prepared PPC is analyzed by using scanning electronic microscope (SEM) and its latent heat is determined by DSC method. Some results from the DSC measurements are presented in Table 3. It shows that the latent heat of the semi-refined paraffin is nearly the same as that of the refined paraffin. Calculated from the table, the ratio of latent heat of form-stable PPC to that of paraffin is 78.9% (refined paraffin), and 77.5% (semi-refined paraffin), which is a little more than the mass percentage of paraffin in both kinds of form-stable PPCs. It means the latent heat of form-stable PPC should also include the sensible heat of HDPE in the phase change temperature range. The typical DSC curves of PPC and HDPE is presented in Fig. 4. As known, the maximum application temperature of the form-stable PPC should be less than the yield point of the corresponding HDPE. In Fig. 4 the third peak in the thermogram for form-stable PPC stands for the phase transition of the HDPE in it. Compared with the thermogram of the HDPE, it can be seen that the paraffin does not have much influence on the yield temperature of the HDPE in the form-stable PPC. Considering applications in low-temperature heat storage, the yield temperature is high enough. It is recommended that one can take the melting point of the paraffin in the form-stable PPC as the operating temperature.

Table 3
Latent heat of form-stable PPC [43].

Form-stable PPC	Sample 1	Sample 2
Paraffin used (mass percentage)	Refined (75%)	Semi-refined (75%)
Latent heat of paraffin (J/g)	198.95	199.63
Latent heat of form-stable PPC (J/g)	157.04	154.73

Xiao et al. [44,45] prepared a shape-stabilized PCM by mixing a technical grade paraffin (melting point T_m = 56–58 °C) with a styrene–butadiene–styrene (SBS) triblock copolymer on a two-roll mixer at a temperature of 100 °C. The mass percentage of paraffin in the composite can go as high as 80%. To improve thermal conductivity of the shape-stabilized PCMs, three parts with weight of exfoliated graphite (EG) were added to 100 parts by weight of the paraffin/SBS composite (paraffin:SBS = 80:20). This was done by adding graphite, EG, into the melted composite at a temperature of 150 °C. A differential scanning calorimeter was used to determine the heats of fusion and phase change point of the shape-stabilized PCMs (Table 4). For thermal cycling tests, 120 g shape-stabilized

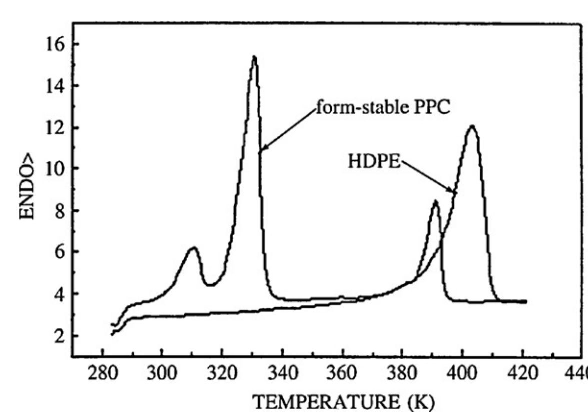


Fig. 4. The typical thermograms of a form-stable PPC and the corresponding HDPE [43].

Table 4
Comparison of experimental and calculated values of latent heat of shape-stabilized PCMs [44,45].

Paraffin and SBS mass ratio	Heat of fusion (J/g)		
	Experimental value	Calculated value	Difference (%)
40:60	81.63	84.2	3.1
60:40	123.5	126.5	2.4
70:30	146.7	147.4	0.5
80:20	165.2	168.4	1.9
100:0	210.5		

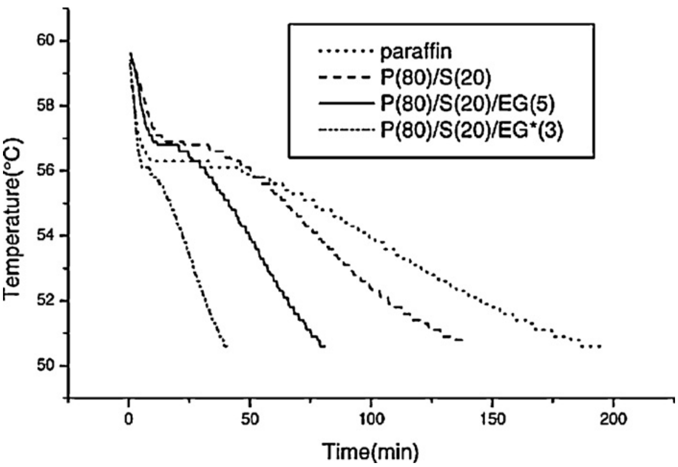


Fig. 5. Cooling curves of pure paraffin and the composite PCMs. T_{ini} = 59.5 °C, T_{bath} = 50 °C [45].

paraffin/SBS composite and 120 g paraffin/SBS/EG composite were moulded to a cylinder with a diameter of 3.8 cm, respectively. The cylinders were directly immersed into a water bath without any container, and a K type thermocouple was inserted in the middle of each of the cylinders. Heating and cooling runs were carried out. For comparison, a cylindrical glass tube with an inside diameter of 3.8 cm containing 96 g paraffin was put into the water bath, and similar cooling and heating runs were carried out. The typical cooling curves are shown in Fig. 5. This figure shows that the adding expanded graphite (three parts) sufficiently enhances thermal conductivity in comparison with paraffin and PCM with five parts of exfoliated graphite Figs. 6 and 7.

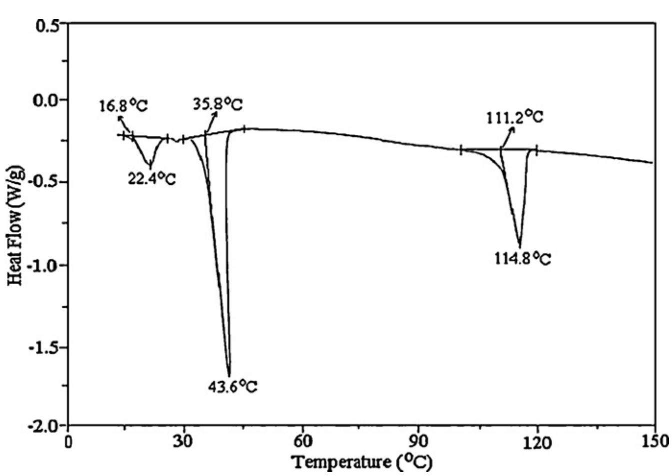


Fig. 6. DSC thermogram of form-stable P1 (77 wt.%)/HDPE composite PCM [48].

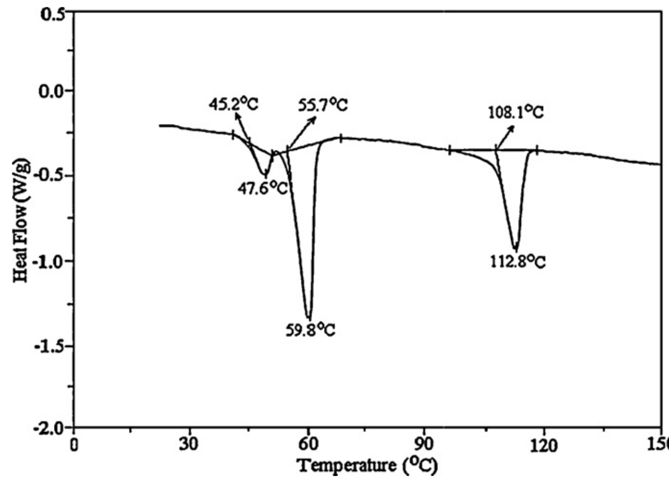


Fig. 7. DSC thermogram of form-stable P2 (77 wt.%)/HDPE composite PCM [48].

Wirtz et al. [46,47] has developed thermal energy storage composites that combine heat storage and structural functionality. The composites were prepared by encapsulation of paraffin waxes in polymer matrices. Room temperature cured bisphenol-A epoxy and styrene–ethylene–butylene–styrene (SEBS) polymers are chosen as matrix materials because of their excellent chemical and mechanical properties. Two paraffin mixtures are used as phase change materials. The first paraffin mixture (IGI 422, Pourret Inc.) is used as the organic phase change material. It melts in the range of 44–58 °C. The other paraffin mixture (BW-422, Blend Waxes Inc., Oshkosh, WI) used melts in the range of 50–60 °C. It was found that IGI 422 paraffin and its polymer composite have two major transition temperatures, one at 45 ± 0.5 °C and a second at 58 ± 0.5 °C. The paraffin mixture has an overall latent heat of 252 J/g and a composite, which is about 75 wt.% paraffin, has a latent heat of 189 J/g, which is 75% of the latent heat of the pure paraffin. The DSC result of paraffin (BW-422) showed that the paraffin has two major transition temperatures, one at 44 ± 1 °C and a second at 55 ± 1 °C. The paraffin has an overall latent heat of 194 ± 5 J/g. In order to prevent the available seepage of liquid paraffin from the SEBS matrix under elevated temperatures and large forces, the exposed surface of the composite system were coated with a thin layer (about 100 μ) of SEBS.

Sarı [48] used two kinds of paraffins with melting temperatures of 42–44 (type P1) and 56–58 °C (type P2) and latent heats of 192.8 and 212.4 J/g to prepare a form-stable PCM. We can see from Table 5 that the maximum weight percentages for both paraffin types in the

Table 5
Thermal characteristics of form-stable PCMs with different mass percent of the paraffins [48].

Test sample	Transition temperature (°C)	Melting point (°C)	Heat of fusion (J/g)
Paraffin 1: HDPE (wt.%)			
50:50	16.3	34.9	95.7
60:40	16.8	35.8	114.8
70:30	17.0	36.6	134.6
75:25	17.4	37.4	143.9
77:23	17.6	37.8	147.6
100:0	23.1	39.8	192.8
Paraffin 2: HDPE (wt.%)			
50:50	42.9	53.8	103.8
60:40	43.6	54.4	125.1
70:30	44.2	54.9	146.1
75:25	44.9	55.4	158.5
77:23	45.2	55.7	162.2
100:0	45.8	56.6	212.4

Table 6
The thermophysical properties of the shape-stabilized PCM developed in [49].

Sample	Melting temperature (°C)	Heat of fusion (J/g)
Paraffin	20.3	119.66
Paraffin/styrene–butadien–styrene/wollastonite (70/25/5)	20.0	86.66
Paraffin/styrene–butadien–styrene/clay1 (70/25/5)	20.4	88.86
Paraffin/styrene–butadien–styrene/clay2 (70/25/5)	21.0	90.37
Paraffin/styrene–butadien–styrene/clay3 (70/25/5)	20.3	96.82
Paraffin/styrene–butadien–styrene/$Mg(OH)_2$ (70/10/20)	20.6	82.97
Paraffin/styrene–butadien–styrene/$Mg(OH)_2$ (70/20/10)	20.7	82.17
Paraffin/styrene–butadien–styrene (70/30)	20.5	87.43
Paraffin/high density polyethylene/diatomite (70/15/15)	20.7	81.21
Paraffin/high density polyethylene/diatomite (70/10/20)	20.1	90.96
Paraffin/high density polyethylene/diatomite (70/20/10)	20.3	87.45
Paraffin/high density polyethylene (70/30)	20.6	87.43
Paraffin/styrene–butadien–styrene (70/30) (surface grafting)	20.7	62.76[a]
Paraffin/high density polyethylene (75/25)	60.0–62.0	130.8
Paraffin/high density polyethylene (80/20)	60.0–62.0	137.9

[a] Some paraffin may be lost during the grafting process.

PCM composites without any seepage of the paraffin in the melted state were as high as 77%. It is observed that the paraffin is dispersed into the network of the solid HDPE by investigation of the structure of the composite PCMs using a scanning electronic microscope (SEM). The melting temperatures and latent heats of the form-stable P1/HDPE and P2/HDPE composite PCMs were determined as 37.8 and 55.7 °C, and 147.6 and 162.2 J/g, respectively, by the technique of differential scanning calorimetry (DSC). Introduction of expanded and exfoliated graphite (EG) into PCM samples in the ratio of 3 wt.% allows to increase the thermal conductivity about 14% for the form-stable P1/HDPE and on about 24% for the P2/HDPE composites.

Zhang et al. [49] developed the form-stable PCMs for building application. The paraffin with the melting point of 20 and 60 °C was chosen as phase change material. As for supporting material, HDPE for a composite was used. In the latter, each component played a different role: powder-like HDPE endowed PCM rigidity; styrene–butadiene–styrene copolymer (SBS) absorbed the paraffin strongly while it was in liquid condition; graphite or carbon fiber acted as a thermal conductive component. The paraffin and the supporting material were mixed evenly and coextruded at about 140 °C in a two-screw extruder. The shape of the product-plate, rod, pellet, etc. varied according to the different application manner. In order to prevent the possible leakage of paraffin, the surface of composite material was grafted and crosslinked. Despite of paraffin's condition (liquid or solid), the polymer network stands still to support the shape. Table 6 presents thermal properties of particular developed form-stable compositions. Table shows that the concentration of 70–80 wt.% of paraffin was proved to be the optimal value.

Cai et al. [50] prepared a shape-stabilized PCM based on high-density polyethylene (HDPE)/ethylene-vinyl acetate (EVA) alloy, organophilic montmorillonite (OMT), paraffin and intumescent flame retardant (IFR). The HDPE and EVA (containing 18 wt.% vinyl acetate) were supplied as pellets by Daqing Petrochemical Company, China Petroleum and Beijing Petrochemical, respectively. The paraffin was available commercially with melting temperature T_m = 56–60 °C and latent heat 167.03 J/g. The ammonium polyphosphate (APP, white power, average particle size:

Table 7
Samples identification and heat of fusion of paraffin/HDP-EVA composites.

Samples	Composition	Latent heat (J/g)
PCM1	Paraffin 60 wt.% + HDPE-EVA 40 wt.%	76.70
PCM2	Paraffin 60 wt.% + HDPE-EVA 20 wt.% + APP-PER 20 wt.%	90.55
PCM3	Paraffin 60 wt.% + HDPE-EVA 18 wt.% + OMT 2 wt.% + APP-PER 20 wt.%	88.15
PCM4	Paraffin 60 wt.% + HDPE-EVA 15 wt.% + OMT 5 wt.% + APP-PER 20 wt.%	91.84

Adapted from [50].

92% <10 μm) and pentaerythritol (PER, white power, average particle size: 92% <10 μm) were provided by Keyan Company. The organophilic montmorillonite (OMT) was prepared by the researchers of our laboratory. The HDPE, VA and desired amounts of OMT were premixed in high-speed blender, and then extruded at 180 °C using a twin-screw extruder. The ratio of HDPE–EVA was fixed as 75/25 by weight. The OMT proportion relative to the polymer matrix (HDPE and EVA) is 2/18 and 5/15 by weight, respectively. The extruded strands were palletized, dried at 80 °C and yielded finally the HDPE–EVA/OMT nanocomposites. Then, the shape-stabilized PCNM with the aforementioned prepared HDPE–EVA/OMT nanocomposites, paraffin and IFR were premixed and prepared by using a twin-screw extruder. The ratio of APP/PER was fixed as 1:1 by weight. The samples are identified in Table 7. The temperature range of the twin-screw extruder was 120–170 °C and screw rotation speed was 450 rpm, thus the shape-stabilized PCNM specimens were obtained. The structures of the HDPE–EVA alloy/OMT nanocomposites are evidenced by the X-ray diffraction (XRD) and transmission electron microscopy (TEM). The structures of the shape-stabilized PCM are characterized by scanning electron microscopy (SEM). PCMs latent heat is determined by differential scanning calorimeter (DSC) method. The SEM and DSC results show that the additives of IFR have little effect on the network structure and the latent heat of shape-stabilized PCNM. The thermal stability properties are characterized by thermogravimetric analysis (TGA).

The typical thermograms of the paraffin, HDPE and the corresponding shape-stabilized PCM are presented in Fig. 8. It can be seen that the paraffin has two peaks of phase change. The first minor peak at the left about 42 °C corresponds to the solid–solid phase transition of the paraffin and the second sharp or main peak corresponding to 58 °C represents the solid–liquid phase change of the paraffin. At the same time, the molten peak of HDPE is also presented, corresponding to around 127 °C. Fig. 8 indicates

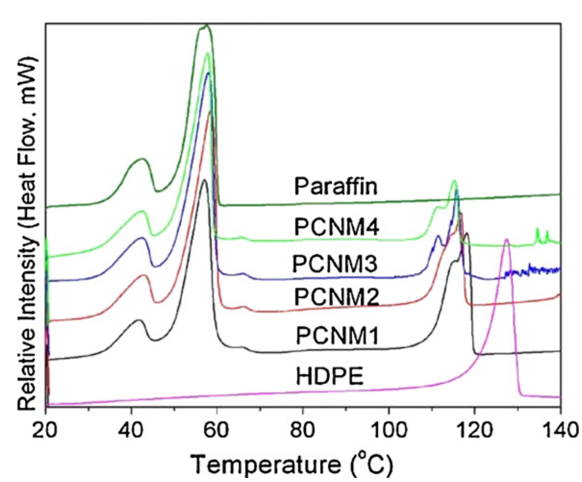


Fig. 8. The DSC curves of the paraffin, HDPE the corresponding shape-stabilized PCM [50].

Table 8
Samples identification and heat of fusion of paraffin/HDP composites.

Samples	Composition (wt.%)	Latent heat (J/g)
PCM1	Paraffin (60) + HDPE (40)	51.42
PCM2	Paraffin (60) + HDPE (20) + MPP(10) + PER(10)	53.92
PCM3	Paraffin (60) + HDPE (15) + MPP(15) + PER(10)	51.02
PCM4	Paraffin (60) + HDPE (15) + MPP(10) + PER(15)	–
PCM5	Paraffin (60) + HDPE (15) + TDE(19) + AO(9)	50.30
PCM6	Paraffin (60) + HDPE (15) + MCA(25)	51.26

Adapted from [51].

that the phase change peaks of the paraffin are still existence in shape-stabilized PCNM. This is because the paraffin is a homologous compound of HDPE, there is no chemical reaction between the paraffin and HDPE in the preparation of the shape-stabilized PCNM. However, the phase change peaks of the paraffin are weaker than the pure paraffin, probably because the three-dimensional network structure partly confines the molecule heat movement of the paraffin in the phase change temperature range. The phase transition peak of the HDPE is ahead of schedule comparing with pure HDPE. The main reasons have two aspects: firstly, the HDPE and EVA, OMT form alloy nanocomposites; secondly, the HDPE and paraffin form polymer alloy in the shape-stabilized PCNM, thereby reducing the melting temperature of HDPE.

The group of Chinese researchers led by Cai et al. [51] conducting investigations on form-stable compositions on the basis of paraffin and high-density polyethylene studied the effects of different additives on their properties. The following products were used: HDPE was supplied as pellets; paraffin (melting temperature T_m = 56–60 °C and latent heat 125.27 kJ/kg); pentaerythritol (PER, powder, average size 92% <10 μm); melamine phosphate (MPP, powder, average size 92% <10 μm); the brominated flame retardant, 1,2-bis(pentabromophenyl) ethan (BPBE, with bromine content 82–83 wt.%, average particle size <5 μm); the antimony oxide (AO, average particle size 8 μm); and melamine cyanurate (MCA, with nitrogen content >98 wt.% and average particle size 5 μm). A twin-screw extruder (TE-35, KeYa, China) was used for the preparation of all samples. Latent heat (see Table 8) of form-stable PCMs was measured with DSC technique, which was carried out in argon atmosphere by means of DT-50 thermal analyzer. The precision of calorimetric and temperature measurements were ±2.0% and ±2.0 °C, respectively. The morphology of samples was investigated by SEM, the result shows that HDPE formed a three-dimensional net structure and the paraffin was dispersed in it, and the addition of flame retardant had no notable effect on the PCM morphology. Flammability properties were characterized by the cone calorimetry. The heat release rate (HRR) peak values and the mass loss rate (MLR) of flame retardant form-stable PCMs have distinctly reduced compared with form-stable PCM.

In the next work, Cai et al. [51] used paraffin, HDPE and organophilic montmorillonite (OMT), pentaerythritol (PER), melamin phospathe (MMP)in order to prepare a dorm stable composition. The HDPE was supplied as pellets by Daqing Petrochemical Company, China Petroleum. Paraffin was available commercially, having melting temperature T_m = 56–60 °C and latent heat 125.27 J/g. The pentaerythritol (PER, powder, average size 92% <10 μm) and melamine phosphate (MPP, powder, average size 92% <10 μm) were supplied by Ke Yan company. The organophilic montmorillonite (OMT) was prepared in the laboratory. The procedure of preparation of the form-stable composition was the same as in [50]. Composition of investigated samples of PCM is given in Table 9.

The typical thermograms of paraffin, HDPE, HDPE/ paraffin hybrid (PCM1) and its HDPE/paraffin/OMT hybrids (PCM2, 4) are presented in Fig. 9. It is obvious that the paraffin has two peaks of phase change: the first phase change peak of paraffin is less,

Table 9
Samples identification and heat of fusion of paraffin/HDPE composites.

Samples	Composition	Latent heat (J/g)
PCM1	Paraffin 60 wt.% + HDPE 40 wt.%	51.42
PCM2	Paraffin 60 wt.% + HDPE 15 wt.% + MPP 15 wt.% + PER 10 wt.%	51.02
PCM3	Paraffin 60 wt.% + HDPE 15 wt.% + OMT 5 wt.% + MPP 10 wt.% + PER 10 wt.%	
PCM4	Paraffin 60 wt.% + HDPE 15 wt.% + OMT 10 wt.% + MPP 10 wt.% + PER 5 wt.%	54.58

Adapted from [52].

corresponding to about 44 °C, while the second peak is very high at nearly 58 °C. The molten peak of HDPE corresponds to around 130 °C. In PCM1, PCM2 and PCM4, the phase change peaks of paraffin still exist, but the first phase change peak of paraffin is weaker than that of pure paraffin, probably because the three-dimensional netted structure and the clay silicate layers partly confine the molecular heat movement of paraffin in the phase change temperature range. The molten peak of the HDPE is ahead of schedule compared with pure HDPE, perhaps the HDPE and paraffin form an alloy and thereby reduce the melt temperature of the HDPE. Compared with the thermogram of pure HDPE, it can be seen that the paraffin, OMT and IFR nearly have no influence on the yield temperature of the HDPE in the form-stable PCM.

Krupa et al. [53] preparated and investigated compositions based on isotactic polypropylene (PP) blended with soft and hard Fischer–Tropsch paraffin wax. The following materials were used: isotactic polypropylene (MFI = 10 g/10 min, density = 0.901 g/cm^3, particle size <30 μm, heat of fusion = 90 J/g, melting temperature = 163.3 °C); hard, brittle, oxidized straight-hydrocarbon chain paraffin wax (average molar mass = 785 g/mol, density = 0.940 g/cm^3, C/O ratio = 18.8/1) – Wax FT; soft paraffin wax (carbon number C18–C40, average molar mass = 374 g/mol, density = 0.919 g/cm^3) – Wax S. The blends were prepared by mixing the components in a 30 ml mixing chamber at 190 °C for 10 min at a mixing rate of 35 rpm. The samples for further characterization were subsequently compressed at 190 °C for 2 min. DSC, DMA, TGA and SEM were used to determine the structure and properties of the blends. Strong phase separation was observed in both cases. Although both grades of paraffin wax are not miscible with PP due to different crystalline structures, it was shown that the hard Fischer–Tropsch paraffin wax is more compatible with PP than the soft one. Both waxes made the PP matrix more plastic. It was found that paraffin waxes melt independently within the PP matrix (up to 40 wt.% of wax), whereas material remains in the solid state. From this point of view, these materials could work as

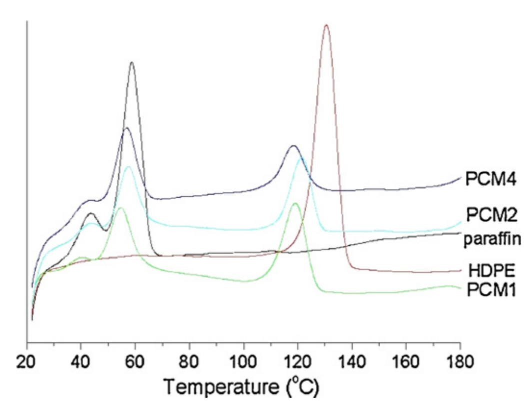


Fig. 9. The DSC curves of paraffin, PCM1, PCM2, PCM4 and the corresponding HDPE [52].

phase change materials. On the other hand, the specific enthalpies of melting which belong to the paraffin wax component are relatively too low to be able to effectively absorb large amounts of energy. For this reason the possibility to use these materials as PCM is limited. Investigation of thermal stability of the materials showed that PP/Wax S blends degrade in two distinguishable steps whereas PP/Wax FT blends degrade in just one step.

In the other work, Krupa et al. [54] studied compositions based on low-density polyethylene blended with soft and hard paraffin waxes. The same paraffins described in previous work [53] were used as phase change storage materials. The low density PE Bralen RA 2–19 (MFI = 1.7 g/10 min, density = 0.916 g/cm^3, particle size < 50 μm, heat of fusion = 109.8 J/g, melting temperature = 107 °C) was used as the structure material. The procedure of preparation and investigation was the same as in [52]. Completely different behavior was observed for the two waxes. The Fischer–Tropsch paraffin wax forms more compact blends than the soft paraffin wax due to cocrystallization with LDPE crystals. TGA results showed that the LDPE/Wax S blends degrade in two distinguishable steps, confirming the immiscibility of these components in the crystalline phase. However, there must be partial miscibility in the molten state, since the DSC results show a shift of the melting peak of LDPE in the blends to lower temperatures, and that of Wax S to higher temperatures compared to the pure components. The phase change enthalpy in all blends increases with increasing wax content in the composite. It is in excellent agreement with the additive rule. The fact confirms that there is no leakage of paraffin wax from the blends during the sample preparation. The melting region of wax FT overlaps with that of LDPE. It is caused by the fact that the melting points of both components are much closer to each other, and it is also due to the much better miscibility of the components. In this case the TGA results show that these blends degrade in only one step, which is typical for miscible blends. The DMA analyses of the blends pointed out an important aspect, which in most cases is neglected. It is the question of which component forms the continuous and which the discontinuous phase. Despite the fact that the highest concentration of Wax S to form a LDPE continuous phase was set to 50 wt.%, it was still not enough to keep the material structure in a consistent shape. Controlled force ramp testing on DMA confirmed poor material strength, especially at temperatures above the wax melting temperature, i.e. temperatures that are interesting for energy storage applications. The highest concentration 40 wt.% of Wax S provides the resistance to the external forces as well as the thermal cycling.

Kaygusuz and Sarı [55] prepared and investigated thermophysical properties of paraffin/high-density polyethylene (HDPE) composites as form-stable solid–liquid phase change material (PCM) for thermal energy storage. Two commercial paraffins of different melting temperatures (type P1; melting point T_m = 48–50 °C and type P2; T_m = 63–65 °C by manufacturer) supplied from Aldrich company were used as PCMs. The density of the selected HDPE as supporting material was found as 0.942 g/cm^3 by volume expansion method. The composite PCMs with amounts of 100 g were prepared by mixing the paraffin and HDPE in melted state and cooled to room temperature. The composite PCMs with different mass percentage of paraffin (50, 60, 65, 70, 73, 76%) were prepared to determine the maximum ratio of the paraffin under which there was no leakage of the paraffin from the composite when the temperature between the melting point of the HDPE and that of the paraffin. Thermal characteristics of paraffin–HDPE composition are presented in Table 10. The mass percentages of paraffins in the composites could go as high as 76% without any seepage of the paraffin in melted state. The dispersion of the paraffin into the network of the solid HDPE was investigated by using scanning electronic microscope (SEM). The melting temperatures and latent heats of paraffins in the form-stable P1/HDPE and P2/HDPE composite PCMs were determined as 44.32 and 61.66 °C, and 179.63 and 198.14 J/g, by the technique of differential scanning calorimetry (DSC), respectively. Typical DSC curves of developed PCMs are given in Figs. 10 and 11. The figures show that the melting points of new form-stable blends are 106.21 and 118.63 °C for P1/HDPE and P2/HDPE composite PCMs, respectively. Furthermore, the thermal conductivity of the composite PCMs was improved about 33.3% for the P1/HDPE and 52.3% for the P2/HDPE by

Table 10
Thermal characteristics of the form-stable PCMs with different mass percent of the paraffins [55].

Test sample	Melting point (°C)	Heat of fusion (J/g)
Paraffin (1): HDPE (wt.%)		
50:50	38.80	138.44
60:40	41.44	150.12
65:35	42.82	163.74
70:30	43.24	171.10
73:27	43.89	174.51
76:24	44.32	179.63
100:0	49.43	228.32
Paraffin (2): HDPE (wt.%)		
50:50	58.14	162.64
60:40	59.21	180.18
65:35	60.02	188.73
70:30	60.93	191.43
73:27	61.28	195.91
76:24	61.66	198.14
100:0	64.48	256.64

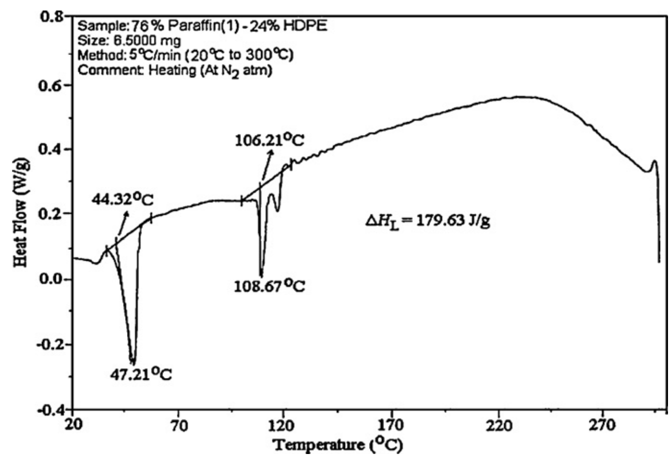


Fig. 10. DSC curve of form-stable P1 (76 wt.%)/HDPE composite PCM [55].

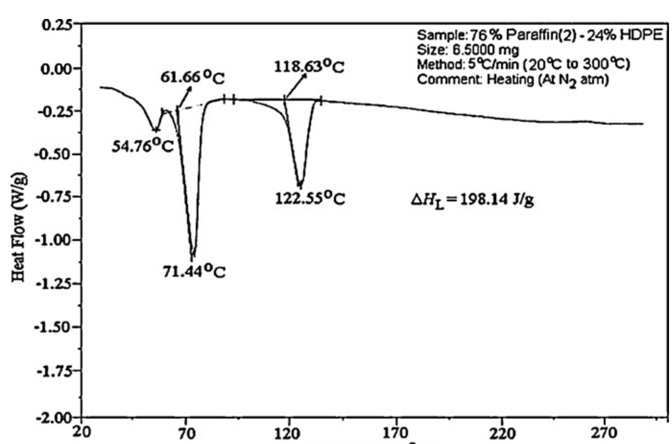


Fig. 11. DSC curve of form-stable P2 (76 wt.%)/HDPE composite PCM [55].

Table 11
Samples identification and heat of fusion of paraffin/HDPE composites.

Samples	Composition (wt.%)	Melting point (°C)	Freezing point (°C)	Heat of fusion (J/g)	Heat of freezing (J/g)
Paraffin (P)		49.73	55.01	163.58	
PCM1	60% P + 40% HDPE	47.71	55.21	78.78	76.46
PCM2	60% P + 20% HDPE + 20% EG	47.70	54.25	88.98	83.48
PCM3	60% P + 20% HDPE + 10% EG + 10% APP	47.83	54.40	93.84	92.48
PCM4	60% P + 20% HDPE + 10% EG + 10% ZB	47.62	54.27	91.21	90.33

Adapted from [56].

introducing the expanded and exfoliated graphite to the samples in the ratio of 3 wt.%.

In the next work Cai et al. [56] used commercial paraffin with melting temperature (T_m = 54–56 °C) and latent heat of 163.58 kJ/kg, ammonium polyphosphate (APP, white powders, average particle size: 92% <10 μm), zinc borate (ZB, $2ZnO{\cdot}3B_2O_3{\cdot}3.5H_2O$) and expandable graphite (EG) with average size of 300 μm and high-density polyethylene (HDPE) for preparing a form-stable composition. A twin-screw extruder was used to prepare the form-stable PCM composites. The temperature range and the screw speed of the twin-screw extruder were set at 120–170 °C and 450 rpm, respectively. The prepared form-stable PCM and its halogen-free flame retardant form-stable PCM composites were compressed and moulded into sheets (3 mm thickness). The detailed compositions of the samples are listed in Table 11.

The thermal properties of composition obtained by DSC measurements are listed in Table 10. According to the table, the melting point and of the form-stable PCM composites approach those of the pure paraffin. However, the latent heat of the paraffin in the form-stable PCM composites decrease slightly compared to the pure paraffin. The latent heat of the form-stable PCM composites containing 60 wt.% paraffin should be about 98.15 kJ/kg by multiplying the latent heat of the dispersed paraffin (163.58 kJ/kg) with its mass fractions (60 wt.%). This may be that the three-dimensional net structure confines the molecule heat movement of the paraffin in the form-stable PCM composites. And the latent heat of paraffin/HDPE composite (PCM1) has more remarkable decreases than the other halogen-free flame retardant form-stable PCM composites. It is believed that the higher amount of HDPE causes the three-dimensional net structure to become more compact and thus molecular heat movements of the paraffin are confined more excessively. But the latent heat of halogen-free flame retardant form-stable PCM composites is slightly higher than that of the PCM1, due to the lower HDPE content with weak net structure, which is in favor of the release of latent heat of the paraffin.

In order to provide form-stable PCMs based on paraffin/high-density polyethylene (HDPE) composites with flame retardant property and high conductivity, Cai et al. [57] used expandable graphite (EG) and ammonium polyphosphate (APP). The high-density polyethylene (HDPE) was supplied as pellets. Paraffin used was a commercial product with melting temperature T_m = 56–60 °C and latent heat of 161.31 kJ/kg. The expandable graphite (average particle size: 300 mm, expansion ratio: 200 ml/g) and the ammonium polyphosphate (APP-II, white powder, average particle size: 92% <10 mm) were used. Some results obtained by DSC measurements, such as phase transition temperature, phase change temperature and latent heat, are listed in Table 12. The latent heat of the form-stable PCM composites containing 60 wt.% paraffin should be about 96.79 J/g by multiplying the latent heat of the dispersed paraffin (161.31 J/g) with its mass fractions. It is believed that the three-dimensional net structure formed by HDPE restricts the thermal molecular movements of paraffin during the phase change. The latent heat of paraffin/HDPE composites (PCM1) has more remarkable decreases than that of the other flame retardant form-stable PCM composites. It should be noted that the melting peak of the HDPE observed in previous experiments is ahead of schedule compared to the pure HDPE. It seems due to the formation of polymer alloy between paraffin and HDPE. Although the melting temperature of the HDPE shows a slight decrease, it is still higher than that of the solid–liquid phase change of paraffin.

Alkan et al. [58] prepared and investigated thermal properties and thermal reliability of paraffin/polypropylene (PP) composite as a novel form-stable phase change material (PCM) for thermal energy storage applications. The paraffin/PP composites were prepared by solution casting method. Solutions of paraffin and PP in n-heptane were prepared in separate beakers and paraffin solution was added to PP solution dropwise. Then n-heptane was casted at room temperature in 15 days. The composites are prepared at 40, 50, 60, 70, 80 w/w% paraffin compositions to obtain the maximum encapsulation ratio without leakage of the paraffin from the composites when the temperature was higher than the melting point of the paraffin. The paraffin/PP composite (70/30 w/w%) is found as the maximum paraffin containing composite and was characterized using Fourier transform infrared spectroscopy (see Figs. 12 and 13), optic microscopy, differential scanning calorimetry (DSC), and thermal gravimetric analysis (TGA) techniques. DSC analysis indicated that the form-stable paraffin/PP composite melts at 44.77–45.52 °C and crystallizes at 53.55–54.80 °C. It has latent heats of 136.16 and 136.59 J/g for melting and crystallization, respectively. The DSC curves of the form-stable PCM before and after 3000 thermal cycles showed that both the endothermic and exothermic peaks belonging to the form-stable PCM are similar. The onset temperatures and phase change enthalpies are almost the same which means that the form-stable PCM is thermally stable and reliable. The melting and crystallization latent heats of the form-stable PCM after 3000 thermal cycling were measured as 116.12 and 116.78 J/g, respectively. After thermal cycling, the deviations of the latent heat of melting of

Table 12
Samples identification and heat of fusion of paraffin/HDPE composites.

Samples	Composition (wt.%)	Transition temperature (°C)	Phase change temperature (°C)	Latent heat (J/g)
Paraffin		36.66	55.19	161.31
PCM1	60% paraffin + 40% HDPE	37.01	55.50	70.10
PCM2	60% paraffin + 15% HDPE + 25% APP	38.07	57.55	86.52
PCM3	60% paraffin + 20% HDPE + 2% EG + 23% APP	37.45	56.01	91.23
PCM4	60% paraffin + 20% HDPE + 4% EG + 21% APP	37.25	56.31	90.89

Adapted from [57].

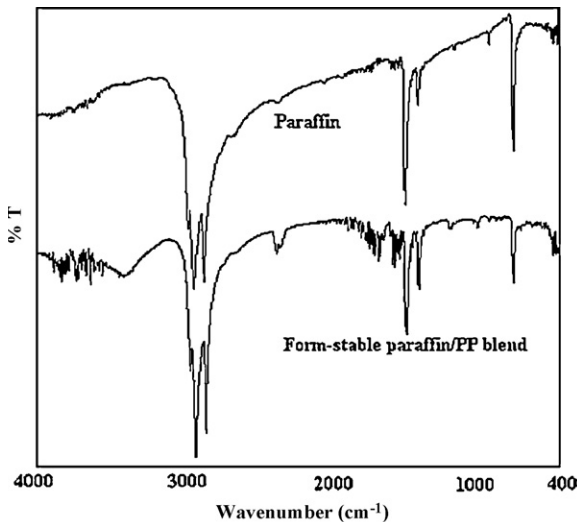


Fig. 12. Fourier transform infrared spectra of paraffin and form-stable paraffin/PP composite [58].

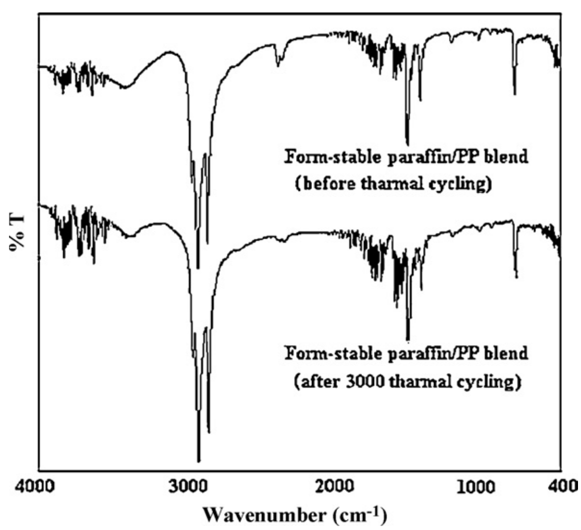


Fig. 13. Fourier transform infrared spectra of form-stable paraffin/PP composite before and after 3000 thermal cycling [58].

the paraffin within the composites are quite low. TGA also showed that the form-stable PCM degrades in two distinguished steps and had good chemical stability.

The flame retardant form-stable phase change materials (PCM) based on high-density polyethylene (HDPE)/ethylene-vinyl acetate (EVA)/organophilic montmorillonite (OMT) nanocomposites and paraffin compounds were prepared by Cai et al. [59]. The flame retardant system consisted of magnesium hydroxide (MH) and microencapsulated red phosphorus (MRP). The structures and properties of the form-stable PCM composites were respectively characterized by X-ray diffraction (XRD), scanning electronic microscope (SEM), thermogravimetry analysis (TGA), differential scanning calorimeter (DSC) and cone calorimeter. The XRD and SEM results showed the paraffin dispersed in the three-dimensional net structure formed by HDPE–EVA/OMT nanocomposites. The TGA results indicated that the loading of the MH/MRP and OMT improved the thermal stability and thermal oxidative degradation properties of the form-stable PCM composites. The DSC measurements (see Table 13) showed that the additives of flame retardant and OMT had little effect on the thermal energy storage properties. The cone calorimeter tests showed that the peak of heat release rate (PHRR) decreased significantly. The decrease in the PHRR as well as compact and homogeneous charred residue after combustion indicated that there was a synergistic effect among the MH, MRP and OMT, contributing to the improved thermal and flammability properties of the form-stable PCM composites.

Cheng et al. [60] preparated and studied thermal properties of a form-stable paraffin/HDPE composite with carbon additivies. For preparation PCMs: a paraffin (melting point: 44 °C) was used as phase change material. HDPE (melt index: 23 g/10 min at 190 °C/5.0 kg, density: 0.957 g/cm^3) was used as supporting material. Expandable graphite (EG) (expansivity: 200 ml/g, average particle size: 50 mesh, carbon content: 99 wt.%). A kind of graphite powder (GP) (carbon content: ≥99.85 wt.%, granularity index (≤30 μm): ≥95%). FT-IR techniques were used in the study to idendify the composite scanning electron microscopy. The thermal conductivities of the shape-stabilized PCMs were measured at 24 °C by HotDisk Thermal Constant Analyzer 2500, and the precision on thermal conductivity was ±3%. The melting temperatures and latent heats of the prepared shape-stabilized PCMs with the additives were measured by differential scanning calorimetry. The calorimetric and temperature measurements accuracy was ±2.0% and ±2.0 °C, respectively. The modified shape-stabilized PCMs were prepared firstly by mixing the melted paraffin with the melted HDPE at about 160 °C (the mass proportion of paraffin and HDPE was 80:20), then adding thermal conductivity enhanced additives to the melted composite samples, stirring for 20–30 min, and finally cooling the melted shape-stabilized PCMs to room temperature. No chemical reaction between paraffin and HDPE was found with infra red spectroscopy. The thermal properties obtained are shown in Figs. 14–16. The carbon additivies change the melting point and heat of fusion of composites insufficiently. On the other hand the thermal conductivity depends on the kind of the carbon added.

Yan et al. [61] prepared and studied some shape-stabilized phase change materials (PCMs), consisting of paraffin and high-density polyethylene (HDPE). In order to develop low-temperature PCMs with high heat of fusion, the mixtures of liquid paraffin, 46# paraffin, 48# paraffin, n-octadecane and n-heptadecane were used as phase change material. The phase change temperatures of these mixtures are between 21 and 28 °C, and they have a high phase change latent heat (Table 14). In order to find the optimal compositions for the form-stable PCMs, HDPE was mixed with paraffin mixtures in proportions of 50–90 wt.%. The

Table 13
Compositions of form-stable composites and their thermal properties.

Samples	Composition (wt.%)					Transition temperature (°C)	Melting temperature (°C)	Latent heat (J/g)
	Paraffin	HDPE–EVA	OMT	MH	MRP			
PCM0	60	40				36.59	55.96	72.35
PCM1	60	15		25		37.57	56.80	82.98
PCM2	60	15		20	5	37.24	55.79	84.11
PCM3	60	12	3	20	5	37.58	56.72	85.01
PCM4	60	10	5	20	5	37.60	56.24	85.08

Adapted from [59].

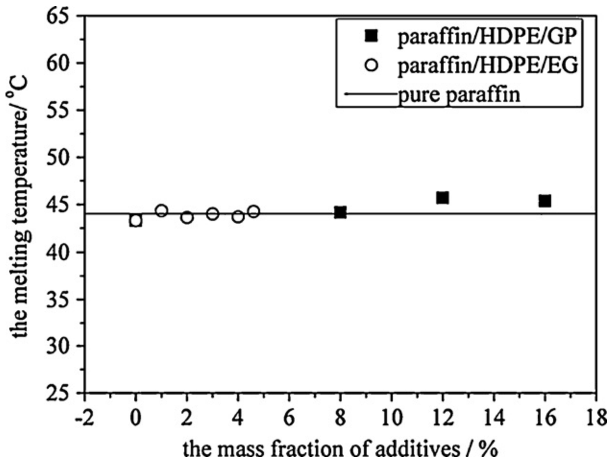


Fig. 14. The melting temperature values of the composite PCMs with respect to the mass fraction of EG and GP [60].

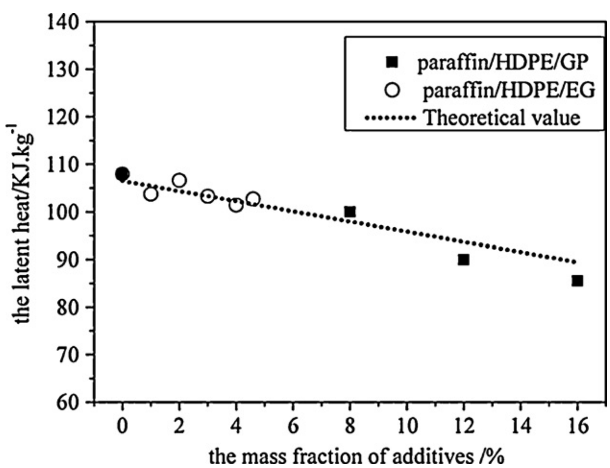


Fig. 15. Latent heat values of the composite PCMs with respect to the mass fraction of EG and GP [60].

phase change temperatures, the phase change latent heats, and the uniformity and stability of the shape-stabilized PCMs were studied experimentally using a differential scanning calorimeter. The composition with different content of HDPE are put into a thermostat container of 40 °C and maintained for 2 h. After that the surfaces of the samples were examined. The experimental results showed that there was a little leakage when the mass content of paraffin was up to 80%, but there was no leakage when the mass content of paraffin

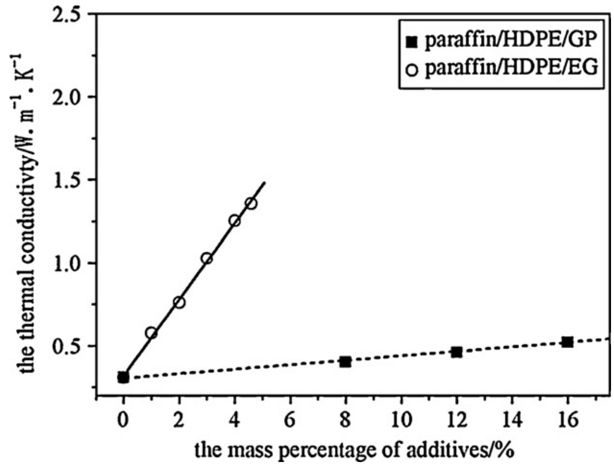


Fig. 16. Thermal conductivity values of the composite PCMs with respect to the mass fraction of EG and GP [60].

was less than 70%. Table 14 presents thermal properties of four samples of form-stable compositions with 70% of phase change materials. It is supposed that the prepared shape-stabilized PCMs are the ideal thermal storage materials to be used in wallboard.

3. Form-stable materials on the basis of fatty acids as latent heat storage materials

Sarı et al. [62] has developed the form-stable phase change materials (PCMs) by composing (Eudragit S) with fatty acids (stearic acid (SA), palmitic acid (PA), and myristic acid (MA)). The compatibility of fatty acids with the Eudragit S is proved by microscopic investigation and infrared (FT-IR) spectroscopy. The melting and crystallization temperatures and the latent heats of melting and crystallization (Table 15) of the form-stable PCMs are measured by DSC method. The maximum mass percentage of all fatty acids in the form-stable PCMs is 70%, and no leakage of fatty acid is observed at the temperature range of 50–70 °C for several heating cycles. Thermal properties obtained from the DSC analysis indicate that the Eudragit S/fatty acid blends as form-stable PCM have great potential for passive solar latent heat thermal energy storage (LHTES) applications in terms of their satisfactory thermal properties and utility advantage.

In order to prepare novel shape-stabilized phase change materials (PCMs), Sarı and Kaygusuz [63] have investigated the compositions of such fatty acids as lauric acid (LA), myristic acid (MA), palmitic acid (PA) and stearic acid (SA) as PCM and poly(vinyl chloride) (PVC) as supporting material. Table 16 shows

Table 14
Thermal properties of some n-alkanes, paraffins and their mixtures.

Sample	Mixture composition (wt.%)	Phase change temperature (°C)	Phase change latent heat (J/g)
48# paraffin		48.6	201.6
46# paraffin		46.5	256.6
n-Octadecane		27.5	224.5
n-Heptadecane		21.7	231.3
Liquid paraffin		−82.5	141.4
Mixture A	50% 46# paraffin/50% liquid paraffin	26.6	130.6
Mixture B	60% 48# paraffin/40% liquid paraffin	25.5	150.5
Mixture C	90% *n*-octadecane/10% liquid paraffin	24.0	248.1
Mixture D	90% *n*-heptadecane/10% liquid paraffin	20.8	235.0
Sample 3	70% mixture A/30% HDPE	27.5	88.6
Sample 8	70% mixture B/30% HDPE	26.2	106.1
Sample 13	70% mixture C/30% HDPE	23.9	177.9
Sample 18	70% mixture D/30% HDPE	21.6	163.2

Adapted from [61].

Table 15
Thermal properties of fatty acids, Eudragit S/fatty acid blends (30/70 wt.%) as form-stable PCMs [62].

Phase change material	Melting point (°C)	Heat of fusion (J/g)	Freezing point (°C)	Heat of freezing (J/g)
Myristic acid (MA)	51.80	198.14	51.4	181.83
Palmitic acid (PA)	60.42	233.24	59.88	237.11
Stearic acid (SA)	66.82	258.98	66.36	263.32
Eudragit S/MA	51.82	132.47	50.47	133.01
Eudragit S/PA	59.60	170.64	59.26	170.92
Eudragit S/SA	66.70	184.22	65.43	184.88

that the maximum composition ratio of all fatty acids in the shape-stabilized PCMs was found 50 wt.% in which no leakage of fatty acid is observed over their melting temperatures for several heating cycles. The miscibility of fatty acids with the PVC and the interaction between the blend components which are responsible for the miscibility has been proved by microscopic investigation and Infrared (IR) spectroscopy. The melting temperature and the latent heat of fusion of the shape-stabilized PCMs are measured by differential scanning calorimetry (DSC) analysis method. The melting temperatures and latent heats of the shape-stabilized PVC/LA, PVC/MA, PVC/PA and PVC/SA (50/50 wt.%) PCMs are determined as 38.8, 49.2, 54.4 and 64.7 °C and 97.8, 103.2, 120.3 and 129.3 J/g, respectively. Note that the experimental determined values in heat of fusion of fatty acid components in form-stable PCMs are in accordance with calculated figures found by using the additive rule. The results indicate that the PVC/fatty acids blends as shape-stabilized PCMs have great potential for passive solar thermal energy applications in terms of their satisfactory thermal properties and advantages of easy preparation with desirable dimensions and direct utility in LHTES applications.

Sarı and Kaygusuz [64] studied the blends of poly(vinyl alcohol) (PVA) with fatty acids (lauric, myristic, palmitic, and stearic acids) to develop shape-stabilized phase change material (PCM). In the blends, the fatty acids, which are dispersed in the solid network of the polymer, act as latent heat thermal energy storage (LHTES) material during its solid–liquid phase change while the polymer (PVA) has function of supporting material due to its structural strength. Therefore, the shape-stabilized fatty acids can keep the same shape in a solid shape without leakage of liquid fatty acids. The results of DSC analysis are presented in Table 17. As it follows from this Table the maximum mixture ratio for all fatty acids in the shape-stabilized form was found as 50 wt.%. The melting temperatures and latent heats of the shape-stabilized lauric, myristic, palmitic and stearic acids were determined as 39.8, 50.2, 56.2, and 67.4 °C and 96.4, 105.3, 121.6, and 132.6 J/g, respectively. The results indicate that the PVA/fatty acids blends as shape-stabilized PCM have great potential for passive solar LHTES applications in terms of their satisfactory thermal properties and utility advantage of without encapsulation.

Kaygusuz et al. [65] prepared and investigated novel shape-stabilized phase change materials (PCMs) by introducing fatty acids (stearic acid [SA], palmitic acid [PA], and myristic acid [MA]) as a PCM in an acrylic resin (Eudragit E) as supporting material. The blends of Eudragit E with fatty acids were prepared by the solution casting method. Eudragit E and one of the fatty acids in chloroform were solved in separate beakers, and fatty acid solution was added to Eudragit E solution dropwise. Then chloroform was casted at room temperature in 15 days. The blends were prepared at 40, 50, 60, 70, and 80% w/w fatty acid compositions to obtain the maximum encapsulation ratio without leakage of the fatty acid from the blends when the blend was heated above the melting points of MA, PA, and SA. The maximum percentage of all fatty acids in the shape-stabilized PCMs was found to be 70 wt.% in which no fatty acid seepage was observed as the blends were heated above the melting points of the fatty acids. Fourier transform infrared (FT-IR) results revealed that the interactions between Eudragit E and fatty acids were only adequate for adhesion of Eudragit E on fatty acid domains. The melting and freezing temperatures and latent heats of the shape-stabilized PCMs were measured by the DSC method and the results were presented in Table 18. It was concluded that Eudragit E/MA, Eudragit E/PA, and Eudragit E/SA blends (30/70 wt.%) have good utility potential for thermal energy storage system owing to easy preparation in desired dimensions, direct usefulness function, and cost effectiveness.

With the aim to develop form-stable PCMs Sarı et al. [66] studied blends of fatty acids such as stearic acid (SA), palmitic acid (PA), myristic acid (MA) and lauric acid (LA) as phase change materials and styrene maleic anhydride copolymer (SMA) as structure material. The prepared form-stable composite PCMs were characterized by using optic microscopy (OM), viscosimetry and Fourier transform infrared (FT-IR) spectroscopy methods, and the results showed that the SMA was physically and chemically compatible with the fatty acids. The ratio of fatty acids was as much as 85 wt.% and no leakage of fatty acid was observed when the temperature of the form-stable composition exceed melting point of fatty acids. The thermal characteristics melting and freezing temperatures and latent heats of the form-stable composite PCMs were measured by using the differential scanning calorimetry (DSC) technique. The results of DSC measurements are presented in Table 19. It seen that the developed form-stable SMA/fatty acid composite PCMs have high potential.

Table 16
Thermal properties of some fatty acids and form-stable compositions on their basis.

Phase change material	Melting temperature of PCM (°C)	Heat of fusion of PCM (J/g)
Lauric acid (LA)	42.6	183.2
Myristic acid (MA)	52.8	198.4
Palmitic acid (PA)	62.4	224.8
Stearic acid (SA)	69.8	238.6
PVC: LA (50 wt.%: 50 wt.%)	38.8	91.6
PVC: MA (50 wt.%: 50 wt.%)	49.2	99.2
PVC: PA (50 wt.%: 50 wt.%)	54.4	112.4
PVC: SA (50 wt.%: 50 wt.%)	64.7	119.3

Adapted from [63].

Table 17
Thermal properties of some fatty acids and form-stable compositions.

Phase change material	Melting temperature of PCM (°C)	Latent heat of PCM (J/g)	
		Experimental	Calculated
Lauric acid (LA)	42.6	183.2	
Myristic acid (MA)	52.8	198.4	
Palmitic acid (PA)	62.4	224.8	
Stearic acid (SA)	69.8	238.6	
PVA: LA (50 wt.%: 50 wt.%)	39.8	96.4	91.6
PVA: MA (50 wt.%: 50 wt.%)	50.2	105.3	99.2
PVA: PA (50 wt.%: 50 wt.%)	56.2	121.6	112.4
PVA: SA (50 wt.%: 50 wt.%)	67.4	132.6	119.3

Adapted from [64].

Table 18
Thermal properties of fatty acids and 30% Eudragit E/70% fatty acid (w/w) blends as form-stablized PCM [65].

Form-stable PCM	Melting point (°C)	Heat of fusion (J/g)	Freezing point (°C)	Heat of freezing (J/g)
Myristic acid (MA)	51.80	178.13	51.74	181.63
Palmitic acid (PA)	60.42	233.24	59.88	237.11
Stearic acid (SA)	66.82	258.98	66.36	263.32
30% Eudragit E/70% MA	51.44	135.62	51.11	134.02
30% Eudragit E/70% PA	58.74	172.43	58.22	172.86
30% Eudragit E/70% SA	65.41	185.64	65.08	185.83

Table 19
Thermal properties of form-stable SMA/fatty acid composite PCMs (15/85 wt.%).

Phase change material	Melting point (°C)	Heat of fusion (J/g)		Freezing point (°C)	Heat of freezing (J/g)	
		Experimental	Calculated		Experimental	Calculated
Stearic acid (SA)	66.87	242.15		66.76	246.74	
Palmitic acid (PA)	60.45	221.42		59.88	226.56	
Myristic acid (MA)	52.44	210.70		52.49	212.65	
Lauric acid (LA)	42.14	190.12		42.20	194.23	
SMA/SA	67.35	202.23	205.83	66.68	204.82	209.73
SMA/PA	60.04	184.54	188.21	59.27	185.18	192.58
SMA/MA	51.75	176.49	180.00	52.07	177.78	180.75
SMA/LA	41.48	160.83	161.67	41.78	163.43	160.00

Adapted from [66].

Alkan and Sarı [67] have introduced the fatty acids into the polymer matrix of poly(methyl methacrylate) (PMMA) in order to develop new kinds of form-stable PCMs for LHTES systems. The fatty acids were introduced successfully into PMMA as much as 80 wt.% and the blends kept their shapes even when they were heated above the melting point of fatty acid. The prepared form-stable SA/PMMA, PA/PMMA, MA/PMMA, and LA/PMMA (80/20 wt.%) blends were characterized by using optic microscopy, viscosimetry and FT-IR spectroscopy methods. The results proved the availability of the attractive interaction between the fatty acid and the PMMA, which resulted in good compatibility of the components of the blends. Thermal properties of the form-stable PCMs (see Table 20) were determined using DSC technique and indicated that they had proper phase temperatures and satisfied latent heat storage capacities for practical LHTES applications. Obviously the form-stable fatty acid/PMMA blends can be considered as candidate PCMs for LHTES applications such as underfloor space heating of buildings and solar energy storage using wallboard and plasterboard impregnated with form-stable PCM due to having good thermal properties.

Wang and Meng [68], using the method of self-polymerization, prepared form-stable PCMs. The eutectic blends of fatty acids were used as phase change storage materials and poly(methyl methacrylate) (PMMA) as supporting material. Fatty acid eutectic mixtures were prepared through melt blending and ultrasonic method. Two selected fatty acids were mixed uniformly at their eutectic ratio in a sealed beaker and kept in the drying oven at 80 °C for 2 h. The mixture was vibrated in an ultrasonic cleaner at 50 °C for 2 min and then conserved in the drying oven at 50 °C. The thermal properties of fatty acids eutectics measured by DSC are listed in Table 21. Fatty acid eutectics introduced into PMMA were as much as 50 wt.%. The developed form-stable PCMs were adjusted to the suitable range for building energy conservation, ranging from 21 to 35 °C. LA–MA eutectic/PMMA PCM was investigated to maximize composition ratio of the form-stable PCMs. Considering the strength of the composite, 70 wt.% of LA–MA eutectic was determined to be optimal and the latent heat of LA–MA/PMMA form-stable PCM was 113.2 J/g. SEM images of the composite PCMs showed that fatty acid eutectic was enwrapped by PMMA so that there was no leakage of melted fatty acid out of the composite during thermal absorbing process. Thermal expansibility of the form-stable PCMs was characterized by the volume expansion coefficient and the results indicated that the composites would be available for building energy conservation.

4. Form-stable materials on the basis of polyethylene glycol as latent heat storage materials

Jiang and Ding [69] have prepared new kinds of solid–solid phase change materials (PCMs) with netted structure. In these materials, the rigid polymer cellulose diacetate (CDA) serves as skeleton, and the flexible polymer polyethylene glycol (PEG) serves as functional branch chain. PEG, a white crystalline solid and chemically pure reagent with average molecular weight from 2000 to 20,000 was used. It was found that if the molecular weight of PEG

Table 20
Thermal properties of form-stable fatty acid/PMMA (80/20 wt.%).

Form-stable PCM	Melting point (°C)	Heat of fusion (J/g)		Freezing point (°C)	Heat of freezing (J/g)	
		Experimental	Calculated		Experimental	Calculated
Stearic acid (SA)	66.87 ± 0.12	242.15 ± 1.78		66.76 ± 0.09	246.74 ± 1.76	
Palmitic acid (PA)	60.45 ± 0.14	221.42 ± 1.65		59.88 ± 0.12	226.56 ± 1.87	
Myristic acid (MA)	52.44 ± 0.11	210.70 ± 1.65		52.49 ± 0.14	212.65 ± 1.96	
Lauric acid (LA)	42.14 ± 0.09	190.12 ± 1.21		42.20 ± 0.11	194.23 ± 1.63	
SA/PMMA	67.31 ± 0.12	187.72 ± 1.89	193.72	66.78 ± 0.11	190.34 ± 2.12	197.39
PA/PMMA	59.98 ± 0.14	173.89 ± 1.78	177.13	59.35 ± 0.09	175.53 ± 1.88	181.24
MA/PMMA	51.00 ± 0.12	166.56 ± 1.94	168.56	50.74 ± 0.13	168.81 ± 1.67	170.12
LA/PMMA	40.96 ± 0.10	149.55 ± 2.02	152.09	41.55 ± 0.11	151.32 ± 1.86	155.38

Adapted from [67].

Table 21
Samples identification and heat of fusion.

Samples	Composition (wt.%)	Melting point (°C)	Latent heat (J/g)
Capric-lauric acids eutectic	CA (67) + LA (33)	22.81	154.16
Capric-myristic acids eutectic	CA (72) + MA (28)	25.36	139.20
Capric-stearic acids eutectic	CA (77) + SA (23)	27.78	122.58
Lauric-myristic acids eutectic	LA (58) + MA (42)	35.18	162.27
PCM1	CA (33.5) + LA (16.5) + PMMA (50)	21.11	76.30
PCM2	CA (36) + MA (14) + PMMA (50)	25.16	69.32
PCM3	CA (38.5) + SA (11.5) + PMMA (50)	26.38	59.29
PCM4	LA (29) + MA (21) + PMMA (50)	34.81	80.75

Adapted from [68].

is less than 2000, the latent heats of obtained PCMs are too small to satisfy our general demands, so they cannot be used practically. If the molecular weight of PEG is larger than 20,000, the latent heats of obtained PCMs become small and their mechanical strengths become very weak. For the same reason, they are also not suitable for practical usage. Therefore in this work, only the specimens with molecular weight 2000, 4000, 6000, 10,000 and 20,000 were studied. For preparation of new composites following chemicals were used: CDA, white loose granules; toluene-2,4-diisocyanate (TDI-80), a chemically pure reagent; acetone, an analytically pure reagent. Fig. 17 demonstrates that the regular change is basically the same in spite of the sample prepared with the PEG of different molecular weight. The enthalpy decreased as the diminution of the weight percentage of PEG and the enthalpy change into zero after the weight percentage of PEG droped to certain value. The correlation between the transition temperatures and the weight percentage of PEG is shown in Fig. 18. The changes of transition temperatures have the similar rules as the enthalpies. The transition temperatures fall down as the weight percentages of PEG decline. It should be noted that the transition temperatures of the composites are much lower than that of pure PEG with the maximum beyond 30 K. There is also the sufficient difference between melting temperature and freezing temperature. Other important fact observed is the enthalpy of PCMs reaches the maximum when the molecular weight PEG is 10,000 and the enthalpy decline when the molecular weight becomes greater or less than this value.

Su and Liu [70] have synthesized a novel polymeric solid–solid phase change heat storage material with polyurethane block copolymer structure (PUPCM) composed of high molecule weight polyethylene glycol (PEG) as soft segment, 4,40-diphenylmethane diisocyanate (MDI) and 1,4-butanediol (BDO) as a chain extender using a two-step process that is shown in Fig. 19. PEG (M_n = 10,000) was degassed and dried in a round flask under high vacuum (20 Pa) at 100–120 °C for 3–4 h. MDI was used as-received. DMF and BDO were dried by 5 Å molecular sieve for 24 h followed by distillation before use. Differential scanning calorimetry (DSC), polarizing optical microscopy (POM), scanning electronic microscopy (SEM) and wide-angle X-ray scanning diffraction (WAXD) tests were conducted to investigate the phase transition behaviors and crystalline morphology. The results of DSC analysis of pure PEG and PUPCM are given in Table 22. It indicates that there is a melting peak at about 66 °C in the heating scanning DSC curve of pure PEG and the latent heat of fusion is 189.6 J/g, while the heating scanning DSC curve of PUPCM shows a melting peak at

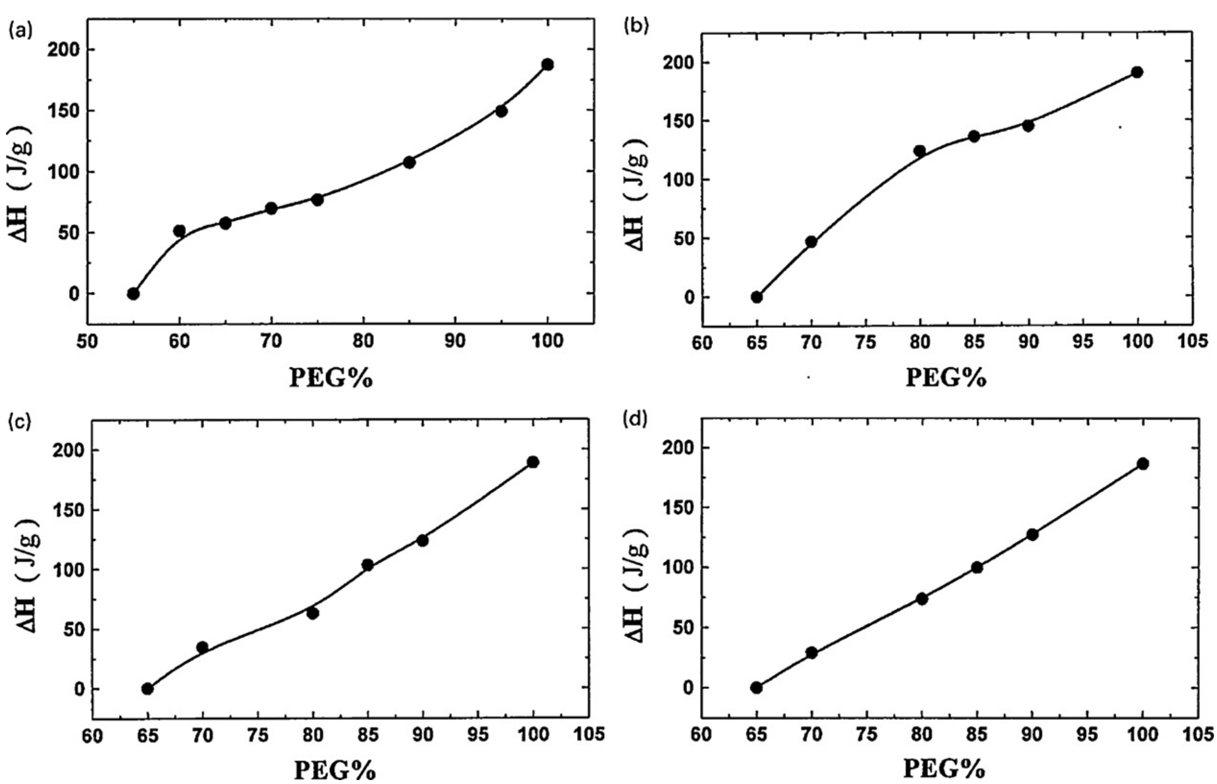


Fig. 17. Relational curves between the enthalpy and the different weight percentage of PEG [69].

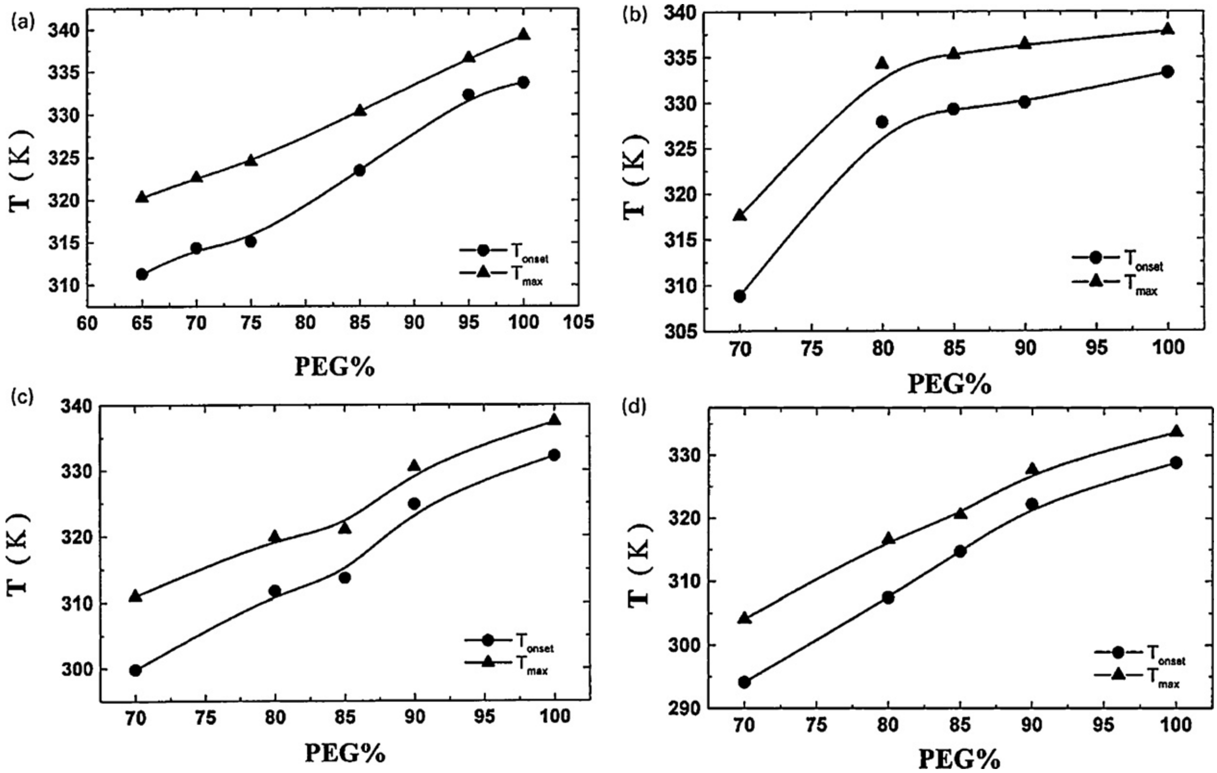


Fig. 18. Relational curves between the transition temperature and the different weight percentage of PEG [69].

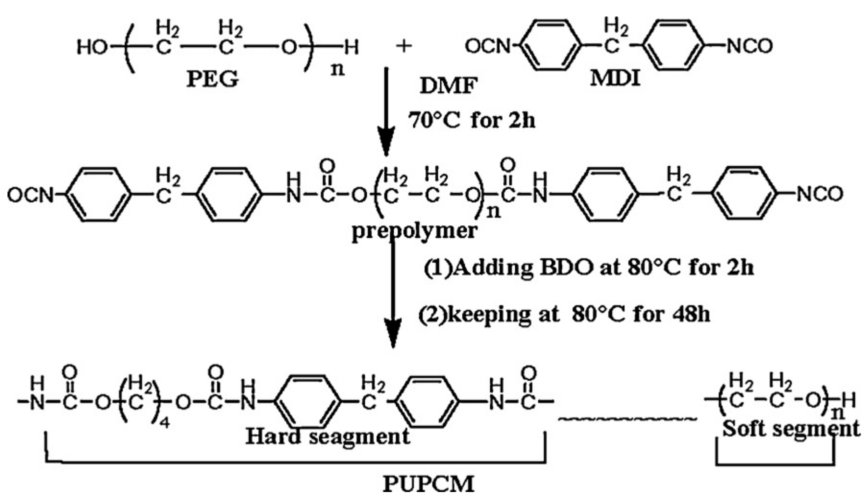


Fig. 19. Synthetic route to PUPCM [70].

65 °C, and the enthalpy is 138.7 J/g. The calculated ratio of PEG in PUPCM corresponds 73–75 wt.%. It is less than experimental value of 88.7 wt.%. Both pure PEG and PUPCM undergo phase transition with high transition enthalpy, but their phase transition states are quite different. Pure PEG's phase transition is a process from solid to liquid condition. Heating some pure PEG in a piece of glass shows that it starts to change from a white crystal solid to a transparent liquid when the temperature is incresed till approximately 50 °C, whereas PUPCM, which is hard and slightly yellow at room temperature, after heating remains solid, and no liquid is observed in the complete heating process, even if the temperature is raised to 100 °C or higher. The results indicated that the PUPCM

Table 22
Transition temperature and transition enthalpy of pure PEG and PUPCM [70].

Sample	Type of phase transition	Latent heat (J/g)		Peak transition temperature (°C)	
		Heating cycle	Cooling cycle	Heating cycle	Cooling cycle
PEG 10000	Solid–liquid	189.6	167.2	65.98	37.61
PUPCM	Solid–solid	138.7	126.2	65.28	38.58

Table 23
Thermal properties of PEG 6000 and HB-PUPCM measured by DSC analysis [71].

Samples	Type of phase transition	Melting point (°C)	Heat of fusion (J/g)	Freezing point (°C)	Heat of freezing (J/g)
PEG 6000	Solid–liquid	67.2	155.1	34.6	152.0
90% PEG 6000	Solid–solid	67.0	138.2	33.2	132.3
80% PEG 6000	Solid–solid	66.4	118.1	20.4	115.8
70% PEG 6000	Solid–solid	62.2	102.8	18.6	100.9
60% PEG 6000	Solid–solid	57.5	91.2	7.8	89.4

showed typical solid–solid phase transition properties, e.g. suitable transition temperature, high transition enthalpy and good thermal stability. However, the substantial difference is observed between transition temperatures in PCMs in heating and cooling mode.

Cao and Liu [71] synthesized and studied a series of novel solid–solid hyperbranched polyurethane phase change materials. For synthesis form-stable PCM the following materials were used. Boltorn® H_2O (second generation, M_w = 1750 g/mol, hydroxyl number equals 470–500 mg KOH/g) was dried at 60 °C under vacuum for overnight prior to use; polyethylene glycol (PEG, M_n = 6000) was degassed and dried in a round flask under high vacuum (20 Pa) at 100–120 °C for 3–4 h; 4,40-diphenylmethane diisocyanate (MDI) was heated to 60 °C and kept at temperature for 2 h and then filtered through a heated filter. N,N-dimethyl-formamide (DMF) was dried by 5 Å molecular sieve for 24 h followed by distillation before use. The synthesis process was similar to the procedure which was used in [65]. The general procedure is as follows: different amounts of dehydrated PEG and excess of MDI in freshly distilled DMF were mixed with stirring in a thermostatic oil-bath at 80 °C under vacuum for 3 h. A predetermined of Boltorn® H_2O was dissolved in dried DMF and added to the mixture. After stirring for another 2 h, the reaction mixture was cast in glass pan. Curing was conducted at 80 °C for 24 h, after which the polymer films with a thickness of 0.2–1.0 mm were obtained. The samples were kept in vacuum at room temperature for 2 weeks before testing. Thermal properties of polyethylene glycol and hyperbranched polyurethane of different concentration of PEG determined by DSC analysis are presented in Table 23. Tests of HB-PUPCM containing 90% PEG 6000 with 100 thermal heating–cooling cycles have given the following results: the melting point and heat of fusion of uncycled sample was 67.05 °C and 138.2 J/g and cycled sample 66.93 °C and 137.8 J/g, respectively. It is easy note that the melting and freezing points differ from each other essentially. Last circumstance is undesirable in typical phase change thermal storage systems.

Alkan et al. [72] composed novel form-stable phase change materials (PCMs) on the basis of polyethylene glycol (PEG) and acrylic polymers like polymethyl methacrylate (PMMA), Eudragit S (Eud S), and Eudragit E (Eud E). The developed PCMs were characterized by optical microscopy, spectroscopy and viscosity techniques. The following chemicals were used as components of PCMs: PMMA (M_w = 120,000 g/mol) without purification; Eudragit S (M_w = 135,000 g/mol), a 1:2 copolymer of methacrylic acid and methyl metacrylate was a commercial product; Eudragit E (light yellow granules, M_w = 150,000 g/mol), a 1:2:1 butyl metacrylate/(2-dimethylamino ethyl) methacrylate/methyl methacrylate statistical copolymer. All acrylic polymers were supplied by Röhm Pharma (Darmstadt, Germany). Chloroform was Merck grade and commercially available. The blends of PEG with PMMA, Eud S, and Eud E were prepared by the solution casting method. Solutions of PEG and acrylic polymers were dissolved in chloroform separately and PEG solution was added to each acrylic solution dropwise. Then chloroform was casted at room temperature in 15 days. The blends were prepared at 50, 60, 70, 80, and 90% w/w PEG compositions to find the maximum available ratio without leakage of the PEG when the temperature was between the melting point of the PEG and that of the acrylic polymer in the blend. Thermal properties of the blends (Table 24) were measured by DSC technique. In the form-stable blends, PEG acted like phase change heat storage material when the acrylic polymers served as supporting material because of their adhesion property. The maximum percentage of PEG was found 80% w/w for any of the blend in which no leakage of PEG occurred for 100 heating/cooling cycles. According to the table, there is difference between melting point and freezing points of PEG as well as the developed blends. These differences are less than in the case of Chinese researchers [69–71].

Sarı et al. [73] prepared and characterized poly(ethylene glycol) (PEG)/poly(methyl methacrylate) (PMMA) blends as novel form-stable phase change materials (PCMs) for latent heat thermal energy storage applications. In the blends, PEG acted as a PCM when PMMA was operated as supporting material. PEG (weight-average molecular weight = 20,000 g/mol, Merck) and PMMA (weight-average molecular weight = 120,000 g/mol, Aldrich) were used without purification. Chloroform was reagent grade and commercially available. PCM preparation procedure was the same as in [72]. Blends were studied at different mass fractions of PEG (50, 60, 70, 80, and 90% w/w) to leakage tests by heating the blends over the melting temperature of the PCM to determine the maximum proportion without leakage. The results of DSC analysis are given in Table 25. The prepared 70/30 w/w % PEG/PMMA blend as a form-stable PCM was characterized with optical microscopy and Fourier transform infrared spectroscopy. Measurements indicated that the form-stable PEG/PMMA blend melted at 58.07 °C and crystallized at 39.28 °C and that it had latent heats of 121.24 and 108.36 J/g for melting and freezing, respectively. Similar measurements were made after thermal cycling of the blend. Its melting point changed from 1.17 to −1.5 to −0.38 °C when its freezing point changed from −0.07 to −0.58 to 1.12 °C after 1000, 2000, and 3000 thermal cycles, respectively. On the basis of these results, we concluded that the form-stable PCM had good thermal reliability in terms of the changes in its phase change temperatures. On the other hand, the latent heat of melting of the PCM changed by −3, −13.5, and −10% and the latent heat of crystallization changed by −5.2, −14.7, and −9.8% after 1000, 2000, and 3000 repeated thermal cycles, respectively. The chemical stability of the form-stable PCM after repeated thermal cycles was also investigated by FT-IR analysis. Fig. 20 illustrates that the FT-IR spectra were identical before and after 3000

Table 24
Thermal properties of some form-stable blends with PEG (80/20 wt.%) [72].

Phase change material	Melting point (°C)	Heat of fusion (J/g)	Freezing point (°C)	Heat of freezing (J/g)
PEG	55.83 ± 0.12	176.10 ± 1.42	46.91 ± 0.23	162.05 ± 1.65
PEG/Eudagit E	56.94 ± 0.21	148.85 ± 1.81	42.73 ± 0.13	144.87 ± 1.72
PEG/Eudagit S	50.96 ± 0.24	144.23 ± 1.21	41.32 ± 0.16	141.53 ± 2.30
PEG /PMMA	56.90 ± 0.17	141.62 ± 2.03	43.15 ± 0.27	140.02 ± 2.10

Table 25
Thermal properties of pure PEG and PEG/PMMA blends [73].

Form-stable PCM	Melting point (°C)	Freezing point (°C)	Heat of fusion (J/g)	Heat of freezing (J/g)
Pure PEG 20,000	61.21	49.35	176.24	154.18
PEG/PMMA (50/50 wt.%)	57.73	38.86	86.28	76.41
PEG/PMMA (60/40 wt.%)	57.81	38.97	102.71	89.16
PEG/PMMA (65/35 wt.%)	57.93	39.10	112.54	97.21
PEG/PMMA (70/30 wt.%)	58.07	19.28	121.24	108.36

thermal cycles. This means that no chemical degradation of the PCM occurred during thermal cycling. However, there is large difference between freezing point and melting point of the developed form-stable blend as it occurred in other form-stable composition with polyethylene glycol.

Fang et al. [74] prepared form-stable polyethylene glycol (PEG)/epoxy resin (EP) composite as a novel phase change material (PCM) using casting moulding method. Reagent grade polyethylene glycol PEG 4000 (average molecular weight of 4000), industrial grade epoxy resin (diglycidyl ether of biphenyl-A, E-51), release agent (Frekote 770-NC), hardener Jeffamine D230 (polyether oligomers terminated at each end with an amine group), promoter n,n-dimethyl-1,3-propanediamine (DMAPA) were used for preparation of the composite. Under 60 °C water bath, 75 g PEG 4000 and 18.5 g epoxy resin E-51 were separately added to 250 ml conical flask, then mechanical agitation caused them uniform dissolution. Based on EP mass percentage, 30% D230 hardener and 5% DMAPA promoter were separately added to the above mentioned flask with quick continuous stirring. After the blend evenly was mixed the air was sucked under vacuum, and poured into preheating mould with coating Frekote 770-NC release agent, then the mold was shifted into a 60 °C drying oven for 24 h. The solidified composite cooled down to the room temperature and became the goal product. The DSC analysis showed 55.3 °C and 186.7 J/g for phase change temperature and the enthalpy of pure PEG. Accordingly, the phase change temperature and the enthalpy of PEG/EP composite was 54.2 °C and 132.4 J/g (the theoretical valve is 140 J/g, calculated by the product of the enthalpy of pure PEG and PEG mass percentage of 75%), respectively. The same phase change behavior existed in the freezing process. Fig. 21 indicated that there is no chemical reaction but physical cross-linking between PEG and EP.

Reagent grade polyethylene glycol (average molecular weight of 10,000) and silicon dioxide were used by Wang et al. [75] for preparation form-stable compositions. Silicon dioxide and PEG solution were each prepared by dissolving silicon dioxide and PEG in water with quick continuous stirring for 12 h afterward the prepared solutions were mixed at room temperature at different weight ratios ranging from 95 to 5 wt.%. After stirring for 3 h, the mixed solution was put into a drying cabinet and heated at 100 °C for 24 h. Then the solid composite was obtained by heating under a reduced pressure at 70 °C for 24 h. The maximum mass percentage of polyethylene glycol dispersed into the PCM composites was determined as 85 wt.%. There was no leakage of the PEG from the surface of the composite up to this mass ratio even when it melted. DSC analysis of pure PEG and PEG/SiO_2 composite is shown in Fig. 22. The developed composite had a large enthalpy of 162.9 J/g and suitable melting temperature (T_m = 61.61 °C). The absence of significant new peaks in Fig. 23 showed no chemical reaction between components.

Wang et al. [76] prepared and investigated a high conductivity form-stable phase change material by blending polyethylene glycol 1000 as latent heat storage material, silica gel as structure-forming material, and β-aluminum nitride powder as thermal conductivity enhancing material. Firstly, Silicon gel and polyethylene glycol with the mass ratio 15/85 were dissolved in water while stirring for 12 h. Secondly, the prepared solutions were added with β-aluminum nitride at different ratios ranging from 5 to 30 wt.% and then mixed at room temperature for 2 h. Afterward, the mixed solution was put into an oven and heated at 100 °C for 24 h. Finally, the solid composite was obtained by heating in a vacuum oven at 70 °C for 24 h. Melting point, heat of fusion thermal conductivity value of the composite PCMs were determined by using DSC technique and the Hotdisk thermal analyzer. Measurement results are presented in Table 26. Obviously, there are significant discrepancies between melting points and freezing points of composite PCM as well as between heat of fusion and heat of freezing. At the same time the increase of β-aluminum nitride content in PCM from 5 to 30% rises thermal conductivity from 0.385 to 0.766 only and simultaneously decreases the specific latent heat of phase change.

Xi et al. [77] realized a two-step procedure for synthesizing a novel polymeric based solid–solid phase change heat storage material (MGPM). At first, a copolymer monomer (PD) containing a polyethylene glycol monomethyl ether (MPEG) phase change unit and a vinyl unit were synthesized via the modification of

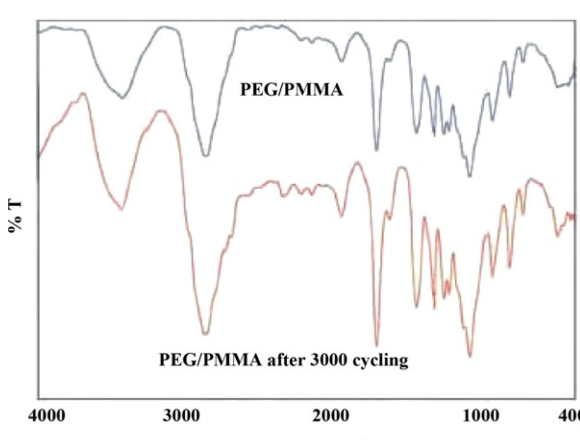


Fig. 20. FT-IR spectra of the form-stable PEG/PMMA blend before and after 3000 thermal cycles [73].

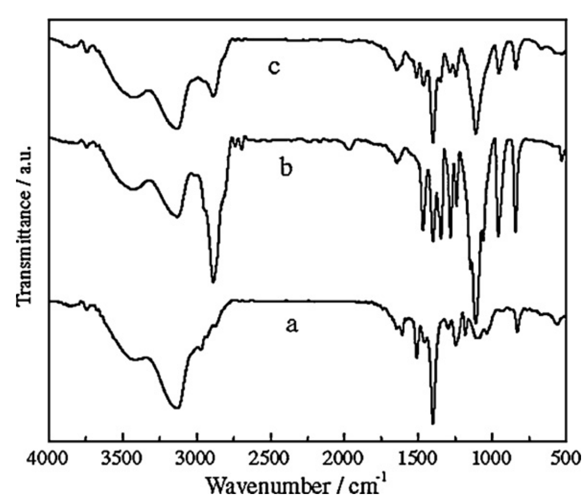


Fig. 21. FT-IR spectra of (a) EP, (b) PEG and (c) PEG/EP [74].

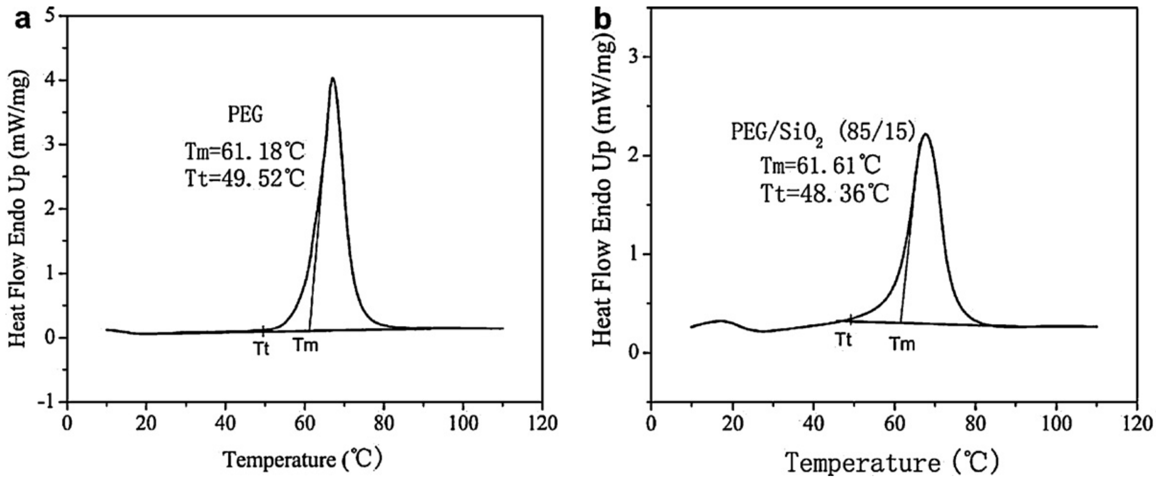


Fig. 22. DSC curve (heating cycle): (a) PEG; (b) PEG/SiO_2 (85/15) [75].

Table 26
Thermal properties of the PEG/SiO_2/β-AlN composite PCMs.

AlN (%)	Melting point (°C)	Heat of fusion (J/g)	Freezing point (°C)	Heat of freezing (J/g)	Thermal conductivity (W/m K)
1	60.41	161.4	45.13	132.9	
5	62.32	154.6	43.96	129.8	0.385
10	58.59	152.8	45.04	128.7	0.446
15	60.93	137.7	44.81	117.6	0.561
20	61.18	129.5	42.39	106.8	0.697

Adapted from [76].

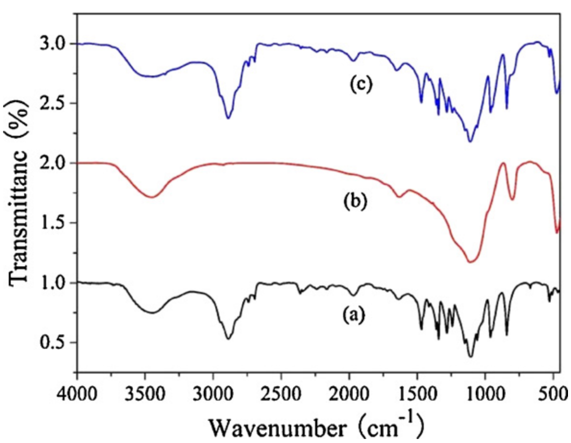


Fig. 23. FT-IR spectrum of (a) PEG, (b) SiO_2 and (c) composite [75].

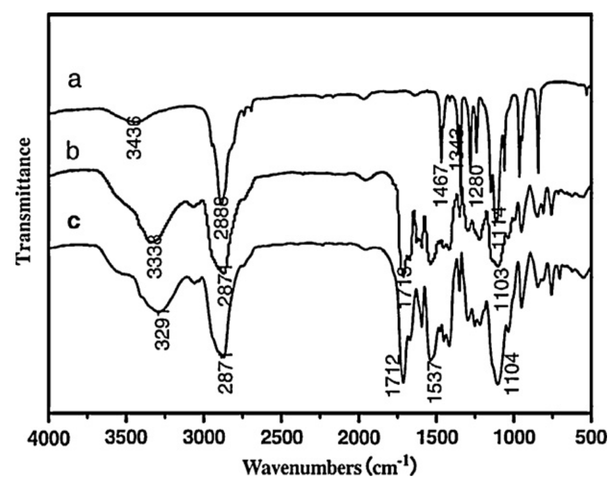


Fig. 24. FT-IR spectra of polyethylene glycol monomethyl ether (MPEG) (a); intermediate novel copolymer monomer (PD) (b) and MGPM (c) [77].

hydrogen group of MPEG. Secondly, by copolymerization of the PD and phenyl ethylene, a novel polymeric based solid–solid phase change heat storage material was prepared. The composition, structure and properties of the novel polymeric based solid–solid phase change material were characterized by IR, ^{1}H NMR, DSC, WAXD, and POM, respectively. The results show that the novel polymeric based solid–solid phase change material possesses excellent crystal properties and high phase change enthalpy. Fig. 24 demonstrates the practical identity of FT-IR spectra of PD and the final composite product. These results prove that the

Table 27
Thermal properties of MGPM preparated with different proportion of PD to phenyl ethylene.

Mole ratio of PD and phenyl ethylene	Type of phase change	MPEG (wt.%)	Heating transition point (°C)	Heating transition latent heat (J/g)	Cooling transition point (°C)	Cooling transition latent heat (J/g)
9:1	Solid–liquid					
1:2	Solid–solid	71	57.7	108.5	18.3	81.6
1:20	Solid–solid	64	55.8	90.3	11.7	63.4
1:30	Solid–solid	53	55.4	75.9	8.4	49.6
1:40	Solid–solid	46	54.0	53.4	4.3	44.0
1:70	Solid–solid	38	53.2	47.2	1.5	33.9

Adapted from [77].

Table 28
DSC results of mPEG and cellulose–graft–PEG copolymers [78].

	PEG content[a] (wt.%)	ΔH_m[b] (J/g)	ΔH_m^*[c] (J/g)	T_c[d] (°C)	ΔH_c[b] (J/g)	ΔH_m^*[c] (J/g)	T_c[d] (°C)
Cellulose–graft–$PEG_{1.1K}$	100.0	140.3	140.3	46.2	137.8	137.8	27.0
	77.4	73.3	94.7	42.8	71.2	92	25.7
	70.5	60.5	85.8	43.3	57.8	82.0	25.1
	57.6	46.0	79.9	40.7	44.7	77.6	26.0
Cellulose–graft–PEG_{2K}	100	183.3	183.3	53.2	181.8	181.8	34.7
	84.3	133.7	158.6	51.0	129.9	154.1	30.7
	75.8	110.9	146.3	50.9	110.4	145.6	30.2
	59.3	81.1	136.8	50.0	80.1	135.1	29.5
Cellulose–graft–PEG_{5K}	100	204.7	204.7	60.1	203.2	203.2	40.6
	90.1	153.6	170.5	58.9	153.1	169.9	39.5
	84.8	141.3	166.6	58.9	140.2	165.3	37.6
	74.1	112.5	151.8	59.0	111.3	150.2	34.9

[a] Calculated by gravimetry: PEG (wt.%) = [mass of PEG (g)/mass of copolymer (g)] × 100%.
[b] Enthalpy of mPEG and its corresponding copolymers during melting and solidifying.
[c] Enthalpy of PEG in its corresponding copolymers during melting and solidifying.
[d] Temperature of melting and solidification

copolymerization of PD and styrene has taken place. In other words, the novel MGPM was prepared. The results of DSC analysis of MGPM are presented in Table 27. We observe the significant discrepancies in heating and cooling transition temperatures as well as in heating and cooling transition latent heat.

Li et al. [78] synthesized a series of cellulose–graft–poly(ethylene glycol) (cellulose–graft–PEG) copolymers as phase change materials (PCMs). In order to prepare the novel heat storage materials the following initial materials were used: microcrystalline cellulose, (poly(ethylene glycol) monomethylether (mPEG) with molecular weight (M_n) of 5000, 2000 and 1100 g/mol (denoted as PEG_{5K}, PEG_{2K} and $PEG_{1.1K}$) and 4,4-diphenylmethane diisocyanate without further purification, expanded graphite (average particle size: 300 nm, expansion ratio: 200 ml/g), the ionic liquid, 1-all-3-methylimidazoliumchloride, prepared as described in literature, dimethylformamide (DMF) and N,N-dimethylacetamide (DMAc) were freshly distilled over CaH_2 under reduced pressure. Anhydrous lithium chloride (LiCl) was dried at 120 °C for12 h in vacuum before use. The compositions obtained were studied by using FT-IR, ^1H NMR, thermomechanical analyzer, X-ray diffraction, polarized optical microscopy, DSC, TGA and SEM. Differential scanning calorimetry indicated that the copolymers showed phase transitions with large thermal storage density (see Table 28), and the phase change temperature is ranging from 40 to 60 °C. The transition temperature and enthalpy can be tailored by changing the molecular weight and the content of poly(ethyleneglycol) (PEG) side chains. The copolymers are solid–solid PCMs with good thermal stability. Expanded graphite (EG) with 2.5 and 10 wt.% was added to the PCMs to improve the thermal conductivity. It was found that the thermal conductivity enhanced significantly with increasing EG content. The cellulose–graft–PEG/EG composite PCM shave potential applications in thermal energy storage and temperature control. Actually, there are thermal hysteresis in melting temperature and freezing temperature.

Zeng et al. [79] prepared and investigated polyaniline (PANI)/1-tetradecanol (TD) compositions. The blends were prepared as follows. 0.03 g of cetyltrimethyl ammonium bromide (CTAB) was dissolved in 90 ml deionized (DI) water. Certain amounts of TD, distilled aniline and 1 ml of concentric HCl were added to this solution. The mixture was vigorously stirred for 2 h in a 50 °C water bath to form an emulsion. The water bath was naturally cooled to room temperature while the stirring continued. As the TD solidified, the emulsion turned to white slurry. The water bath was replaced by an ice-water bath. After the temperature of the mixture was cooled to 0–5 °C, 10 ml of ammonium persulfate (APS)-DI water solution was poured into it. The molar ratio of the aniline and APS was fixed to be 1:1. The mixture was stirred vigorously overnight and the ice-water bath was naturally warmed to room temperature. The mixture was left stand still to precipitate the solid materials. The supernate and the solid material floating on the surface were decanted by means of decantation. The precipitation was mixed with DI water and left stand still again. This procedure was repeated till the supernatant was nearly colorless. Afterward, the mixture was filtered and washed with DI water till the moment when the filtrate was totally colorless. The residue was collected and dried in a vacuum desiccator. The studied samples and results of DSC analysis are given in Table 29. Thus, S1 has the highest phase change enthalpy (162.97 J/g) in the composites. Latent heat of S2 is 162.64 J/g and is very close to that of S1. It was found that the highest TD mass fraction in the form-stable PCM is about 73% and will not increase anymore even the raw materials ratio is higher than this value. The reason can be interpreted as follows: in the reaction mixture, the amount of the surfactant, CTAB, is certain and the maximum amount of TD that can be emulsified by CTAB is certain. When the TD mass in the mixture exceeds this value, the exceeded TD would form big granule floating on the water surface and be decanted even if it has been composed with PANI. So in the present system, the highest TD mass fraction is about 73%.

Liao with other colleagues [80] developed and investigated a novel hyperbranched polyurethane/poly(ethylene glycol) doped with pentaerythritol (D-HBPU). The general synthesis procedure of doped hyperbranched polyurethane with 90-wt.% soft segment content (SSC) as follows: dehydrated PEG 6000 9.95 g with a little pentaerythritol 0.05 g and excess of L-MDI 1.0275 g in freshly distilled DMF were mixed and stirred in a thermostatic oil-bath at 80 °C for 5 h. A predetermined of Boltorn™ H_2O (0.0837 g) was dissolved in dried DMF and added to the mixture (molar ratio: —NCO/—OH = 1). After stirring for another 2 h, the reaction mixture

Table 29
Thermal properties of PANI/1-tetradecanol compositions.

Sample	TD mass fraction in composite PCM (%)	Melting temperature (°C)	Heat of fusion (J/g)
1-Tetradecanol (TD)	100.00	34.85	221.23
S1	73.64	33.54	162.97
S2	73.49	33.77	162.64
S2	60.37	33.25	133.62
S4	58.83	32.74	119.14
S5	37.23	33.38	82.39
S6	29.89	34.23	66.14
S7	15.92	34.85	35.23

Adapted from [79].

Table 30
Thermal property of HBPU and D-HBPU measured by DSC analysis [80].

Samples	Phase transition	Transition temperasture (°C)		Entahlpy of phase change transition (J/g)	
		Heating cycle	Cooling cycle	Heating cycle	Cooling cycle
HBPU	Solid–solid	55.7	30.8	115.7	112.4
D-HBPU	Solid–solid	59.0	36.8	125.0	120.6

Table 31
Phase change enthalpies of the PEG/AC PCMs with various PEG molecular weights [81].

Sample	PEG 1500/AC	PEG 4000/AC	PEG 6000/AC	PEG 10000/AC
Fusion enthalpy (J/g)	81.3	83.1	90.2	85.2
Solidification enthalpy (J/g)	72.8	75.7	85.1	81.4

was cast in a glass pan. Heating at 80 °C in a vacuum oven for 24 h took place, after which the polymer films were obtained. The samples were kept in vacuum at room temperature for 2 weeks before testing. Hyperbranched polyurethane with 90-wt.% SSC has the same process of synthesis. The composite material prepared was investigated by Fourier transform infrared spectroscopy, differential scanning calorimetry, thermogravimetric analyses, wide-angle X-ray diffraction (WAXD), and polarization optical microscopy (POM). Results of the investigation showed that D-HBPU was a typical solid-state PCM with better heat storage property and thermal resistance when compared with hyperbranched polyurethane (see Table 30).

Recently Feng et al. [81] preparated and investigated of polyethylene glycol/active carbon composites as shape-stabilized phase change materials. Chemically pure polyethylene glycol (PEG), a white crystalline solid was chosen as phase change material. The average molecular weights of PEG are 1500, 4000, 6000 and 10,000. The granular active carbon was produced by physical steam activation of carbonized coco nut shell at 1000 °C. PEG/AC PCMs were prepared by a physical blending and impregnation method. PEG was melted and dissolved in absolute ethanol. AC was added to the PEG solution while stirring and the solution was then stirred vigorously for 4 h. After this, the mixture was dried at 80 °C for 72 h, so that the ethanol solvent would evaporate and the shape stabilization of the composites above PEG's melting point could be investigated. The PEG content in the PEG/AC PCMs varied from 30 to 90 wt.%. When the composite PCMs were kept at 80 °C (above the melting point of PEG) for 3 days, some leakage of the liquid phase was found when the weight percentage of PEG in the composites was higher than 80 wt.%. The results of DSC analysis are presented in Table 31. It was observed that the phase change temperatures of the PEG/AC PCMs with the same PEG weight percentage increased with the rise in PEG molecular weights. Meanwhile the phase change enthalpies first increased and then decreased with the increase in PEG molecular weights (shown in Table 31), and the phase change enthalpy of the PEG 6000/AC PCM was the largest among four samples. Since the supercooling of PCMs is very important for application, the changes in phase change temperatures of PCM composites depending on PEG content and molecular weights are presented in Fig. 25. Thus, the extent of supercooling is about 20 °C.

5. Form-stable materials with solid–solid phase change

Some organic molecular crystals have polymorphic transformations. They are characterized by high enthalpies of solid–solid transitions and a low enthalpy of fusion. Such organic "plastic crystals" are potential thermal energy storage materials that undergo solid–solid phase transitions storing a significant amount of thermal energy and can be incorporated in practical applications such as drywall and Trombe walls in passive solar buildings.

5.1. Organic form-stable materials with solid–solid phase change

With the purpose to identify tetrahedral substances in addition to pentaerythritol that have high entropies of transition as a consequence of many possibilities for conformational disorder, Murrell and Bleed [82] determined thermal properties of some plastic crystals. All data obtained with a DuPont 900 Differential Thermal Analyzer at a heating rate of 15 °C/min in the air atmosphere are presented in Table 32. As seen from the table, the most investigated substances have high transition latent heat. The peculiarity of plastic crystals is interesting for thermal energy storage applications.

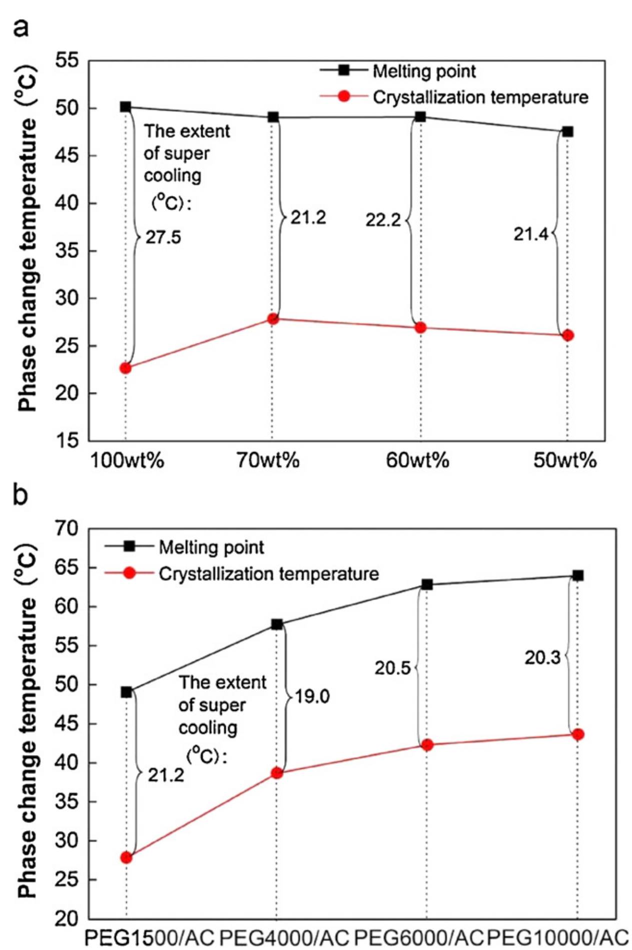


Fig. 25. Comparisons of the phase change temperature and the extent of supercooling for pure PEG and the PEG/ACPCMs. (a) – PEG1500/AC and (b) – 70% PEG/AC [81].

Table 32
Transition and fusion enthalpy for various substances.

Substance	Transition temperature (°C)	Transition latent heat (J/g)	Melting point (°C)	Heat of fusion (J/g)
Pentaerythritol	182–183	301	258	37
2-hydroxymethyl-2-methyl-1,3-propanediol	81	193	197	45
2,2-dimethyl-1,3-propanediol	40–43	131	125–126	45
2,2-dimethyl-1-propanol	−31	51	51–54	46
2-amino-2-hydroxymethyl-1,3-propanediol	131–134	283	166–169	25
2-amino-2-methyl-1,3-propanediol	78–80	239	110–112	28
2-hydroxymethyl-2-nitro-1,3-propanediol	80–82	148	Decomposition at 184 °C	
2-methyl-2-nitro-1,3-propanediol	79–80	190	149–153	28
2-methyl-2-nitro-1,3-propanol	35–39	144	88–89	31
2,2-dimethylpropionic acid	152–135	288	194–197	27
2,2-bis(hydroxymethyl)propionic acid	7–9	86	32–36	24
Tetramethylammonium chloride	265–265	90	Sublimation	

Adapted from [82].

Table 33
Typical properties of polyhydric alcohols.

Polyhydric alcohol/Formula	Transition temperature (°C)	Melting point (°C)	Latent heat of transition (J/g)	Heat capacity[a] (J/g °C)	Density (g/cm^3)	Thermal conductivity (W/m K)
Pentaerythritol (PE) $C-(CH_2OH)_4$	187	269	269	2.84	1.33	1.0
Trimethylol ethane (TME) $CH_2-C-(CH_2OH)_3$	82	198	174	2.75	1.22	0.51
Neopentylglycol (NPG) $(CH_2)_2-C-(CH_2OH)_2$	48	126	139	2.76	1.19	0.36
60 mol.% NPG/40 mol.% TME	26	140	76	2.64	1.07	0.23
67 mol.% NPG/33 mol.% TMP[b]	24	102	61			
90 wt.% TME/10 wt.% graphite	81	198	174		1.26	0.64

Adapted from [83–85].
[a] Just above the transition temperature.
[b] TMP = Trimethylpropane, $(CH_2OH)_3CCH_2CH_3$.

Taking into account high latent heat of crystal transformation in some plastic crystals and their potential use in thermal energy storage components and systems for solar and other applications, Benson et al. [83–85] carried out the investigation of thermal properties of some polyhydric alcohols. The compounds were obtained as technical reagent or purified grades of chemicals. Most of the experiments were conducted on as-received reagent grade compounds. In some cases, additional purification was achieved by recrystallization from water. Some thermal analyses were also conducted on technical grade materials for comparison with the pure compounds. Typical results of measurements are summarized in Table 33. A limited number of thermal cycling experiments were done in order to evaluate the stability of a typical mixture of polyols. Fig. 26 shows three DSC recordings of one such mixed sample. The sample contained 87.5% trimethylol ethane plus 12.5% neopentylglycol (molar percentages) and was cycled throughout the solid-state transition temperature range 320–370 K for 732 times at 20 K/min. The observed variation in enthalpies and transition temperatures are within the measurement uncertainties.

Taking into account high potential of solid–solid transition for thermal energy storage, Font et al. [86] carried out calorimetric study of PE/NPG and PG/NPG blends. In order to avoid the problems sublimation and vaporization the sample mixtures were prepared from water solutions at room temperature. The all measurements were done with using aluminum crucibles, which were sealed to prevent sublimation of components. The thermal analysis of the binary mixtures PG/NPG and PE/NPG was done with a heat flux scanning calorimeter (HFDSC) working in differential form like in the DTA technique. The signal was collected with two thermoelectric modules Melcor FC 06-32-06L connected in opposition. These detector elements can be used in a temperature range from −100 to 100 °C and have a high sensitivity, which allows to work without amplification. A a standard probe Pt-100 Ω was used for temperature measurement. The most interesting data obtained are presented in Table 34. As it is seen from the table during cooling the transition temperature range starts about 5 °C lower than that of heating. In the NPG/PG mixtures the existence of thermal hysteresis between the endothermic transition of the heating and the exothermic process corresponding to the cooling is observed. This thermal hysteresis may reach a ΔT of 15 °C (difference between the onset temperatures). The greatest difference in ΔH between heating and cooling transition occurs for samples of pure NPG (of the order of 10%). For these mixtures the difference between the

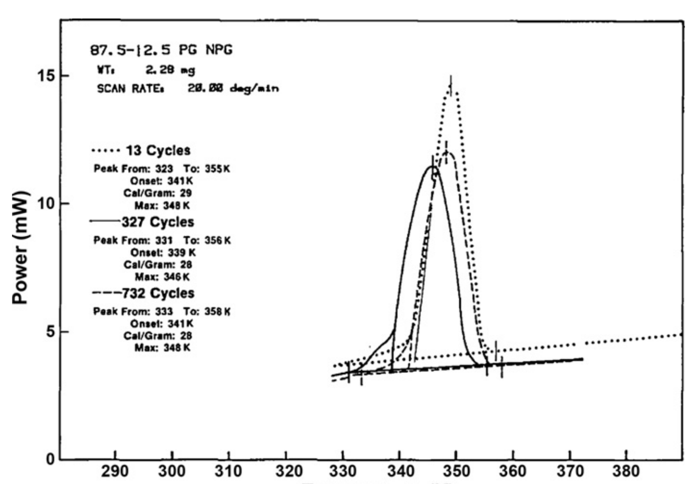


Fig. 26. DSC curves of 87.5% PG/12.5% NPG composition after 13, 327 and 732 complete thermal cycles through the solid-state transition [83].

Table 34
Transition parameters (ΔH – latent heat; T_i – start temperature; T_f – end temperature) of different concentration of PG/NPG for cycle 100.

Fraction of penta-glycerine (PG)	Heating			Cooling		
	ΔH (kJ/mol)	T_i (°C)	T_f (°C)	ΔH (kJ/mol)	T_i (°C)	T_f (°C)
0	13.5	37	44	12.0	32	29
9	11.0	19	29	9.7	19	15
17	10.2	12	40	8.3	10	0
23	9.8	12	28	8.0	3	−5
29	9.6	13	33	6.8	−3	−12
33	10.4	15	40	6.7	3	−5
40	8.5	11	48	7.0	11	3
45	11.7	29	55	8.4	22	8
50	13.6	43	70	11.5	41	28
55	14.0	45	68	11.2	51	23
60	13.0	37	65	9.0	37	15
65	13.6	53	72	12.2	50	30
70	13.6	44	74	10.5	43	30
75	14.2	50	72	12.6	47	34
83	14.9	57	79	12.5	60	42
90	18.1	64	83	17.4	65	53
100	18.4	78	86	17.8	73	62

Adapted from [86].

beginning temperatures of the transformation compared to pure NPG may reach ΔT as high as 30 °C.

Having studying PG/NPG in his previous work [86], Font et al. found that the latent heat of transition and beginning of the transition in heating and cooling modes depend on the concentration of PG in PG/NPG composition. In the considered work [87], the behavior of two NPG/PG mixtures with mass concentrations of 33% (mixture A) and 70% (mixture B) of PG (see Table 35) under different thermal treatments was studied. All measurements were made with a differential heat flux calorimeter. Mixture A is cooled from the plastic phase (45 °C) to temperatures of 5 and 10 °C, maintaining it at these temperatures over different periods of time. Then it is heated again up to 45 °C (treatment A-I). The transition II ∼ I on direct heating (without stopping at intermediate temperatures) begins at 15 °C, while the direct process on cooling starts at 3 °C. Therefore the temperatures 5 and 10 °C are included on the interval that corresponds to the thermal hysteresis of the transition. For the same sample we have carried out a different type of treatment (treatment A-II). The sample is cooled from phase I (45 °C) to different temperatures T (see values of T in Table 36) maintaining it at T during 12 h. Later, it is heated up to 45 °C. Similar measurements were also made with mixture B.

Yaving summarizing the results of this work, it can be said that when cooling the samples from plastic phase and holding them at a temperature higher than the initial temperature of the transition on direct cooling (without stopping at intermediate temperature), conversion to crystalline phase takes place. The degree of conversion evolves exponentially with time at which the mixture is maintained. The same can be observed for the mixture with 33% of PG the existence of an exponential evolution of the conversions degree of with respect the temperature for a fixed time. In our point of view, when the samples of PG/NPG mixture are cooling from the plastic phase to the temperature below the transition temperature, supercooling is taking place. It is known that the polyalcohols are characterized by their ability to be supercooled. The supercooling phenomenon explains the results obtained in considered paper.

Taking into consideration the attractiveness of some organic plastic crystals as perspective solid–solid phase change materials for thermal energy storage, the group of researchers led by Prof. J.Ll. Tamarit have investigated the binary systems of neopentylglycol (NPG), pentaglycerine (PG), pentaerythritol (PE), tris (hydroxymethyl) aminomethane (TRIS) and 2-amino-2-methyl-1,3-propanediol AMPL [88–91]. The thermal measurements were made with two heat flux calorimeters working in differential form. The calibration of two calorimeters has been made using Joule effect (dissipation of about 1 J into sample crucible). The temperatures in both calorimeters have been measured with a PT-100 Ω standard probe. In the phase diagram of the PG/NPG, two interesting points were found: the presence of an invariant eutectoid (eutectoid temperature 24.9 °C; 0.29 ± 0.02 molar fraction of PG); a total miscibility in the plastic phase and a Gibbs minimum point at 106.4 °C and 0.21 ± 0.02 molar fraction of PG. The binary system of PE/PG is characterized by a total miscibility in crystal and plastic phases. In the binary system of TRIS/AMPL, an eutectoid invariant

Table 35
Effect of maintaining time of mixture A on its transition latent heat in heating mode for treatment A-I.

Mixture maintaining temperature 5 °C		Mixture maintaining temperature 10 °C	
Maintaining time (min)	ΔH (kJ/mol)	Maintaining time (min)	ΔH (kJ/mol)
10	0.54	45	0.13
30	1.09	60	0.42
45	3.69	75	0.49
60	4.45	120	1.67
90	8.47	135	2.14
140	8.18	180	4.18
180	9.07	225	5.47
240	9,27	270	5.93
300	9.40	360	8.56
420	9.47	480	7.51
720	9.05	630	7.58
		720	7.81
		825	7.81

Adapted from [87].

Table 36
Effect of maintaining temperature of mixture A on its transition latent heat in heating mode (maintaining time 12 h) for treatment A-II [87].

Mixture maintaining temperature (°C)	ΔH (kJ/mol)
0	10.12
2	9.81
3	9.05
7	8.97
10	7.81
11	6.75
13	4.34
15	1.98
16	1.33
20	0

Table 37
Thermal properties of some alcohols and amines with solid–solid transition.

Substance	Formula	Transition temperature (°C)	Transition latent heat (J/g)	Melting point (°C)	Heat of fusion (J/g)
Pentaerythritol	$C_5H_{12}O_4$	187.5 ± 1.0	301.1 ± 3.0	261.3 ± 1.0	38.2 ± 0.7
Pentaglycerine	$C_5H_{12}O_3$	80.3 ± 1.0	179.8 ± 0.8	186.0 ± 1.0	34.1 ± 0.8
Neopentylglycol	$C_5H_{12}O_2$	40.0 ± 1.0	135.4 ± 4.8	125.0 ± 1.0	38.4 ± 1.0
TRIS	$C_4H_{11}NO_3$	133.6 ± 1.0	280.7 ± 14.0	169.5 ± 1.0	26.4 ± 1.6
AMPL	$C_4H_{11}NO_2$	79.4 ± 1.0	221.6 ± 11.5	109.2 ± 1.0	26.8 ± 1.9

Adapted from [88–91].

Table 38
Transition parameters of pentaerythritol (PE)/trimethylolpropane (TMP) system.

Composition (mol.%)	Solid-state transition temperature (°C)	Transition latent heat (J/g)	Melting point (°C)	Heat of fusion (J/g)
PE (55%) – TMP (45%)	57.37	55.36	174	88.79
PE (50%) – TMP (50%)	57.49	63.63	166	48.02
PE (40%) – TMP (60%)	57.64	72.02	158	42.75
PE (30%) – TMP (70%)	57.96	94.24	150	37.84

Adapted from [92].

was observed at 72 ± 1 °C and 0.18 molar fraction of AMPL. Unfortunately, the latent heat of solid–solid transition of the observed eutectoid composition has not been measured. The thermal properties of pure compounds measured in present works are summarized in Table 37.

Zhang and Yang [92] has studied the heat capacities and enthalpies of phase transition for mixtures of pentaerythritol and trimethylolpropane in different mole ratios over the superambient temperature range with an automated adiabatic calorimeter. Samples for the experiments were prepared in the following manner. Pentaerythritol reagent was sublimed and recrystallized from distilled water twice. Its purity was found to be 99.96% by means of chemical analysis. Trimethylolpropane reagent was recrystallized from dry ether. The purity was found to be 99.12 mol% from the analysis of its equilibrium melting curve. Two purified substances were mixed and grounded into fine powder in the desired mole ratios. The mixture was heated to produce a clear liquid, and grounded into a fine powder again after cooling to room temperature. The results of measurement of thermal effect in compositions under investigations are given in Table 38. As seen from the table, the mixture composed of 30% PE and 70% TMP has acceptable solid–solid transition temperature 57.96 °C and latent heat 94.24 J/g.

A group of Japanese researchers at the Kinki University [93–95] measured low-temperature heat capacity of high purity trimethyloletane (TME) or neopentanetriol (NPT) ($C_5H_{12}O_3$) and neopentylglycol (NPG) ($C_5H_{12}O_2$). A low-temperature adiabatic calorimeter described previously in [96] was used for the heat capacity measurement. The heat capacity was determined by a discontinuous heating mode. The sample temperature was measured to a precision of 0.1 mK for about 10 min prior and after each energizing period. The amount of supplied energy was chosen so as to give the resulting temperature increment of 1–2 K in the normal region and 0.05–0.1 K in the transition region. The purity of each sample was determined to be 99.99% for NPG and 99.96% for NPT. The crystals of NPT and NPG undergo the first order transition at (85 ± 0.1) and (41.3 ± 0.1) °C, respectively. The amount of the enthalpy of transition is particularly large both for NPG (120.2 J/g) and NPT (176.8 J/g).

After consideration neopentylglycol (NPG) and pentaglycerine (PG) as high potential solid-state thermal energy storage material, Son and Morehouse [97] investigated the composition of these plastic crystals with salt hydrates such as magnesium chloride hexahydrate and sodium sulphate decahydrate. Thermal properties of phase change materials to be investigated are summarized in Tables 39 and 40. As follows from Table 39, the transition temperatures of compositions on the basis of PG salt hydrates observed at temperatures exceed melting points of salts. Consequently, these salts at noted transition temperature should be in liquid state. However, there is no information regarding the seepage of liquid phase in [97], as well as thermal stability of these compounds.

In the frame of the investigations already started, the international research group [98,99] has studied the binary systems with TBN, MNP, NPA, NPG, PG, TRIS and PE. The experimental technique was the same as in previous studies [86–91]. The eutectoid invariants were registered. Unfortunately the data on thermal effects of eutectoid compositions have not been reported. Along with determination of characteristic parameters of binary systems, the thermal properties of some pure plastic crystals were measured (see Table 41).

Wang et al. [100,101] investigated heat storage performance of the binary systems of neopentylglycol (NPG)/pentaerythritol (PE) and neopentylglycol (NPG)/trihydroxy methyl-aminomethane (TAM) as solid–solid phase change materials. Experimental samples were prepared in the following sequence: the desired ratio of NPG and PE or NPG and TAM was put into a mortar, after that

Table 39
PCM property values.

Materials	Transition temperature[a] (°C)	Transition latent heat[b] (J/g)	Specific heat[c] (J/g°C)
Solid–solid			
Neopentylglycol (NPG)	48	119	2.7
Pentaglycerine (PG)	82	139	2.8
Solid–liquid			
Magnesium chloride hexahydrate (MCH)	117	169	2.3
Sodium sulphate decahydrate (SSD)	31	186	3.1
Mixtures (molar ratio)			
NPG–MCH (7:3)	43	87	1.5
NPG–MCH (9:1)	42	101	2.1
NPG–SSD (7:3)	39	56	0.2
NPG–SSD (9:1)	40	108	1.4
PG–MCH (7:3)	85	56	1.0
PG–MCH (9:1)	85	67	
PG–SSD (7:3)	70	260	0.7
PG–SSD (9:1)	87	241	2.0

Adapted from [97].
[a] ±1 °C.
[b] ±1 J/g.
[c] ±10%.

Table 40
PCM property values.

Materials	Description/Mixture	Measured thermal conductivity (W/m °C)*
Solid–solid		
Neopentylglycol (NPG)	100%	0.24
Pentaglycerine (PG)	100%	0.36
Solid–liquid		
Magnesium chloride hexahydrate (MCH)	100%	0.62
Sodium sulphate decahydrate (SSD)	100%	0.57
Mixtures (molar ratio)		
NPG–PG	10–90%	0.28–0.32
NPG–SSD	10–30%	0.48–0.52
NPG–MCH	10–30%	0.51–0.55
PG–SSD	10–30%	0.49–0.53
PG–MCH	10–30%	0.50–0.59
Matrix/PCM		
Aluminum/NPG	7%	7.11
Aluminum/NPG	14%	14.77

Adapted from [97].
* Measurement uncertainty of ±10%.

pure ethyl alcohol was poured into the mixture. Then the infrared light was used in order to totally volatilize ethyl alcohol from the mixture. Finally, the infrared light was taken away and the material was cooled to room temperature and grinded into powder. Thermal properties of binary compositions determined by DSC technique are given in Table 42.

It was found that the second phase change peak should be mainly considered in the binary system NPG/PE or NPG/TAM with smaller NPG fractions meanwhile the first peak should be mainly considered when the NPG fraction is larger. When the NPG fraction is larger, it is better to use the second phase change enthalpy in applications which have a working temperature lower than 40 °C, but for the smaller NPG fractions, the first phase change enthalpy is too small, so it is better to use it in applications which have a working temperature higher than 140 °C. The effects of some important factors, such as sealing of the container, adding silicone oil and graphite powder to the mixture and the preparation techniques of the experimental samples are observed. The decrease of the second solid–solid phase change temperature of the binary system of NPG/PE or NPG/TAM is larger than that of PE or TAM, but the decrease of the first solid–solid phase change temperature of the binary system is smaller than that of NPG, which is caused by the bigger change of the force and length of the hydrogen bonds in the binary system. For effective prevention of volatilization of the experimental samples it is preferable to use the method of crystallization from ethyl alcohol during the process of preparation.

Taking into account high potential of using plastic crystal as thermal energy storage, a group of researchers led by D. Chandra [102–104] has investigated heat capacity of PE (99%), PG (99%), NPG (99%), NPA (99%), Tris (99.9%) and AMPL (99%) obtained from the Aldrich Corporation. An ordinary differential scanning calorimeter system as well as modulated DSC was used to make heat capacity measurement. A sapphire crystal supplied by Perkin Elmer Corporation was used to standardize the heat capacities of these phase change materials (PCMs). Specimens (approximately 5 mg each) were used in tightly sealed aluminum sample pans. The results of measurements are presented in Tables 43 and 44.

Witusiewicz et al. [105] studed the binary organic alloy system 2-amino-2-methyl-1,3-propanediol (AMPD) with neopentylglycol (NPG) and measured the temperature and enthalpy of melting of pure compounds by means of differential scanning calorimetry (DSC). The final purity of the AMPL and NPL was assessed by DSC using the Pyris™ Software and was found to be 99.95 wt.%. Experiments and calculations show that the binary AMPD–NPG system exhibits an eutectic reaction with the eutectic point at 378.3 K

Table 41
Thermal properties of plastic crystals with solid–solid transition.

Compound	Formula	Transition temperature (°C)	Transition latent heat (J/g)	Melting point (°C)	Heat of fusion (J/g)
TBN	$(NO_2)C(CH_3)_3$	−13.2	45.0	25.3	24.8
MNP	$(NO_2)(CH_3)_2C(CH_2OH)$	38.3	122.8	90.7	26.6
NPA	$(CH_3)_3C(CH_2OH)$	−37.8	31.6	56.6	28.4
Neopentylglycol	$(CH_3)_2C(CH_2OH)_2$	41.2	119.3	126.6	41.7
Pentaglycerine	$(CH_3)C(CH_2OH)_3$	83.5	174.3	201.2	39.3
TRIS	$(NH_2)C(CH_2OH)_3$	133.6	280.7	169.5	30.5
Pentaerythritol	$C(CH_2OH)_4$	187.5	293.8	266.0	38.2

Adapted from [98,99].

Table 42
Experimental results of performance of solid–solid phase change heat storage of the monophyletic systems of NPG, PE and TAM and binary systems of NPG/PE and NPG/TAM [101].

Material	First transition temperature (°C)	Second transition temperature (°C)	First transition latent heat (J/g)	Second transition latent heat (J/g)
PE	185.4		339.55	
NPG	42.4		119.10	
TAM	132.4		295.61	
$NPG_{0.382}PE_{0.618}$	32.0	169.8	18.17	147.73
$NPG_{0.582}PE_{0.412}$	34.0	160.3	26.20	83.02
$NPG_{0.618}PE_{0.382}$	35.0		33.16	
$NPG_{0.764}PE_{0.236}$	37.0		46.14	
$NPG_{0.854}PE_{0.146}$	37.4		51.50	
$NPG_{0.910}PE_{0.090}$	36.6		68.15	
$NPG_{0.382}TAM_{0.618}$	35.6		27.08	
$NPG_{0.582}TAM_{0.412}$	36.1		43.64	
$NPG_{0.618}TAM_{0.382}$	36.6		62.19	
$NPG_{0.764}TAM_{0.236}$	37.7		75.29	
$NPG_{0.854}TAM_{0.146}$	38.1		121.03	
$NPG_{0.910}TAM_{0.090}$	38.6		143.30	

Table 43
Equations for heat capacities of the polyalcohols and the amines in the α, γ and liquid phases in various temperature ranges [103].

Materials	Phases	Equation	Temperature range
NPA	γ	$Cp_{\gamma} = 1.830(\pm 0.098)T - 329.718(\pm 30.643)$	305–322.5 K
	Liquid	$Cp_{L} = 0.678(\pm 0.018)T + 54.918(\pm 6.507)$	337.5–382.5 K
NPG	α	$Cp_{\alpha} = 1.168(\pm 0.141)T - 162.094(\pm 43.611)$	305–312.5 K
	γ	$Cp_{\gamma} = 0.466(\pm 0.015)T + 110.905(\pm 5.549)$	332.5–390 K
	Liquid	$Cp_{L} = 0.318(\pm 0.070)T + 187.519(\pm 30.144)$	407.5–447.5 K
PG	α-1	$Cp_{\alpha\text{-}1} = 0.654(\pm 0.055)T - 2.698(\pm 17.367)$	305–322.5 K
	α-2	$Cp_{\alpha\text{-}2} = 0.924(\pm 0.055)T - 100.452(\pm 18.469)$	330–347.5 K
	α-3	$Cp_{\alpha\text{-}3} = 1.918(\pm 0.156)T - 444.825(\pm 54.950)$	350–355 K
	γ-1	$Cp_{\gamma\text{-}1} = 0.472(\pm 0.043)T + 138.041(\pm 16.881)$	377.5–412.5 K
	γ-2	$Cp_{\gamma\text{-}2} = 0.460(\pm 0.027)T + 148.751(\pm 11.555)$	415–447.5 K
PE	α-1	$Cp_{\alpha\text{-}1} = 1.253(\pm 0.005)T - 180.015(\pm 1.839)$	307.5–412.5 K
	α-2	$Cp_{\alpha\text{-}2} = 2.154(\pm 0.093)T - 542.564(\pm 39.794)$	415–437.5 K
	α-3	$Cp_{\alpha\text{-}3} = 4.348(\pm 0.228)T - 1501.120\ (\pm 101.390)$	440–450 K
	γ	$Cp_{\gamma} = -0.926(\pm 0.228)T + 913.335(\pm 109.096)$	472.5–485 K
AMPL	α-1	$Cp_{\alpha\text{-}1} = 0.993(\pm 0.049)T - 130.005(\pm(15.431)$	305–322.5 K
	α-2	$Cp_{\alpha\text{-}2} = 0.981(\pm 0.057)T - 134.587(\pm 18.926)$	327.5–337.5 K
	Liquid-1	$Cp_{L\text{-}1} = 0.580(\pm 0.098)T + 119.436(\pm 39.017)$	387.5–412.5 K
	Liquid-2	$Cp_{L\text{-}2} = 0.402(\pm 0.021)T + 204.310(\pm 8.659)$	415–522.5 K
TRIS	α-1	$Cp_{\alpha\text{-}1} = 0.695(\pm 0.056)T - 18.355(\pm 17.700)$	305–322.5 K
	α-2	$Cp_{\alpha\text{-}2} = 0.755(\pm 0.014)T - 48.044(\pm 5.056)$	327.5–387.5 K
	γ	$Cp_{\gamma} = 0.817(\pm 0.105)T + 58.404(\pm 45.690)$	430–440 K

Table 44
The thermal properties of neopentylglycol and some polyalcohol amine derivatives.

Substance	Transition temperature (°C)	Transition latent heat (J/g)	Melting point (°C)	Heat of fusion (J/g)
NPG (neopentylglycol)	38.03	116.40	123.98	40.18
TRMP (trimethylolpropane)	54.6	121.9	59.5	6.7
AMPL (2-amino-2-methyl-1,3-propanediol)	77.90 ± 0.28	223.97 ± 1.51	107.11 ± 0.57	26.20 ± 0.51
TRIS (tris(hydroxymethyl)aminomethane	131.97 ± 0.37	318.38 ± 4.18	167.44	29.52

Adapted from [103,104].

and 42.2 mol% NPG. Thermal properties of neopentylglycol and 2-amino-2-methyl-1,3-propanediol measured in this work are given in Table 45.

The investigations of heat storage performances of NPG (neopentylglycol), TAM (tris(hydroxymethyl)aminomethane), PE (pentaerythritol), and AMPD (aminoglycol) and their mixtures as solid–solid phase change materials for solar energy applications, conducted by Gao et al. [106] with using DSC technique, gave very important results. It was found that pure AMPD was not suitable for practical applications due to its wide ranges of charge and discharge temperatures and its high hygroscopic property. The specific sample preparation process has significant impact on the heat storage performance of the mixtures of polyalcohols. If the experimental samples are prepared with the proper processes, there will usually be only one peak presented in the DSC curves instead of two peaks, as reported by some studies. Due to the poor heat storage performance and high hygroscopic property of AMPD, the binary mixtures of AMPD/NPG and AMPD/TAM do not have practical application values. At the same time, the binary mixtures of AMPD/PE with a high or low weight ratio of AMPD still are found to have potential practical application values. The experimental results also showed that a mixture of more than two polyalcohols does not have better performance than a binary mixture.

Tong et al. [107] measured the low-temperature heat capacity $C_{p,m}$ of 2-amino-2-methyl-1,3-propanediol (AMPL) in the temperature range from 78 to 405 K by adiabatic calorimetry. The temperatures and the molar enthalpies of solid–solid and solid–liquid phase transitions were determined to be 78.45 °C, 24.33 ± 0.02 kJ/mol (234 J/g) and 107.48 °C, 4.01 ± 0.01 kJ/mol (38.1 J/g), respectively. The thermal stability of the compound was investigated by DSC and TG techniques.

The employees of the German company Gally et al. [108] disclosed a set of dialkyammonium salts with high enthalpy of solid–solid transitions (see Table 46). Thermal transition parameters were determined by using DSC techniques. The majority of the offered compounds have undergone subcooling. In some cases, the subcooling may be sufficient (up to 28 °C). Moreover, the enthalpy of solid–solid transition in cooling mode is less than in heating of the compounds with deep supercooling (Table 46).

In the next work [109], the group of researchers from Merck KGaA continued the investigation of a series of symmetrical dialkyl ammonium salts, DC_nX. They have prepared and characterized DC_nX with regard to the temperature and enthalpy of solid–solid phase transitions, temperature of melting, thermal stability as well as the reversibility of the phase transitions. The number of carbon atoms, C_n varied between 8 and 18 and anions X halides, nitrate,

Table 45
Thermal properties of NPG and AMPD.

Substance	Transition temperature (°C)	Transition latent heat (J/g)	Melting point (°C)	Heat of fusion (J/g)
NPG (neopentylglycol)	48.8	116.8	130.0	42.5
AMPD (2-amino-2-methyl-1,3-propanediol)	79.7	226.2	103.3	26.1

Adapted from [105].

Table 46
Some dialkylammonium salts with solid–solid phase transitions.

Amine	Acid	Heating transition onset temperature (°C)	Heating transition latent heat (J/g)	Cooling transition onset temperature (°C)	Cooling transition latent heat (J/g)	Subcooling (°C)	Melting point (°C)
Dihexylamine	Nitric acid	10	110	−8	90	18	>100
Dioctylamine	Chloric acid	14	112	14	122	0	>100
Dioctylamine	Acetic acid	36	177	20	163	16	46
	Nitric acid	44	154	26	144	18	>100
Dioctylamine	Formic acid	45	145	17	127	28	>100
Didecylamine	Hydrogen chloride	49	117	43	113	5	>100
Didecylamine	Chloric acid	54	140	41	131	13	>100
Didodecylamine	Chloric acid	54	168	47	155	7	>100
Didodecylamine	Formic acid	56	156	45	145	11	87
Didecylamine	Hydrogen bromide	56	102	50	100	6	>100
Didecylamine	Nitric acid	57	153	44	149	13	>100
Didecylamine	Acetic acid	58	151	53	140	5	68
Didodecylamine	Acetic acid	64	178	63	163	1	76
Didodecylamine	Hydrogen chlor	65	132	60	127	5	>100
Didodecylamine	Propeonic acid	66	169	66	164	1	73
Didecylamine	Formic acid	67	161	46	148	21	79
Didodecylamine	Nitric acid	69	160	62	161	7	>100
Didodecylamine	Nitrogen bromide	78	124	65	119	6	>100

Adapted from [108].

chlorate, perchlorate and hydrogen sulphate had been chosen. The measurement results obtained by using DSC techniques are given in Table 47. As seen from the table, with dependence on chain length and anion type, the transition temperatures are varied from 20 to 100 °C. The large difference between melting and transition temperatures was found. This factor is very important for solid–solid transition materials, which can be used as phase change thermal energy storage materials. The most important factor is high mass specific solid–solid transition enthalpies reaching values of 185 J/g, which makes this class of substances attractive for heat storage applications.

5.2. Organo-metallic form-stable materials with solid–solid phase change

The research group from Instituto Chimico at the University of Naples (Italy) was the first scientific group which began the wide and systematic investigations of chemical and thermal properties of organo-metallic salts [110–136]. Due to the authors' limited access to the early papers published in Italian scientific journals as well as in other journals, we consider only the most important results of these researchers, which were summarized in some international journals.

In 1975 Landi and Vacatello [127] presented the results of their studies on order–disorder solid–solid phase transitions in some alkylammonium tetrachlorometallates (Table 48). All the compounds were recrystallized twice from absolute ethanol. The synthesis of the Fe(II) compounds was performed in absence of oxygen, and the resulting tetrachloroferrates were handled in nitrogen atmosphere. The crystals of the Fe(II) salts are pale yellow platelets, while those of the Hg(II) and Zn(II) salts are white platelets. The thermal behavior has been examined by means of a Perkin Elmer DSC-1 differential scanning calorimeter. All the observed transitions were reproducible both in temperature and enthalpy after heating and cooling cycles throughout transition temperatures, with exception of the Fe(II) salts, whose behavior was somewhat different. When a sample is heated above 200 °C the transition peaks at lower temperatures became broad and difficult to analyze. The total reproducibility was observed in samples not heated above 200 °C. All solid–solid transitions in the temperature

Table 47
Thermal characteristics of some dialkylammonium salts.

Compound	Transition temperature (°C)	Transition latent heat (J/g)	Melting point (°C)	Difference between melting and transition temperatures (°C)
DC_8Cl[a]	21	132	247	226
DC_8ClO_4	23	108	266	243
DC_8ClO_4	32	122	171	139
DC_8NO_3[a]	45	176	190	145
$DC_{10}Cl$	48	119	228	180
$DC_{10}ClO_3$	55.5	154	178	123
$DC_{10}Br$	57	100	243	186
$DC_{10}NO_3$	60	179	181	121
$DC_{12}ClO_3$[a]	61.5	159	165	104
$DC_{12}ClO_4$[a]	62	159	260	198
$DC_{12}Cl$[b]	65	123	208	142
$DC_{12}NO_3$	66	185	174	108
$DC_{12}Br$[a]	73	113	227	154
$DC_{18}ClO_4$[a]	88.1	185	230	122
$DC_{18}Cl$[b]	91.2	174	177	86
$DC_{18}I$[b]	93	116	194	101
$DC_{18}NO_3$[a]	93.5	186	147	54
$DC_{18}Br$[b]	98	135	188	90

Adapted from [109].
[a] Heating rate: 2 K/min.
[b] Heating rate: 5 K/min.

Table 48
Thermal properties of some organo-metallic compounds.

Alkylammonium tetrachlorometallate	Molar weight	Type of transition	Heating		Cooling	
			Transition temperature (°C)	Latent heat of transition (J/g)	Transition temperature (°C)	Latent heat of transition (J/g)
$(C_{12}H_{25}NH_3)_2MnCl_4$	569.47	Solid–solid	45	68.5	39	68.5
$(C_{12}H_{25}NH_3)_2CuCl_4$	578.08	Solid–solid	47	72.6	41	72.6
$(C_{12}H_{25}NH_3)_2CoCl_4$	573.47	Solid–solid	90	78.5	69	83.7
		Solid–liquid	166	13.8	159	14.3
$(C_{12}H_{25}NH_3)_2ZnCl_4$	579.92	Solid–solid	90	79.3	72	87.9
		Solid–liquid	166	12.4	157	15.0
$(C_{12}H_{25}NH_3)_2HgCl_4$	715.13	Solid–solid	52	37.7	43	37.7
		Solid–liquid	202	49.2	196	49.2
$(C_{12}H_{25}NH_3)_2FeCl_4$	570.38	Solid–solid	46	77.1	33	75.4
		Solid–liquid	202	70.1	192	70.3
$(C_{16}H_{33}NH_3)_2MnCl_4$	681.69	Solid–solid	72	88.0	65	82.1
		Solid–solid	91	16.1	88	17.6
$(C_{16}H_{33}NH_3)_2CuCl_4$	690.30	Solid–solid	72	52.1	66	56.5
		Solid–solid	81	10.9	73	14.0
		Solid–solid	87	20.3	83	20.3
$(C_{16}H_{33}NH_3)_2CoCl_4$	685.69	Solid–solid	105	113.7	85	112.3
		Solid–liquid	171	11.7	165	11.2
$(C_{16}H_{33}NH_3)_2ZnCl_4$	692.13	Solid–solid	103	106.9	88	112.7
		Solid–liquid	163	11.1	158	11.7
$(C_{16}H_{33}NH_3)_2HgCl_4$	827.34	Solid–solid	81	58.0	71	58.0
		Solid–liquid	196	31.4	190	31.4
$(C_{16}H_{33}NH_3)_2FeCl_4$	682.60	Solid–solid	71	79.1	56	79.1
		Solid–solid	94	17.6	80	17.6
		Solid–liquid	192	57.1	186	58.6

Adapted from [127].

range 25–100 °C were revealed by microscopic observations, while transitions around 170 °C for cobalt and zinc compounds and transitions around 200 °C for Fe and Hg compounds correspond to the melting, giving in all the cases liquid-crystalline materials which become isotropic around 260 °C. Slow decomposition was, however, observed in all the cases in the range of stability of the liquid-crystalline phases, the decomposition rate increasing rapidly with increasing temperature, so that no reliable enthalpic data on the liquid crystal-isotropic transitions could be obtained.

In the next works, the grope of scientists at the University of Naples [121,123] prepared and studied behaviors of organo-metallic salts such as $(C_nH_{2n+1}NH_2)_2ZnCl_2$ and $(C_nH_{2n+1}NH_2)_2CuCl_2$. Compounds were prepared by mixing hot ethanolic solutions of zinc (copper) chloride and alkylamine in the molar ratio 1:2. After boiling for 5 min, the resulting solutions were allowed to cool to room temperature, the white precipitates filtered and recrystallized twice from absolute ethanol and dried in vacuum. The thermograms of all the compounds were registered between 190 and 470 K on a Perkin-Eimer DSC-I apparatus at the scanning rate of 8 K/min in nitrogen atmosphere. Pure reference compounds were used to calibrate the temperature scale. Transition enthalpies were obtained with using a weighed sample of indium (ΔH_m = 28.5 J/g) as a reference standard. The reported transition enthalpies represent mean values of several measurements on independent samples. The standard deviation is in the order of 5% for each set of measurements. The results of measurements are presented in Tables 49 and 50. Comparison of thermal properties of salts considered with behaviors of akrylammonium tetrachlorometallates shows that the enthalpy of solid–solid transition in the first type of compounds is less or compatible with heat of fusion while in the latter type this value is sufficiently more than in the first type.

In the paper published in 1980 [120], the researchers from the University of Naples summarized the results of previous investigations of the whole class of compounds $(C_nH_{2n+1}NH_3)_2MCl_4$ where M is divalent metal atom and $8 \le n \le 18$. These compounds were termed “layer perovskites” because of M = Mn, Cu, Hg, Fe and their structure resembles that of the mineral Perovskite, $CaTiO_3$. From the general formula given above, it can be inferred that the hydrocarbon regions of the layer perovskites consist of long chain alkylammonium groups ionically bonded to an inorganic support. These linear alkyl chains are the origin of the peculiar thermal behavior of the perovskite compounds. Transition thermal parameters for perovskite compounds determined by Busiko et al. are shown in Table 48. As seen from the table, the compounds are characterized by high enthalpy reversible

Table 49
Thermal properties of some organo-mettallic compounds.

Organo-metallic salt	Molar weight	Transition temperature (°C)	Transition latent heat (J/g)	Melting point (°C)	Heat of fusion (J/g)
$(C_{10}H_{21}NH_2)_2CuCl_2$	449.05	79	47.0	133	96.2
$(C_{12}H_{25}NH_2)_2CuCl_2$	505.16	79	35.8	132	99.4
$(C_{14}H_{29}NH_2)_2CuCl_2$	561.27	104	51.8	131	103.7
$(C_{16}H_{33}NH_2)_2CuCl_2$	617.37	103	66.6	129	105.6
$(C_{18}H_{37}NH_2)_2CuCl_2$	673.48	109	78.7	127	104.0

Adapted from [121].

Table 50
Thermal properties of some organo-mettallic compounds.

Organo-metallic salt	Molar weight	Transition temperature			Melting point (°C)	Transition latent heat			Heat of fusion (J/g)
		First (°C)	Second (°C)	Third (°C)		First (J/g)	Second (J/g)	Third (J/g)	
$(C_6H_{13}NH_2)_2ZnCl_2$	338.68	−4	154		167	3.9	25.2		41.6
$(C_8H_{17}NH_2)_2ZnCl_2$	394.79	−23	28		149	3.0	48.4		50.9
$(C_{10}H_{21}NH_2)_2ZnCl_2$	450.89	−38	3	31	144	4.0	12.0	4.2	49.0
$(C_{12}H_{25}NH_2)_2ZnCl_2$	507.00	4	62–70		140	2.6	55.4		47.5
$(C_{14}H_{29}NH_2)_2ZnCl_2$	563.11	69–78			134	64.1			46.3
$(C_{16}H_{33}NH_2)_2ZnCl_2$	619.22	37	78–95		131	1.8	69.7		47.0

Adapted from [123].

solid–solid phase transitions in the temperature range 0–100 °C. Thermal and structural studies conducted previously showed that these phase changes involve the hydrocarbon regions only, leaving the inorganic layers quite unchanged, and consist mainly in the transition of the linear alkyl chains from conformationally ordered state, in which the carbon–carbon skeletal bonds are a planar zig-zag sequence, to a disordered one, in which the chains gain a conformational freedom comparable with that they would have in the melt. The compounds considered are chemical stable up to 200 °C and have notable transition latent heat. Therefore they were suggested for storing solar energy Table 51.

Li et al. [137] synthesized a series of bis(n-alkylammonium) tetrachlorometallates and studied their solid–solid phase transitions using DSC and IR technique. $M(II)Cl_2$ (M = Cu, Zn, Hg, Mn, Co, Ni), HCl alkylamine and absolute ethanol used here were analytical reagents. Perovskite compounds were obtained as platelets by mixing hot ethanolic solutions of chlorides of metals, HCl and alkylamine in a 1:2:2 molar ratio. The solutions were concentrated by boiling, then allowed to cool to room temperature and filtered. The products were recrystallized twice from absolute ethanol. The results of DSC analysis are given in Table 52. As seen from the table, transition temperatures of C_nM_n, C_nCo, C_nZn and C_nCu lie between

Table 51
Thermal properties of some alkylammonium tetrachlorometallates ($(n\text{-}C_nH_{2n+1}NH_3)_2MCl_4$).

Metall	*n*	Transition temperature (°C)			Melting point (°C)	Transition latent heat (J/g)			Heat of fusion (J/g)
		First	Second	Third		First	Second	Third	
Co	9	72			160	51.1			11.8
	10	82			165	71.6			13.7
	11	85			164	65.9			13.8
	12	90			166	78.7			13.8
	13	90			164	79.7			11.0
	14	97			167	93.3			10.3
	15	44	100		168	3.3	79.0		10.2
	16	105			171	113.8			11.7
	17	52	105		170	15.4	101.1		85.0
Mn	9	14				63.1			
	10	35				68.0			
	11	43				85.6			
	12	45				69.3			
	13	58	70			87.5	12.6		
	14	66	78			81.6	14.2		
	15	67	89			95.9	15.8		
	16	72	91			87.8	16.6		
	17	76	80	100		90.1	14.1	20.3	
Cu	9	15				52.7			
	10	33				53.5			
	11	40				70.4			
	12	47				72.9			
	13	60	71			79.6	16.5		
	14	65	75			66.8	17.2		
	15	70	85			81.8	17.8		
	16	72	81	87		52.1	12.1	20.2	
	17	79	88	95		75.4	12.4	20.5	
Hg	8	41				10.9			
	9	19	30			9.3	9.7		
	10	45				27.8			
	11	50			203	29.0			36.0
	12	59			202	39.0			34.5
	13	67			200	46.6			38.4
	14	73			198	47.2			34.4
	15	80			197	51.7			37.4
	16	81			195	51.7			33.1
Fe	12	46			202	77.2			70.3
	16	71	94		192	78.8	17.9		57.1
Zn	12	90			166	81.1			12.7
	16	103			163	108.8			11.3

Adapded from [120].

Table 52
Thermal properties of some bis(n-alkylammonium) tetrachlorometallates.

Bis(n-alkylammonium) tetrachlorometallates	Molar weight	Transition temperature			Melting point (°C)	Transition latent heat			Heat of fusion (J/g)
		First (°C)	Second (°C)	Third (°C)		First (J/g)	Second (J/g)	Third (J/g)	
$(C_{10}H_{21}NH_3)_2CuCl_4$	521.97	33.77	36.91			55.1	7.51		
$(C_{10}H_{21}NH_3)_2ZnCl_4$	523.82	80.14			162.79	82.8			18.1
$(C_{10}H_{21}NH_3)_2MnCl_4$	513.36	32.80				70.3			
$(C_{10}H_{21}NH_3)_2CoCl_4$	517.36	77.71				74.3			
$(C_{12}H_{25}NH_3)_2CuCl_4$	578.08	52.54	59.07			59.1	11.0		
$(C_{12}H_{25}NH_3)_2ZnCl_4$	579.92	88.23			155.95	104.9			15.3
$(C_{12}H_{25}NH_3)_2MnCl_4$	569.48	54.05	56.42			74.2	6.6		
$(C_{12}H_{25}NH_3)_2CoCl_4$	573.47	60.71	87.97			33.7	59.96		
$(C_{16}H_{33}NH_3)_2CuCl_4$	690.30	72.8	81.59	96.02		57.1	8.0	14.6	
$(C_{16}H_{33}NH_3)_2ZnCl_4$	692.13	99.13			160.49	125.3			12.2
$(C_{16}H_{33}NH_3)_2MnCl_4$	681.69	73.13	90.96			87.6	16.9		
$(C_{16}H_{33}NH_3)_2CoCl_4$	685.69	93.42	99.70			10.6	104.2		13.8

Adapted from [137].

55.1 and 125.3 °C. They are potential thermal energy storage materials. C_nNi, C_nCd, C_nHg were found unsuitable for thermal storage use, because C_nNi has poor thermal stability; moreover, C_nCd and C_nHg has lower latent heat for these application in the low temperature.

A novel solid–solid phase change heat storage material developed by Li and Ding [138] was prepared via the two-step condensation reaction of high molecule weight polyethylene glycol (PEG 10000) with pentaerythritol (PE) and 4,40-diphenylmethane diisocyanate (MDI). Fourier transforms infrared spectroscopy (FT-IR), differential scanning calorimetry (DSC), thermogravimetric analyses (TGA), polarization optical microscopy (POM) and wide-angle X-ray diffraction (WAXD) measurements were employed to investigate their ingredients, thermal properties and crystalline behaviors. The results showed that PEG/MDI/PE tertiary cross-linking copolymer had typical solid–solid phase transition property, high enthalpy reaching 152.97 J/g and suitable transition point at 58.68 °C. The thermal resistance of PEG/MDI/PE copolymer was improved by the introduction of rigid phenyl groups and crosslinked groups. Initial decomposition temperature increased by about 17 °C, compared with pristine PEG 10000. Furthermore, the PCM still kept solid state when heated to 150 °C for the cross-linking structure that restricted the soft segment's free movement at high temperature. So it is obvious that the novel solid–solid PCM will be a promising heat storage material and have a very wide application.

6. Microcapsulated form-stable materials

Having considered the paraffin leakage and lipophilicity, Liu with colleagues [139,140] encapsulated form-stable PCMs composed of 80 wt.% paraffin and 20 wt.% HDPE into inorganic silica gel polymer by *in situ* polymerization. A differential scanning calorimeter (DSC) is used to measure the thermal properties of the PCM. Moreover, the Washburn equation associated with the wetting properties of powder materials is used to test the hydrophilic–lipophilic properties of PCM. The results of these tests are given in Table 53. From the table it can be concluded that the higher the mass percentage of the silica gel as coating material is, the better the hydrophilicity of the microencapsulated PCMs. To obtain better hydrophilicity, the relevant enthalpy has to be reduced accordingly. The experiments demonstrated that when the mass percentage of paraffin is 62.35 wt.%, the slope of the Washborn equation is only 0.23 cm^2/min and is nearly zero, and most of the form-stable materials are not encapsulated. When the mass percentage is 55.76 wt.%, there is a flex point on the curve of the slope, and the value is 3.36 cm^2/min. The hydrophilicity is good enough to meet demands of the architecture field. After all optimal

Table 53
Thermal properties of microcapsulated PCMs containing paraffin.

Number	Weight percentage of paraffin (%)	Melting point (°C)	Specific enthalpy (J/g)	Slope of the Washburn equation (cm^2/min)
1[a]	0.00		0.00	6.34
2	11.23	19.56	24.14	5.85
3	20.35	19.88	45.17	5.43
4	24.39	19.20	54.14	5.32
5	27.32	18.55	60.67	5.12
6	32.09	19.38	71.23	4.95
7	37.54	22.60	83.34	4.82
8	39.08	22.03	86.76	4.74
9	44.40	22.43	98.59	4.56
10	46.43	20.21	103.07	4.32
11	53.54	22.33	118.62	3.73
12	55.76	21.50	123.78	3.36
13	58.64	21.32	130.19	2.46
14	62.35	21.34	138.42	0.23
15	69.12	22.01	153.46	0.03
16[b]	79.31	22.26	176.07	0.00
17[c]	100.00	17.08	222.1	0.00

Adapted from [139,140].

[a] Sample of blank test.
[b] Form-stable phase change material of 79.39 wt.% paraffin.
[c] Refined paraffin.

Table 54
The thermal properties of PEG powder and electrospun PEG/CA composite fibers before and after 100 heating–cooling cycles [141].

Sample	Melting point (°C)	Heat of fusion (J/g)	Freezing point (°C)	Heat of freezing (J/g)
PEG powder	64.18	177.38	37.72	167.75
Cycled PEG powder	62.14	158.90	36.96	155.38
PEG/CA fibers	58.47	86.03	38.96	65.15
Cycled PEG/CA fibers	57.59	85.91	38.23	64.95

products with melting point 21.5 °C and heat of fusion 123.78 J/g containing about 56 wt.% paraffin are proposed to be used in the building field.

7. Electrospun form-stable materials

Chen et al. [141] prepared ultrafine fibers of polyethylene glycol/cellulose acetate (PEG/CA) composite using electrospinning technique. PEG acts as a model phase change material (PCM) and CA acts as a matrix. An appropriate amount of cellulose acetate (CA, M_n = 29 kg/mol, degree of substitution, DS = 2.45, Aldrich) was dissolved in N,N-dimethylacetamide (DMAc) and acetone mixture (DMAc/acetone = 1/2, w/w) at a concentration of 15 wt.%. PEG (M_n = 10 kg/mol, Guangzhou Chemical Agent Company, China) was added to the CA solution (PEG/CA = 1/1, w/w) under constant stirring for 2 h. The morphology observation from the electrospun PEG/CA composite fibers revealed that the fibers were cylindrical and had a smooth external surface. PEG was found to be both distributed on the surface and within the core of the fibers. The thermal properties of the composite fibers were determined by DSC analysis and are presented in Table 54. Typical DSC curves of PEG and PEG/CA composition are shown in Fig. 27. The results indicated that the thermo-regulating function and the thermal properties of fibers were reproducible after 100 heating and cooling cycles. At the same time it should be noted the electrospun PEG/CA composite is characterized by the shortage such as thermal hysteresis in phase change temperature and latent heat.

Chen et al. [142] have prepared the ultrafine fibers based on the composites of polyethylene terephthalate (PET) and a series of fatty acids, lauric acid (LA), myristic acid (MA), palmitic acid (PA), and stearic acid (SA) via electrospinning as form-stable phase change materials (PCMs). LA, MA, PA, and SA were purchased from Bodi Chemical Reagent Co., Ltd. China. Dichloromethane (DCM) and trifluoroacetic acid (TFA) were purchased from Sinopharm Group Chemical Reagent Co., Ltd. China (both are analytical reagent grade). PET (M_n = 20,000 g/mol) was donated by Zhejiang Xiangsheng Group Co., Ltd. China. All received chemicals were used without further purification.

The solutions including 15 wt.% PET was prepared by adding PET in a 2/1 volume ratio of DCM/TFA mixture. The PCM samples were prepared with fatty acid while adding to PET solution with different fatty acid/PET mass ratios from 50 to 150 wt.%. These mixtures were separately stirred for 1 h. Electrospinning was performed at 20 °C in air and using a homemade equipment. During the electrospinning, each of the prepared solutions was placed in a 5 ml syringe and was fed by a syringe pump at a rate of 3 ml/h. The metallic needle (0.8 mm diameter) was connected to the power supply BPS-20 with a fixed voltage at 16 kV. An aluminum flat sheet was grounded and used as the collector. The distance between the needle and the collector was fixed at 20 cm. The fibers were randomly deposited on the collector to form fibrous non-woven fiber mats. The fiber mats were dried in vacuum at room temperature for 24 h to remove residual solvent.

The morphology and thermal properties of the composite fibers were studied by means of field emission scanning electron microscopy (FE-SEM) and differential scanning calorimetry (DSC). It was found that the average fiber diameter increased generally with the content of fatty acid (LA) in the LA/PET composite fibers. The fibers with the low mass ratio maintained cylindrical shape with smooth surface while the quality became worse when the mass ratio was too high (more than 100/100). The results of DSC analyses are shown in Figs. 28 and 29. As seen from the charts, the latent heat of the composite fibers was increased with the growth of LA content and the phase transition temperature of the fibers has no obvious variations compared with LA. It indicates that the PCM/polymer mass ratio plays an important role in the latent heat of the form-stable PCM/polymer composite fibers, but has less effect on their phase change temperature. In contrast, both the latent heat and phase transition temperature of the fatty acid/PET composite fibers varied with the type of the fatty acids, and could be well maintained after 100 heating–cooling thermal cycles, which demonstrated that the composite fibers had good thermal stability and reliability. Therefore, the electrospun fatty acids/PET composite fibers are promising in serving as form-stable PCMs for thermal energy storage.

In the next paper Chen et al. [143] has developed ultrafine fibers of PCM/polymer composites as a novel shape-stabilized

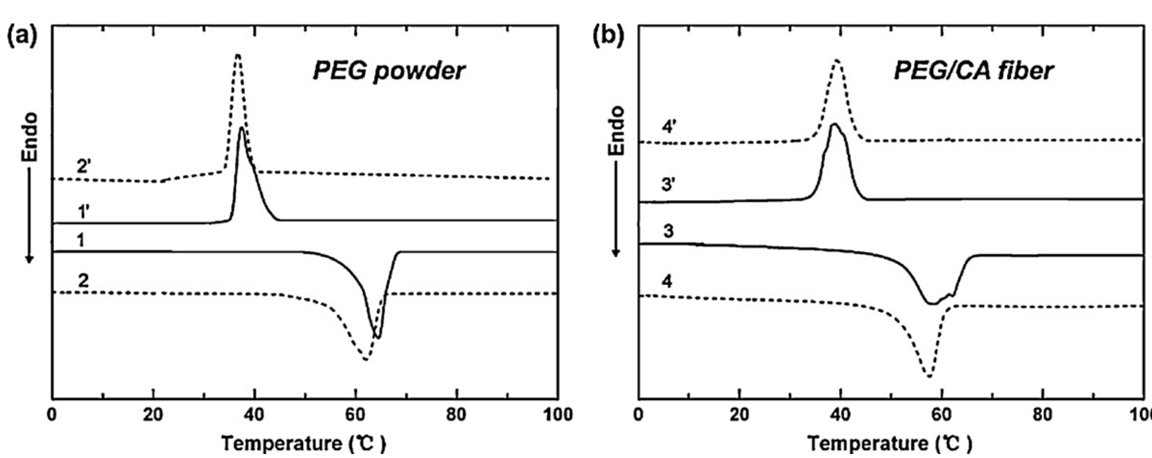


Fig. 27. DSC curves of (a) PEG powers and (b) the electrospun PEG/CA composite fibers before (solid line) and after (dashed) 100 heating cooling cycles [141].

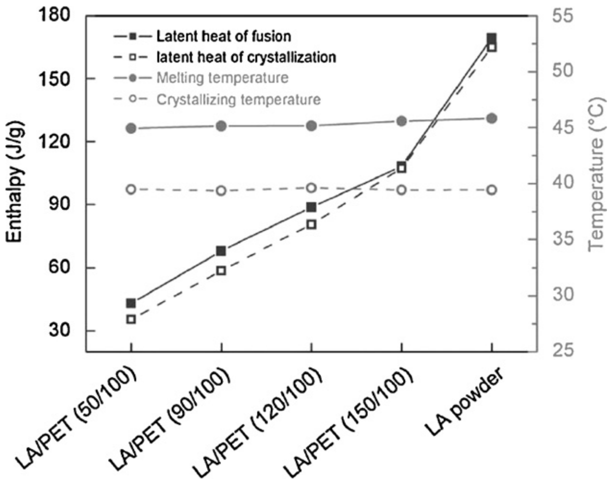


Fig. 28. The latent heat and phase transition temperature of LA powder and LA/PET composite fibers with different mass ratios [140].

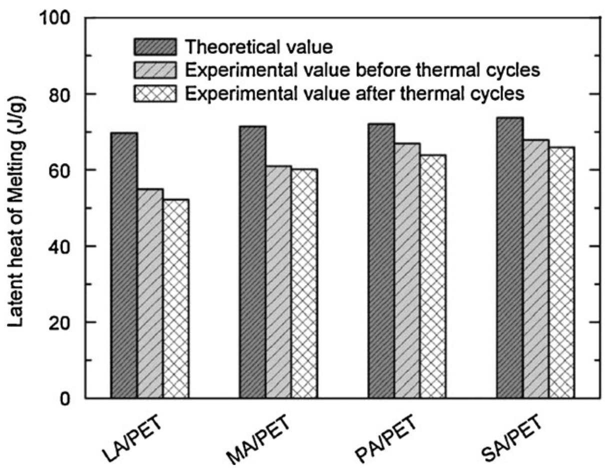


Fig. 29. Theoretical and experimental values of enthalpy of the four types of electrospun fatty acids/PET (70/100) composite fibers before and after 100 heating–cooling cycles [142].

polymer-matrix phase change material (PCM) via electrospinning technique. Ultrafine fibers of lauric acid/polyethylene terephthalate (LA/PET) composite (1:1, w/w) prepared were characterized by field-emission scanning electron microscopy (FE-SEM),

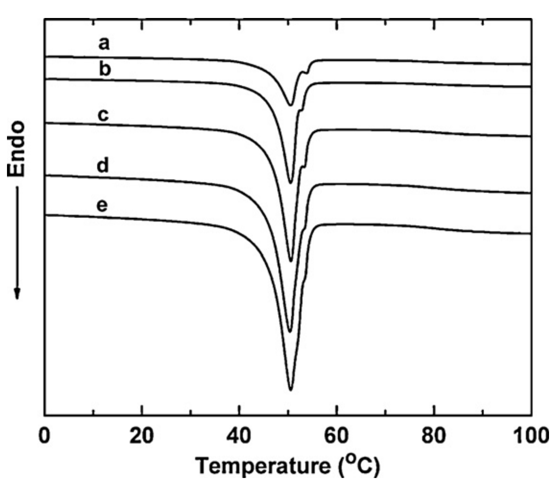


Fig. 30. DSC curves of electrospun SS/PET composite fibers with different mass ratios: (a) 10/100; (b) 20/100; (c) 30/100; (d) 40/100 and (e) 50/100 [144].

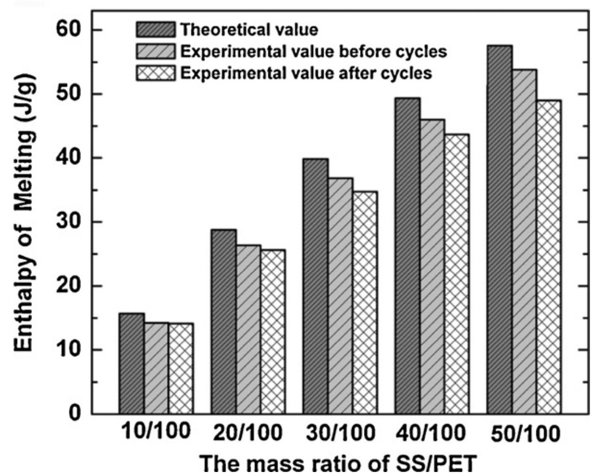


Fig. 31. Theoretical and experimental values of enthalpy of electrospun SS/PET composite fibers before and after thermal cycles [144].

differential scanning calorimetry (DSC) and tensile testing. The electrospun fibers had cylindrical shape with smooth surface and the average fiber diameter was about 710 nm. The composite fibers also showed high latent heat of melting and crystallization, which was 70.76 and 62.14 J/g, respectively. The prepared composite fibers were melted at 45.14 °C and crystallized at 38.57 °C.

Another novel form-stable phase change material was prepared by Chen et al. [144] using two-step procedure. In the first stage, the stearyl stearate (SS) was synthesized by esterification of stearyl alcohol and stearic acid. Then the ultrafine composite fibers of SS/polyethylene terephthalate (PET) were prepared via electrospinning. The structure of SS, morphology and thermal properties of SS/PET composite fibers were characterized by FI-IR, FE-SEM and DSC, respectively. Thermal properties of SS measured by DSC technique are given in Table 55. The average diameter of SS/PET composite fibers measured from the SEM images increased gradually with the growth of SS percentage, and the morphology of the composite fibers had no obvious variation after thermal treatened, which confirmed the developed material had the feature of form-stable phase change. The results from DSC (see Figs. 30 and 31) showed that the enthalpy of the composite fibers increased with the rise in SS content, but the variation of SS percentage in the composite fibers had insufficient influence on phase transition temperature of the fibers. In addition, the thermal performances of the fibers could be maintained well after 100 heating–cooling thermal

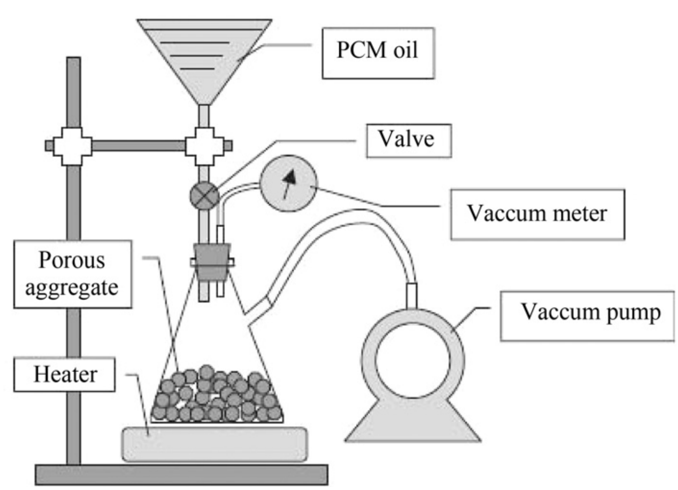


Fig. 32. Schematic drawing of the vacuum impregnation setup [146].

Table 55
The thermal properties of stearyl stearate before and after thermal cycles [142].

Sample	Melting point (°C)	Heat of fusion (J/g)	Freezing point (°C)	Heat of freezing (J/g)
Original	55.1	172.7	49.7	175.0
Thermal cycled	52.9	159.0	48.3	157.3

Table 56
The thermal properties of the original and the crosslinked electrospun PEG/CA composite fibers before and after 100 heating–cooling cycles [145].

Sample	Melting point (°C)	Heat of fusion (J/g)	Freezing point (°C)	Heat of freezing (J/g)
Original	58.47	86.03	38.96	65.15
Cycled original	57.59	85.91	38.23	64.95
Crosslinked	52.14	36.79	40.99	25.92
Cycled crosslinked	52.12	36.72	40.98	25.85

cycles, which indicated that the composite fibers had good thermal stability and reliability.

In order to further improve the thermal stability sequel as well as the water-resistant ability (because PEG is water soluble polymer) of the electrospun PEG/CA composite fibers which were developed before [139], the surface of fibers were crosslinked by Chen et al. [145] using toluene-2,4-diisocyanate (TDI) as a crosslinking agent. The morphology and the thermal properties of the crosslinked fibers were investigated using scanning electron microscopes (SEM), differential scanning calorimeter (DSC) and thermogravimeter (TG), respectively. Electrospun PEG/CA composite fibers (~0.1 mm thickness) were immersed in 10 wt.% TDI/toluene solution at 40 °C. And then the catalyst, dibutyltin dilaurate (1 wt.%, respect to TDI), was dropped to the solution. After 4 h the fibers filtered from the reaction system were Soxhlet extracted with ether for 24 h and dried under vacuum at 30 °C for 24 h. It was found that the crosslinking enhanced the water-resistant ability and the thermal stability of fibers. Simultaneously, there is a significant drop in phase change temperature and latent heat and improving thermal stability of the the results of DSC analysis given in Table 56.

8. Form-stable materials on the bases of expanded materials as structure material

In order to enhance heat storage capacity in concrete products, Zhang et al. [146] put forward a two-step procedure to produce thermal energy storage concrete (TESC). First, a phase change composition (PCC) was made from porous aggregates and liquid PCM by vacuum impregnation. Then, thermal TESC was produced using PCC, Portland cement, and other raw materials. Butyl stearate with melting point 18 °C was used as phase change material. Porous aggregates, including one kind of expanded shale aggregate and two kinds of expanded clay aggregates, were used as supporting materials of PCM. The characteristics of porous aggregates used are shown in Table 57. The porosity of these materials is high and varies from 34 to 75%. It was very difficult for them to absorb large quantity of liquid (water) by simple immersion. The main reason is that the pore space of the aggregates was blocked up with the air, which prevented liquid from entering the pore space. If the air in the inner pores of the porous materials is evacuated before immersion, the aggreates can absorb large quantity of liquid. As shown in the fifth column of Table 57, up to 72.5% of water was absorbed by the porous aggregates after vacuum evacuation. In the PCM absorption process of porous aggregates, the vacuum evacuation setup (Fig. 32) was used. The results of the measurement of thermal properties of the concretes under investigation are shown in Fig. 33. TESC was made from Portland cement, sand, TESAs and water. For comparison, normal concrete and concrete with plain porous aggregates were also prepared. OC1, OC2, and OS were used to denote concretes made with TESAs that are C1, C2, and S porous aggregates with incorporation of PCM. The present experiments showed that the PCM can penetrate into pore space with diameter of 1–2 μm and occupy up to 75% of the total pore space of the porous materials. As seen from the results of DSC test, the thermal energy storage capacity of TESC produced by the two-step method is comparable with that of one commercially available PCM product. This means that the two-step method proposed in this paper is feasible and has potential application in the field of building energy conservation.

In the next paper Zhang et al. [147] presented the results of developing the composite materials with using porous materials such as: the expanded fly ash granules (FL), expanded clay granules of small size (SZ), expanded clay granules of large size (SL),

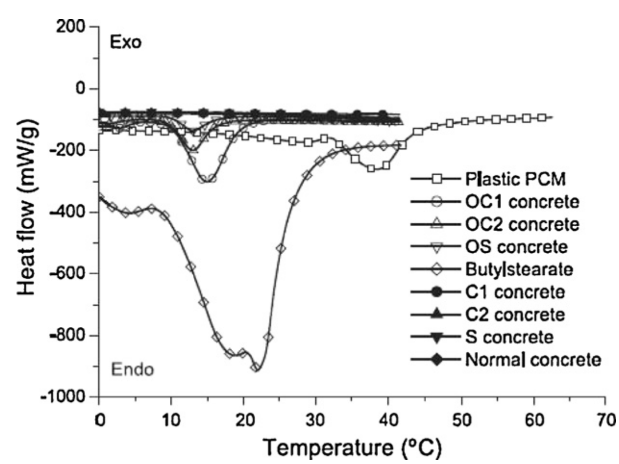


Fig. 33. DSC curves of different materials [146].

Table 57
Basic properties of porous materials.

Porous aggregate	Density (g/cm^3)	Porosity (MIP) (%)	Water-absorbing capacity by simple immersion (%)	Water-absorbing capacity by vacuum impregnation (%)	PCM-absorbing capacity (%)
Superlite clay aggregate – C1	0.76	75.6	11.0	72.5	68.0
Normal clay aggregate – C2	1.25	41.9	5.9	42.5	15.0
Shale aggregate – S	1.39	33.8	4.1	15.0	6.7

Adapted from [146].

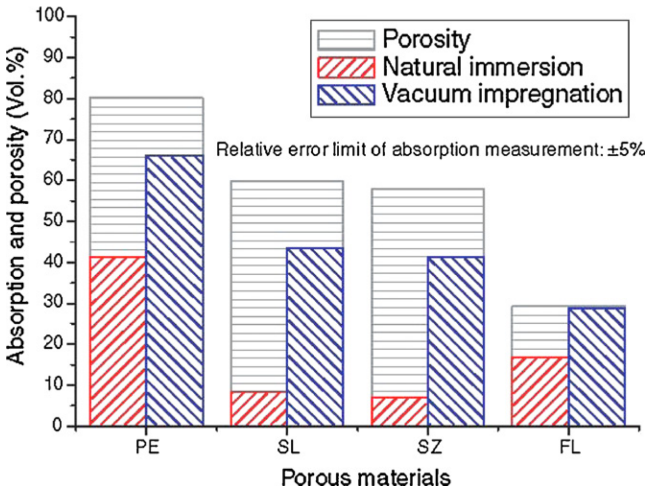


Fig. 34. Comparison between vacuum impregnation and natural immersion [147].

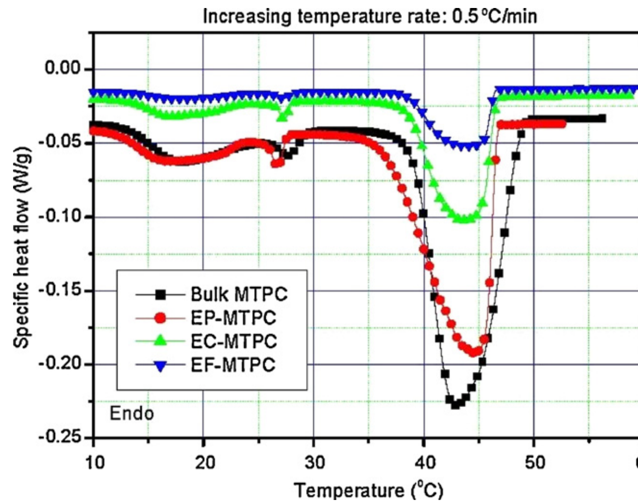


Fig. 35. DSC curves of MTPC confined in porous materials and bulk MTPC [148].

and expanded perlite granules (PE). The average diameter of porous granules was for FL 10 mm, SZ 3 mm, SL 10 mm and PE 2 mm, respectively. The procedure of vacuum impregnation was similar that in [146]. The lauric acid was used as phase change material. As follows from the results of DSC test, the thermal energy storage capacity of TESC produced by the two-step method is comparable with that of one commercially available PCM product. This means that the two-step method proposed in this paper is feasible and has potential application in the field of building energy conservation. The data obtained are given in Fig. 34. As seen from the figure, there is the substantial difference between absorption results of the vacuum impregnation and natural one. Vacuum impregnation method is effective for loading porous materials with organic PCMs. Up to 65% of PCMs by volume can be loaded in porous materials by means of this method. In addition, its setup is quite simple, cheap and easy of scale-up. The key parameters in the vacuum impregnation method consist in immersion time and processing temperature, which should be optimized. The tests of different protective covers for composite granules showed that the covers of latex had the best result.

In the other work, Zhang et al. [148] investigated vacuum impregnation of capric acid (CA) and commercial paraffin (MTPC) into porous materials: expanded perlite granule (EP), expanded clay granule (EC) and expanded fly ash granule (EF), which was previously used in [146,147]. The results of DSC analysis of composite porous materials are shown in Figs. 35 and 36. Comparison of these two figures showed that quite different phase change behaviors were found for capric acid and paraffin, in porous materials. For capric acid, which has a functional group of —COOH, a remarkable elevation of melting temperature was observed when it was confined in the porous materials with alkaline spots on their inner pore surface. As for paraffin, which has only inactive functional groups of $—CH_2$ and $—CH_3$, no elevation or depression of the melting temperature was found when it was confined in these alkaline porous materials.

Khudhair et al. [149] used also the two-step procedure for preparing the phase change concrete. The grinded pumice was sifted using a 10-mesh sieve and dried for 24 h in an oven at 120 °C. The prepared aggregates were then placed in a flask connected to a vacuum pump so that the air is evacuated from the pores within the pumice aggregates. The pressure of the system was monitored and evacuation process continued for about 10 min at a vacuum pressure of 75 kPa. The paraffin RT20 as PCM was allowed to flow into the flask to a level so that all the pumice aggregates in the flask become totally immersed. Following this, the vacuum was released and the air was allowed to enter the flask, which caused the liquid PCM to penetrate into all the pore spaces within the pumice aggregates. This process was repeated for liquid paraffin at 30, 40, 50, 60, and 70 °C. Fig. 37 shows the time dependence of PCM absorbed by pumice. It is seen that there is a rapid uptake of PCM during the first minute. Followed by a slower uptake, the saturation was achieved in about 10 min. There was very little additional paraffin uptake after 10 min. The DSC measurements of the PCM and composite pumice (CP) showed that there are endothermic peaks at about 22 °C and exothermic peaks at about 18 °C. The measured latent heat of the PCM was 162.5 J/g while the measured latent heat of the CP was 72.5 J/g. By taking the mass fraction of PCM as 48.3%-wt, the latent heat of the CP was calculated as 78.5 J/g, which is sufficiently close to the measured value. The produced CP has been incorporated in the concrete mix in the second step with mass ratio of paraffin at 10 wt.%. It was found that the mechanical strength of CP-concrete was comparable to that of plain concrete.

Li and Li [150] from Hong Kong University of Science and Technologies used vacuum impregnation to enhance heat storage capacity of porous insulation materials. The expanded perlite was chosen as the porous material and paraffin with melting point 43 °C as phase change material. Vacuum impregnation was similar to the one that used in [146]. The corresponding measurements showed that the average diameter of pores was 80 μm. The DSC analysis

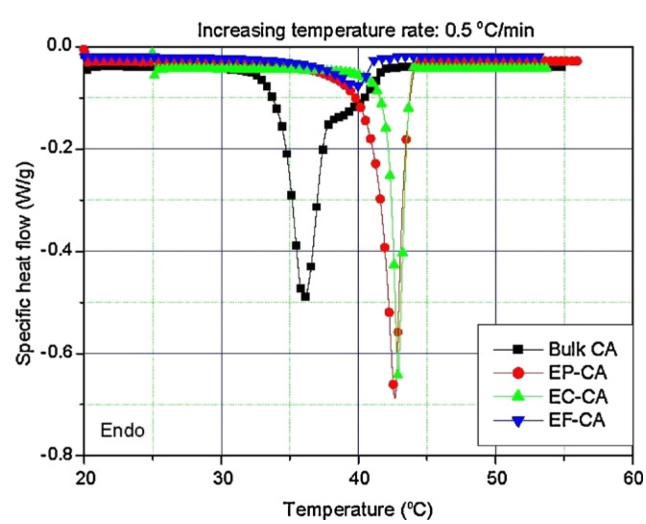


Fig. 36. DSC curves of CA confined in porous materials and bulk CA [148].

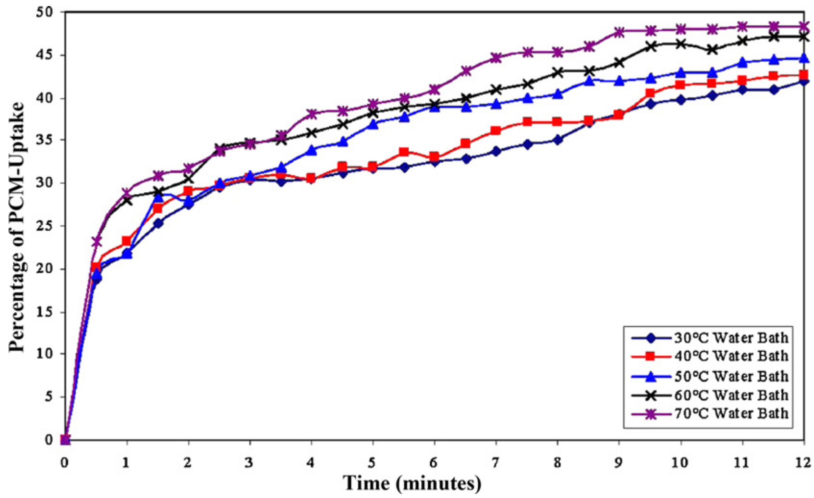


Fig. 37. Experimental saturation curves of PCMPA using the vacuum impregnation process [149].

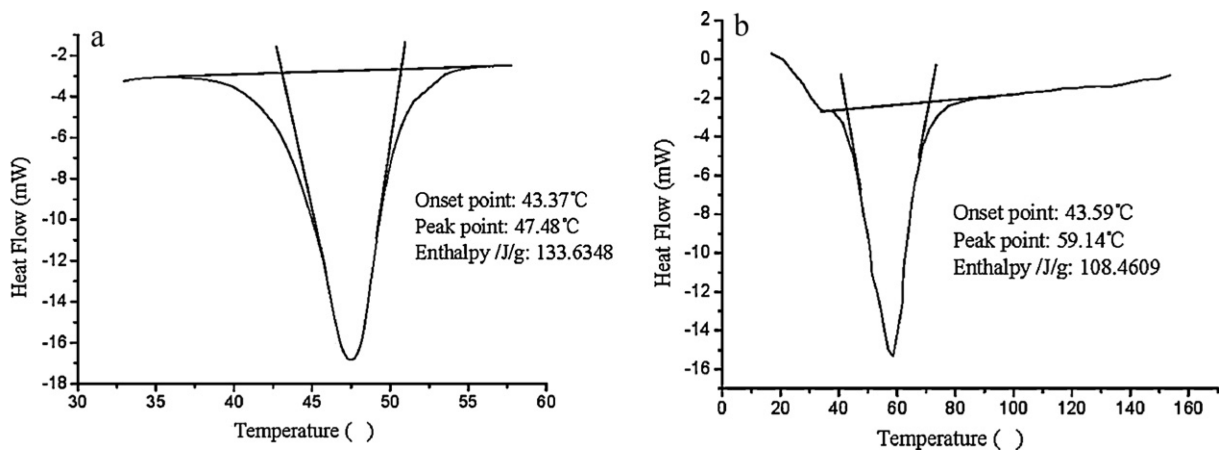


Fig. 38. DSC analysis curves for pure paraffin (a) and composition paraffin/perlite (b) [150].

of thermal properties of pure paraffin and paraffin/perlite is presented in Fig. 37. Comparison of Fig. 38a and b shows that the fraction of paraffin in paraffin/perlite composition is as much as 81%. Two small identically shaped cubicles were made with panels. One of them used expanded perlite as aggregate and the other used granular phase change composites. These two cubicles were placed into a thermal chamber which could simulate variation of temperatures between 20 and 60 °C in the heating mode and from 60 to 0 °C in cooling mode both at rate of 0.5 °C/min. And the cubicles were instrumented with thermocouples, than the inner temperatures were continuously monitored within certain time. Fig. 39 illustrates air temperature variations inside of cubicles. As seen from the figure, three points can be highlighted: firstly, is the cubicle without paraffin has a maximum temperature and it is 3 °C higher than that with paraffin; secondly the maximum temperature with paraffin is obtained about 40 min later without paraffin, that is, the thermal inertia of the panel is higher; thirdly, the thermal inertia appears again due to the freezing of paraffin when temperature falls.

Sarı with his co-workers [151–154] developed a set of heat storage composite materials on the basis of perlite and some organic substances with using vacuum impregnation procedure was similar that which was used in [146,147]. The composition preparated was studied by infra-red spectroscopy and differential scanning calorimetry. The commercial chemicals with purity of 96–98% were used as phase change storage components. The maximum proportion of capric acid (CA) as phase change material (PCM) in the composite was found as 55 wt.%. Thermal properties of CA/expanded perlite (EP) composition are summarized in Table 58. As seen from the table the thermophysical properties of the composition are stable enough and composite material has high latent heat.

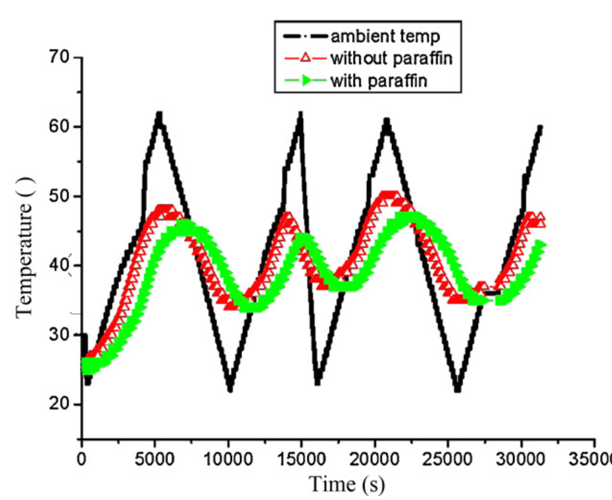


Fig. 39. Thermal behaviors of cubicles made with perlite and composites [150].

Table 58
The changes in thermal properties of the CA/EP composite PCM with respect to thermal cycling number [151].

Number of thermal cycling	Melting point (°C)	Freezing point (°C)	Heat of fusion (J/g)	Heat of freezing. (J/g)
0	31.80	31.61	98.12	90.06
1000	31.32	31.36	96.98	94.42
3000	29.16	31.30	93.43	88.39
5000	30.25	31.52	95.54	90.60

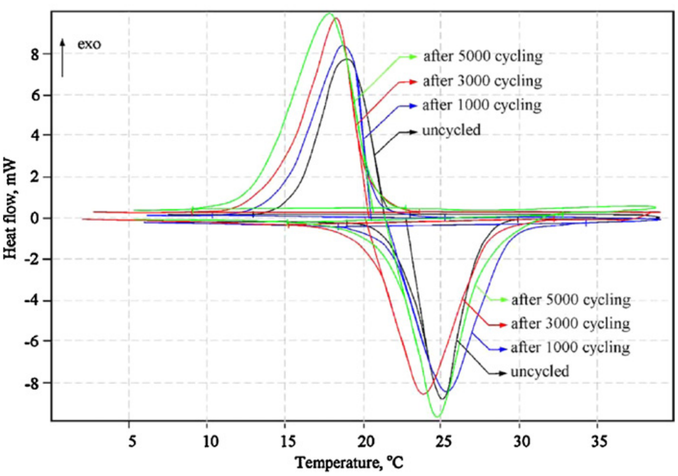


Fig. 40. DSC curves of the form-stable CA–MA/EP composite PCM before and after thermal cycling [152].

In work [152], the eutectic mixture of capric (CA) and myristic (MA) acids was impregnated under vacuum into expanded perlite. The phase change temperature of the eutectic blend lies in the range of 21.10–22.61 °C and the heat of fusion varies from 154.83 to 156.42 J/g. The CA–MA eutectic mixture as PCM is confined in the porous EP by mass fraction of 55% without melted PCM seepage from the composites. The developed form-stable composition underwent the phase change at 20.70–21.70 °C. The heat of fusion of the composition varies in the range of 85.40–89.75 J/g. The tests showed that the new composite material is stable (see Fig. 40).

In order to determine the maximum absorption of lauric acid by expanded perlite in vacuum, the blends of lauric acid with 30, 40, 50, 60 and 70 wt.% were prepared [153]. It was established that the composite with 60% lauric acid did not lose the phase change material. The melting point of the form-stable composition was found as 44.1 °C and the heat of fusion as 93.4 J/g. The DSC curves of the composition are depicted in Fig. 41. As seen from the figure the melting temperature does not undergo any sufficient changes after 1000 thermal cyclings.

The paraffin, with melting temperature 42–44 °C, was used in work [154] for vacuum impregnation of perlite. As the experiments showed, the paraffin could be absorbed in pores of expanded perlite as much as 55 wt.% without melted phase change material seepage from the composite. The thermal properties of the paraffin/perlite composition can be found in Table 59. As it follows from the table, the multiple thermal cycling does not deteriorate the composition performances.

Karaipekli and Sarı [155,156] used vermiculite (VMT) as structure skeleton for preparing heat storage composition with eutectic blends of fatty acids. The procedure of vacuum impregnation was similar that which was used in above considered works. The fraction of the eutectic mixtures of fatty acids in the obtained compositions was as follows:

- 20% in the capric-myristic acid/vermiculite composition;
- 40% in the capric-lauric acid/vermiculite composition;
- 40% in the capric-palmitic acid/vermiculite composition;
- 40% in the capric-stearic acid/vermiculite composition.

Thermal properties of the compositions on the basis of vermiculite are summarized in Tables 60 and 61. As it follows from the tables, the developed compositions are very stable and they can be used in passive solar buildings.

Nomura et al. [157] investigated the ability of porous materials to absorb phase change heat storage materials. Erythritol was selected as the PCM and expanded perlite (EP), diatom earth (DE), and gamma-alumina (GA) were selected as porous materials. Erythritol has high heat of fusion 354.7 J/g and high melting temperature 118 °C. The noted properties make it attractive for thermal energy in industry where there are the thermal wastes at present. The results of tests are shown in Figs. 42 and 43. The advantage of vacuum impregnation is obviously for EP only, as for DE and GA the vacuum impregnation does not sufficiently increase the share of PCM in composite compared to the ordinary impregnation. It was also found that the content of erythritol is decreased and stabilized at 75% from the initial mass in thermal cycling. Obviously, the

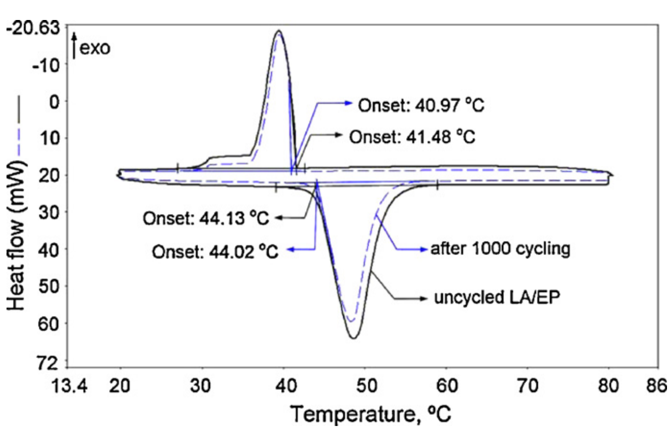


Fig. 41. DSC curves of the form-stable LA/EP composite PCM before and after thermal cycling [153].

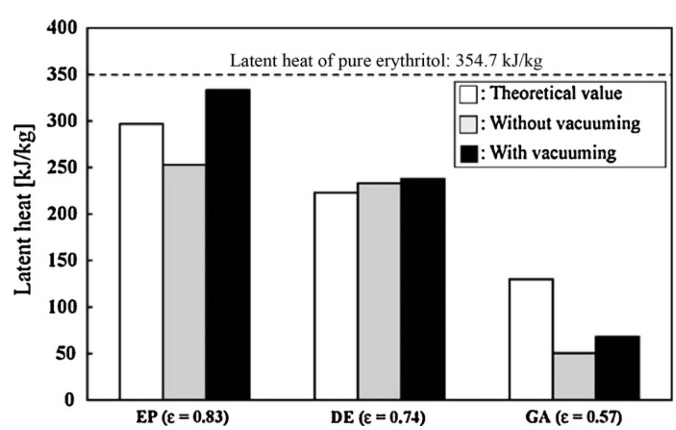


Fig. 42. Comparison between vacuum impregnation treatment and impregnation treatment for each porous material [157].

Table 59
Thermal properties of paraffin/EP composite PCM with respect to thermal cycling number [152].

Number of thermal cycling	Melting point (°C)	Freezing point (°C)	Heat of fusion (J/g)	Heat of freezing (J/g)
0	42.27	40.79	87.40	90.25
1000	42.00	40.83	93.42	94.67
3000	42.61	41.82	92.85	93.56
5000	42.45	41.84	95.19	96.08

Table 60
Thermal properties of form-stable CA–MA/VMT composite PCM with respect to thermal cycling number [155].

No of thermal cycling	T_s (°C)	T_p (°C)	T_e (°C)	ΔH_m (J/g)	T_s (°C)	T_p (°C)	T_e (°C)	ΔH_f (J/g)
0	19.75	23.35	26.41	27.46	17.05	14.54	10.12	31.42
500	19.56	22.03	26.51	30.64	18.08	15.31	11.23	31.30
1000	19.42	21.07	26.63	30.66	18.27	15.42	11.84	31.84
2000	19.48	21.20	25.92	31.78	18.06	17.85	14.19	31.75
3000	19.43	21.60	25.83	25.92	16.72	16.54	13.35	27.41

Table 61
Thermal properties of eutectic mixtures of fatty acids and the form-stable composite PCMs.

Phase change material	T_m (°C)	ΔH_m (J/g)	ΔH_m (J/cm^3)	T_m (°C)	ΔH_f (J/g)	ΔH_f (J/cm^3)
CA-LA	19.62	149.95	13285	19.41	148.99	13200
CA-LA/VMT	19.09	61.03	2496	19.15	58.09	2376
CA-LA/VMT after 5000 cycles	19.01	60.70	2483	18.86	59.43	2431
CA-PA	23.12	156.44	13829	22.15	150.29	13284
CA-PA/VMT	23.51	72.05	2959	21.44	67.24	2745
CA-PA/VMT after 5000 cycles	23.13	70.03	2859	20.97	68.55	2808
CA-SA	25.39	188.15	16595	25.20	184.11	16238
CA-SA/VMT	25.64	71.53	2914	24.90	69?64	2837
CA-SA/VMT after 5000 cycles	25.12	71.46	2911	24.29	68.93	2808

Adapted from [156].

maximum diameter of the pore in which the liquid phase change material can be kept is 10 μm.

9. Application of form-stable materials

Barrio et al. [158] conducted the tests of small floor radiant heating system (see Fig. 44) for maintaining comfort temperature. The prototype unit is the simulation heating space of 1 m^3. The storage material bed has a depth of 2.5 cm and a surface of 1 m × 1 m. That corresponds to a mass of 18 and 40 kg for NPG (as tested storage material) with solid–solid phase transition and sand as (reference to the sensible storage material). Some thermal properties of NPG we considered previously. In the tests, the commercial grade NPG was used in flakes, with a density of 720 kg/m^3 and a thermal conductivity of 0.29 W/(m °C), both at room temperature. The specific heat values at 20 and 50 °C are 1.67 and 2.5 J/(g °C), respectively. The sand used in the simulation had a density of 1600 kg/m^3 and a thermal conductivity of 0.37 W/(m °C), at room temperature. Its specific heat at 20 °C is 3.3 J/(g °C). The energy stored by the sand as sensible heat between 20 and 40 °C, is 69 J/g. The system NPG was much more efficient in temperature regulation, allowing an adequate utilization of the off-peak electricity during the charging period. Results obtained in that study show the promising perspectives of the solid–solid phase transition for thermal storage in building materials.

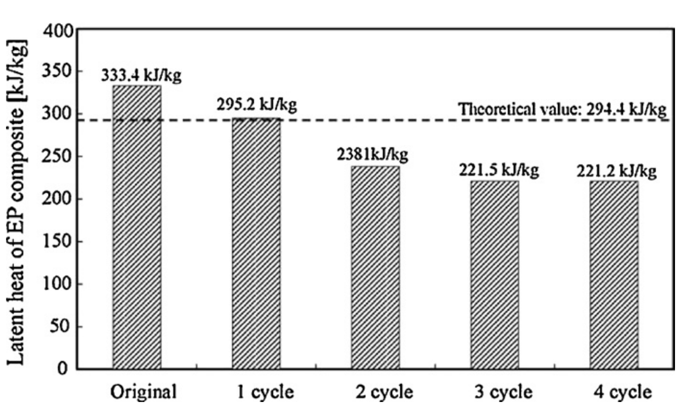


Fig. 43. Latent heat of EP/erythritol composites (impregnation time: 1.8 ks) in cyclic heating and cooling process [157].

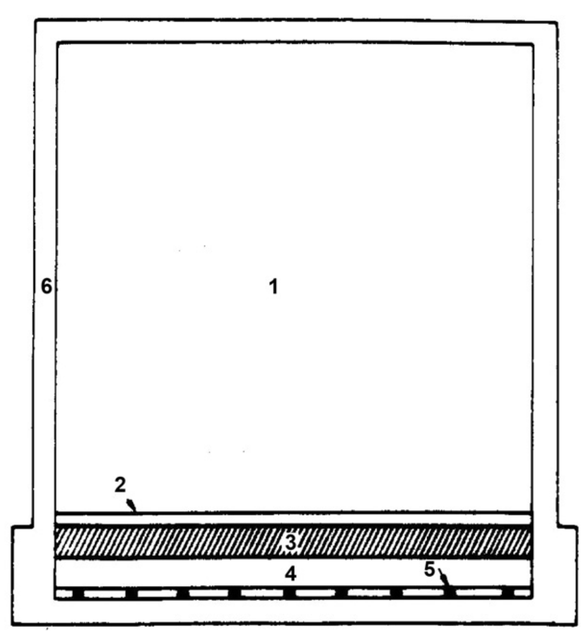


Fig. 44. Scheme of the prototype used in our simulation: (1) space heating, (2) tile pavement, (3) thermal resistance, (4) storage material, (5) electric resistance, (6) thermal insulation [158].

Table 62
Time of charging different points in the solid-solid PCM for different temperatures in the hot face.

Distance from the top (cm)	Time of charge for a temperature of 65 °C (min)		Time of charge for a temperature of 53 °C (min)	
	Simulation	Experimental	Simulation	Experimental
1	106	110	250	240
2.5	458	490	752	720
4	875	930	1501	1430
5	1252	1520	2252	1920

Adapted from [159].

Table 63
Properties of aluminum foam samples.

Metal fraction $(1-\varepsilon)$	Pore size (pores per inch)	Density ρ_{foam} (kg/m^3)	Conductivity k_{foam} (W/m K)	Conductivity $k_{composite}$ (W/m K)
0.077	5	207.5	7.6	4.3
0.084	20	227.3	8.3	4.9
0.090	10	244.1	8.9	5.0

Adapted from [160].

Font et al. [159] carried out theoretical and experimental studies of some characteristic physical parameters required to construct a thermal storage unit for domestic hot water storage systems. A phase change material in solid state was used to store solar energy. The NPG used, commercial grade, has been compressed with density value of 0.9 g/cm^3. The thermal conductivity has been determined at different temperatures. The obtained mean values are: 0.11 W/(m °C) in the monoclinic phase, in the range of 20–30 °C, and 0.08 W/(m °C) in the cubic phase, between 45 and 50 °C. The measured thermal conductivity was differed from values reported in [97,158]. Latent heat and transformation temperature from monoclinic to cubic phases of NPG have been measured by means a Setaram DSC92 differential calorimeter. This phase change starts at 39 °C, regarding the peak temperature 42 °C and the latent heat 122 J/g. To verify the validity of the theoretical model, the results of the simulation were compared with the ones that were obtained experimentally. A container of 50 × 40 × 5 cm was made for this purpose. The NPG in the container was charged by means of an electrical resistance placed on the top face (50 × 40). The other faces were maintained by insulation from the surroundings, using fiber glass. At different points in the PCM, the temperature were measured with chromel-alumel thermocouples sited on the top and at 1, 2.5, 4 and 5 cm from the top (probes nos. 1, 2, 3, 4, and 5, respectively). Two tests were conducted: charge of the PCM maintaining the top face of the container at two different temperatures, 65 and 53 °C. The results of the calculation and experiments are given in Table 62. For the utilization of solar radiation, a period of 8 h charge is adequate. As the experiments showed, approximately 8 h were required for charging the PCM, keeping in mind that the the temperature of the top face was 65 °C and the charger was placed 2.5 cm away from the face. It was found that the restitution of the latent heat takes place in a period of about 16 h. So, it may be concluded that the maximum distance between the pipes must be 5 cm to accomplish the charge and restitution periods must be between 8 and 16 h.

Bauer and Wirtz [160] studying the problems related to the cooling during the peak of variable power dissipating devices operation via the latent heat effect and developed and investigated a plate-like structure that consists of a central core of foamed aluminum, packed with a PCM (see Fig. 45). As Fig. 45 shows, two thick aluminum plates (1.0 mm each) are glued to 12.7 mm thick sheets of aluminum foam (Duocel, ERG Aerospace) with a thermally conductive epoxy (OMEGABOND-200, Omega Engineering). Pure pentaglicerine (PG), as the PCM, was used in the experiments. The latent heat of PG is 183 J/g, and transition occurs at 86 °C. Three sandwich-structures, having three different foamed

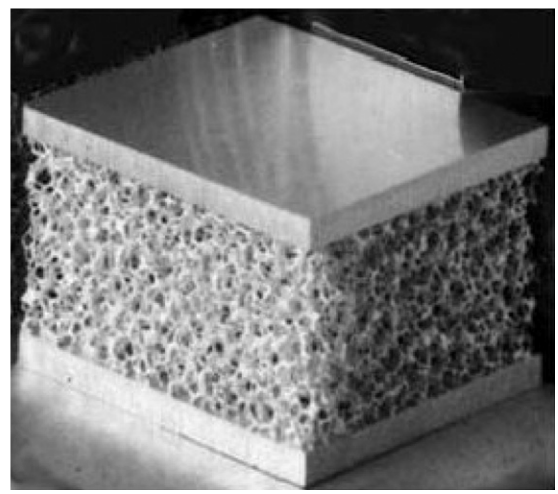


Fig. 45. Thin aluminum plates are bonded to the foamed aluminum [160].

aluminum porosities were constructed and tested. In each case, the void-volume of the foamed aluminum was packed with PG in a density of approximately 0.65 g/cm^3. Measurements (Table 63) showed that the PCM slightly augments the effective thermal conductivity. An increase in aluminum foam metal fraction results in in the growth of effective thermal conductivity of the composite because only about 2% of the heat flow goes through the PCM, and the interfacial bond resistance decreases due to increase contact area. The trade-off is that as there is an increase in aluminum foam metal fraction, while the volumetric latent heat decreases (Fig. 46); thus, the storage time is reduced. Fig. 47 demonstrates

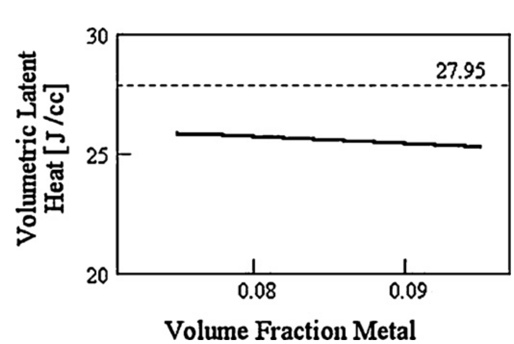


Fig. 46. Composite effective latent heat as a function of metal fraction [160].

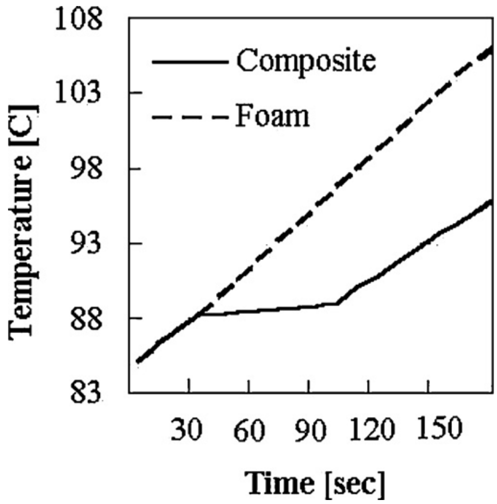


Fig. 47. Latent heat effect demonstrated by comparing the temperature versus time plots for the empty foamed aluminum and of the composite [160].

the TES-effect by comparing the temperature and time plots of the empty aluminum foam to the composite. The experiment consists of insulating a sample and the heater plate. The heater plate supplies approximately 58.5 W of power to the system; it is estimated that 10% of the heat is lost to the environment.

Zheng and Wirtz [161,162] developed a thermal response model for designing a hybrid thermal energy storage (TES) heat sink. Based on the optimization result, a prototype TES-volume was built and a test rig was established to calibrate the performance model. The test rig consisted of a 100 mm square flat plate heat source; the prototype TES-volume; and, a 100 mm square, water-cooled cold-plate heat sink. These elements are clamped together. A thin layer of conductive paste filled the interface between each element. Fig. 48 shows the assembly with insulation removed, prior to being filled with PCM. For experiments, all external surfaces of the test rig were insulated with a layer of balsa wood. It consisted of 12.7 mm thick upper and lower aluminum heat spreader plates sandwiching 46.1 mm thick × 50.8 mm high conducting plates. These plates are inserted into 6.3 mm deep grooves milled in the surface of the upper and lower heat spreader plates so that the height of the TES-volume was 38.1 mm. The plate-to-plate spacing of the TES-volume is approximately 1.15 mm. The total storage volume (excluding heat spreader plates) was 393.3 cm^3; so, the volume available for PCM storage was approximately 208.4 cm^3. Powdered PG was packed between the plates with a density of 0.75 g/cm^3. A

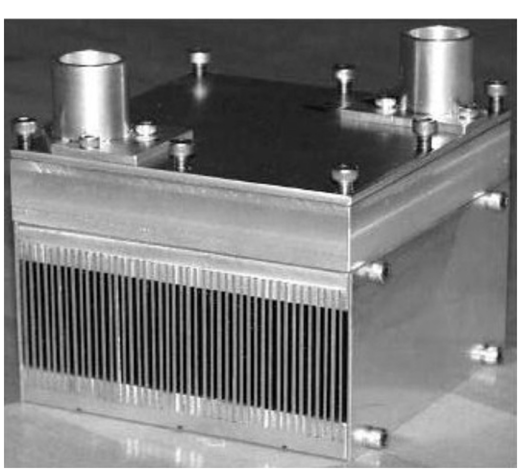


Fig. 48. Assembly of test rig [161,162].



Fig. 49. Appearance of the experimental house [164].

comparison of the simulation results showed excellent agreement between simulation and measurement for the low input power increment.

A group of researchers at the Tsinghua University (China) led by Prof. Y. Zhang [163–166] used the form-stable composition plates to study the work of an under-floor electric heating system with thermal energy storage. The dimensions of the experimental house (see Fig. 49) were 3 m (depth) × 2 m (width) × 2 m (height). It had a 1.6 m × 1.5 m double-glazed window facing south, covered by black curtain. The roof and walls were made of 100-mm-thick polystyrene wrapped by metal board. The under-floor heating system included 120-mm-thick polystyrene insulation, electric heaters, 15-mm-thick PCM, some wooden supporters, 10-mm-thick air layer and 8-mm-thick wood floor. Fig. 50 illustrates the structure of the heating system. The electrical heaters were working during the valley period (23:00–7:00). They stopped working when their temperatures were more than 65 °C and the time was from 7:00 to 23:00. The indoor temperature, outdoor temperature, solar radiation, electricity consumption were measured and recorded every 5 min. The air outlets and air inlets were open, and the air supply fans were working from 9:00 to 16:00 and they stopped working after this period. The simulation and experimental studies showed that the indoor temperature can be increased effectively with the air supply during the working hours. Thus, the temperature of the PCM plate was kept at the phase transition temperature during whole the day, even heaters stopped working. The time of the total electrical energy consumption was shifted from the peak period to the off-peak period, which would provide significant economic benefits because of the different day and night electricity tariffs. It is impossible to do any assessment related to commercial availability of this project due to short-term duration of experiments, absence of any information on energy flows and cost characteristics.

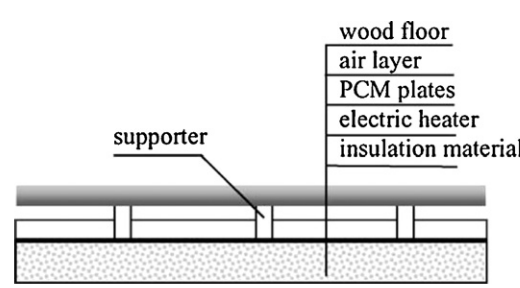


Fig. 50. Schematic of electric floor heating system with shape-stabilized PCM plates [164].

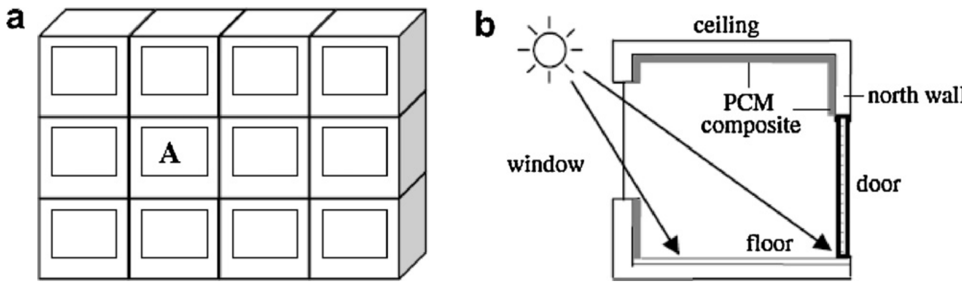


Fig. 51. Schematic of the simulated room: (a) location of the simulated room A in the building; (b) profile of the room A with PCM composite [167].

Zhou et al. [167–170] from Tsinghua University (China) conducted theoretical and experimental investigations on passive solar building. A typical south-facing middle room in a multi-storey building in Beijing, China, is serving as a model room for analysis, which has only one exterior wall (the south wall) and others are all interior envelopes (room *A* shown in Fig. 51). The dimension of the room is assumed to be as 3.9 m (length) × 3.3 m (width) × 2.7 m (height). The south wall is externally insulated with 60-mm-thick expanded polystyrene (EPS) board. There is a 2.1 m × 1.5 m double-glazed window in the south wall and a 0.9 m × 2 m wood door in the north wall which is adjacent to another room or the corridor. The floor is a typical wood floor with the air layer. PCM composite plates are attached to the inner surfaces of four walls and the ceiling as linings. The internal walls of the room were made of mixed type PCM-gypsum and shape-stabilized PCM plates developed previously [49,171,172]. The following conclusions were obtained from those investigations. To maximize the benefit from the energy storage, shape-stabilized phase change material (SSPCM) plates were used:

(1) the melting temperature and heat of fusion should be optimized according to the conditions in that paper, the appropriate melting temperature is about 20 °C and the heat of fusion should not be less than 90 J/g;
(2) it is the inner surface convection, rather than the internal conduction resistance of SSPCM, that limits the latent thermal storage;
(3) thin PCM plates with large areas are advantageous and the effect of PCM plates located in the inner surface of interior wall is superior to that of exterior wall (the south wall);
(4) obviously, the external thermal insulation influences both operating effect and the period of the SSPCM as well as the indoor temperature in winter;
(5) SSPCM plates create a heavyweight response to the lightweight constructions with the rise of the minimum room temperature at night by up to 3 °C for the case studied;
(6) the SSPCM plates really absorb and store the solar energy during the daytime and discharge it later and improve the indoor thermal comfort degree at nighttime.

Yan et al. [173] used a shape-stabilized PCM to prepare a cement phase change wallboard. The shape-stabilized PCM consisted of paraffin mixture (70%) and high-density polyethylene (30%) as support material. The paraffin mixture was developed previously in [60] and included 50% $46^{\#}$ paraffin and 50% liquid paraffin. The phase change temperature of the shape-stabilized PCM was 27.5 °C, and the phase change latent heat was 88.6 J/g. The shape-stabilized PCMs and grout were mixed to prepare shape-stabilized PCM walls. Cement and fine sand were mixed in the container in the proportions of 1:2, and then the mashed shape-stabilized PCMs were added into the container. The mixtures were stirred as some water was added into the mixture. The mixtures were put into the mould and wallboards were prepared. Three pieces of shape-stabilized phase change wallboards and one piece of ordinary wallboard without PCMs were prepared. The size of all the wallboard samples was 300 × 300 × 30 mm. The shape-stabilized PCM wallboard was placed in a heat box. Five measuring points were placed in the center and four corners of the wallboard. Heat flow was given by a heater in one side of the wallboard. In the experiment, the temperatures and heat flow values of the measuring points were tested by the multi-point heat flow meter. The wallboard was heated for 2 h, and then allowed to cool for 4 h in the open air. It was found that both the thermal flow through the phase change wallboard and the fluctuation in the thermal flow are smaller than those of the common wallboard. The bigger the content of phase change material in wallboard, the smaller the thermal flow and its fluctuation. The results showed that prepared PCM wallboard has good thermal performance and therefore it has high potential for the cooling of buildings.

10. Conclusions

We considered practically all types of form-stable phase change materials (FSPCM). The majority of researchers of the FSPCMs attribute to main advantages of form-stable PCMs with the insignificant volume change at phase change in comparison with solid–liquid phase change and opportunity to use them in some cases without encapsulation. It should be noted that the following properties of phase change storage materials to be used for latent heat storage were highlighted [174] as desirable:

- a high value of the phase change (transition) heat and specific heat per unit volume and weight;
- melting (transition) temperature which matches the application;
- a low vapor pressure (<1 bar) at the operational temperature;
- a chemical stability and non-corrosiveness;
- a PCM should not be hazardous, highly inflammable or poisonous;
- a PCM should have a reproducible crystallization without degradation;
- a PCM should have a small supercooling degree and high rate of crystal growth;
- a PCM should have a small volume variation during solidification;
- a high thermal conductivity;
- a PCM should be abundant and low at cost.

The simplicity and effordability of technologies for production of composite PCMs should be noted as well.

Taking into consideration the above mentioned requirements we could make the following conclusions:

1. The form-stable compositions, on the basis of paraffins as heat storage component, meet the most of noted requirements. High-density polyethylene, styrene–butadien–styrene, styrene–ethylene–butylene–styrene can be used as the structure materials. The share of paraffin in the composition can be

as high as 75–80 wt.% and latent heat of phase change observed in experiments is close to theoretical value. The technology of production of these compositions is very simple and on their basis heat storage products can be made in the form plates, spheres or cylinders. Long term performances (thermal cycling up to 3000–5000), upper limit of operating temperature and compatibility of these compositions with potential heat transfer agent (water, air, etc.) should be tested before commercial production.

2. There are other very perspective materials for the form-stable PCMs such as the compositions on the basis of fatty acids as thermal energy storage element. Poly(methyl methacrilate) (PMMA), styrene maleic anhydride (SMA), acrylic resins (Eudragit E, Eudragit S) can be recommended as structure-forming matrix. The share of fatty acids in the form-stable compositions with PMMA, SMA and Edragit E and Eudragit S reaches from 70 to 85 wt.% of theoretically available value. The use of poly (vynil alcohol), poly (vynil chloride) is less preferable, since the share of fatty acids in composition with these compounds does not exceed 50 wt.%. The form-stable compositions with fatty acids are also needed in corresponding tests which were mentioned earlier.
3. It was found that all form-stable compositions contained polyethylene glycol and considered to undergo supercooling which for some compositions reaches up to 20 °C and more. Supercooling of latent heat storage materials is undesirable since it decreases the performances of storage units. Despite of high latent heat in phase change, the application of form-stable PCMs with polyethylene glycol as well as the other phase change materials, which undergo the significant supercooling, is sufficiently limited.
4. High transition latent heat of crystal polyalcohols, other organic and metalloorganic salts as perspective materials for thermal energy storage attracted the attention of many researchers. Results of investigations considered in paragraph 4 showed that these crystals have a set of disadvantages, such as: supercooling, high solubility in water (the most wide-spread heat transfer agent) and high volatility of polyalcohols. If supercooling may be decreased by special measures, the latter shortages can be overcomed only by encapsulation of solid–solid PCMs. It is expected that the similar solid–solid PCMs can be applied in passive systems of temperature control.
5. The microcapsulated form-stable materials, similar to those which were developed by Liu et al. [139,140] with melting point 21.5 °C and latent heat 123.78 J/g, can find the wide application in passive solar buildings if these materials will be produced at reasonable cost.
6. The promising stable materials, in the form of ultrafine fibers, were made by the group of Chinese researchers led by C. Chen by means of electrospinning. Fabrication of warm clothers with fibers are undergoing the phase changes on retention of high textile performances and very important for cold regions. From this point of view, the use of fibers consisting of polyethylene glycol is more preferable since freezing of phase change material occurs at the temperatures of 37–38 °C. This level of temperatures is similar to the temperature of human body. In general case, fabrication of warm clothers with fibers, which undergo phase change at 20–25 °C, is more appropriate. These temperatures are more comfortable for human body and the heat losses at those temperatures are signifantly less than the temperatures at which the ultrafine fibers, made by Chen et al., undergo phase change.
7. The form-stable compositions, on the basis of phase change materials and porous structure materials, present another perspective class of heat storage materials. The porous expanded materials as perlite, vermiculite, concrete, etc. are abundant and cheap. At present there are many phase change materials with high heat of fusion and suitable melting point, which can be used as latent heat storage component. As shown above, the absorbing capacities of porous materials in the process of simple impregnation are very limited. Only vacuum impegnation of PCM into porous structure can provide the maximum share of storage material in the composition. The cheap commercial production of building products with vacuum impregnated latent heat storage materials gives opportunities for worldwide application of PCMs in passive solar buildings.
8. At present, we have a few samples of application of form-stable materials. It is due to the fact that they are prepared in small (laboratory) quantity. The data collected and analyzed in present review show the great potentials of the form-stable heat storage materials. Alongside with further investigations and developments of new FSPCMs, the efforts of researchers should be focused on solving engineering issues of their production at reasonable costs.
9. As far it known, the FSPCM products are not commercially produced currently and therefore we could not compare their cost with that of solid–liquid PCM products.
10. Thus, the development of form-stable PCM products is in the initial stage and it is necessary to conduct a lot of applied investigations directed to provide acceptable production tecnologies and demonstrate the profitable spheres of their application.

References

[1] Buildings Energy Datebook 2006. US Department of Energy and Annual Energy Review 2007. DOE/EIA-0384 (2007). Energy Information Administration, U.S. Department of Energy. June 2008. Available at http://www.eia.doe.gov/aer/pdf/aer.pdf.
[2] Kornevall C. EPBD – the EU's buildings platform. Stakeholders want to move on quicker despite the slow start in many Member States. Available at http://www.eeb-blog.org/2008/02/epbd-the-eus-bu.html.
[3] Schaetzle WJ, Brett CE, Grubbs DM, Seppanen MS. Thermal energy storage in aquifers: design and applications. Pergamon; 1980.
[4] Schmidt FW. Thermal energy storage and regeneration (series in thermal and fluids engineering). McGraw-Hill; 1981.
[5] Beckmann G, Gill PV. Thermal energy storage: basics-design-applications to power generation and heat supply (course in mathematical physics). Springer-Verlag; 1984.
[6] Garg HP, Mullick SC, Bhargava A, Solar K. Thermal energy storage. Holland: Reidel Publishing Company; 1985.
[7] Garg HP. Advances in solar technology: collection and storage systems. Kluwer Academic Publishers; 1987.
[8] Hadorn J-C. Guide to seasonal heat storage. Ottawa: Swiss Federal Energy Office and Swiss Association of Engineers and Architects; 1990.
[9] Dinter F, Geyer M, Tamme R. Thermal energy storage for commercial applications. Springer-Verlag; 1991.
[10] Dinçer İ, Rosen MA. Thermal energy storage systems and applications. 2nd ed. Chichester: A John Wiley and Sons, Ltd; 2011.
[11] Lane GA. Solar heat storage: latent heat material. Vol. 1. Background and scientific principles Boca Raton: CRC Press; 1983.
[12] Lane GA. Solar heat storage: latent heat material. Vol. 2. Technology Boca Raton: CRC Press; 1985.
[13] Mehling H, Cabeza LF. Heat and cold storage with PCM: an up to date introduction into basics and applications. Berlin: Springer; 2008.
[14] Abhat A. Short term thermal energy storage. Energy Build 1981;3(1):49–76.
[15] Abhat A. Short term thermal energy storage. Revue Phys Appl 1980;15(3):477–501.
[16] Feldman D, Shapiro MM, Banu D. Organic phase change materials for thermal energy storage. Sol Energy Mater 1986;13(1):1–10.
[17] Feldman D, Shapiro MM, Banu D, Fuks CJ. Fatty acids and their mixtures as phase change materials for thermal energy storage. Sol Energy Mater 1989;18(3–4):201–6.
[18] Kenisarin MM. Short-term storage of solar energy. 1. Low temperature phase change materials. Appl Sol Energy 1993;29(2):46–64.
[19] Himran S, Suwono A, Ali Mansoori G. Characterization of alkanes and paraffin waxes for application as phase change energy storage medium. Energy Sourc 1994;16(2):117–28.
[20] Zalba B, Marin JM, Cabeza LF, Mehling H. Review on thermal energy storage with phase change: materials, heat transfer analysis and applications. Appl Therm Eng 2003;23(3):251–83.
[21] Farid MM, Khudhair AM, Razak SAK, Said AH. A review on phase change energy storage: materials applications. Energy Convers Mgmt 2004;45(9–10):1597–615.

[22] Khudhair A, Farid M. A review on energy conservation in building applications with thermal storage by latent heat using phase change materials. Energy Convers Mgmt 2004;45(2):263–75.
[23] Rozanna D, Chuah TG, Salmiah A, Choong TSY, Sa'ari M. Fatty acids as phase change materials (PCMs) for thermal energy storage: a review. Int J Green Energy 2004;1(4):495–513.
[24] Sharma CD, Sagara K. Latent heat storage materials and systems. A review. Int J Green Energy 2005;2(1):1–56.
[25] Tyagi VV, Buddhi D. PCM thermal storage in buildings: a state of art. Renew Sustain Energy Rev 2007;11(6):1146–66.
[26] Kenisarin M, Mahkamov K. Solar energy storage using phase change materials. Renew Sustain Energy Rev 2007;11(9):1913–65.
[27] Zhang Y, Zhou G, Lin K, Zhang Q, Di H. Application of latent heat thermal energy storage in buildings: state-of-the-art and outlook. Build Environ 2007;42(6):2197–209.
[28] Pasupathy A, Velraj R, Seeniraj RV. Phase change material-based building architecture for thermal management in residential and commercial establishments. Renew Sustain Energy Rev 2008;12(1):39–64.
[29] Zhu N, Ma Z, Wang S. Dynamic characteristics and energy performance of buildings using ph ase change materials: a review. Energy Convers Mgmt 2009;50(9):3169–81.
[30] Agyenim F, Hewitt N, Eames P, Smyth M. A review on materials, heat transfer and phase change problem formulation for latent heat thermal energy storage systems (LHTESS). Renew Sustain Energy Rev 2010;14(2):615–28.
[31] Baetens R, Jelle B, Gustavsen A. Phase change materials for building applications: a state-of-the-art review. Energy Build 2010;42(9):1361–6.
[32] Gil A, Medrano M, Martorell I, Lázaro A, Dolado P, Zalba B, et al. State of the art on high temperature thermal energy storage for power generation. Part 1 – concepts, materials and modellization. Renew Sustain Energy Rev 2010;14(1):31–55.
[33] Medrano M, Gil A, Martorell I, Potau X, Cabeza LF. State of the art on high temperature thermal energy storage for power generation. Part 2 – case studies. Renew Sustain Energy Rev 2010;14(1):56–72.
[34] Kenisarin MM. High-temperature phase change materials for thermal energy storage. Renew Sustain Energy Rev 2010;14(3):955–70.
[35] Zhao CY, Zhang GH. Review on microencapsulated phase change materials (MEPCMs): fabrication, characterization and applications. Renew Sustain Energy Rev 2011;15:3813–32.
[36] Cabeza LF, Castell A, Barreneche C, deGracia A, Fernández AI. Materials used as PCM in thermal energy storage in buildings: a review. Renew Sustain Energy Rev 2011;15(3):1675–95.
[37] Kuznik F, David D, Johannes K, Roux J-J. A review on phase change materials integrated in building walls. Renew Sustain Energy Rev 2011;15(1):379–91.
[38] Tyagi VV, Kaushika SC, Tyagi SK, Akiyama T. Development of phase change materials based microencapsulated technology for buildings: a review. Renew Sustain Energy Rev 2011;15(2):1373–9.
[39] Fan L, Khodadadi JM. Thermal conductivity enhancement of phase change materials for thermal energy storage: a review. Renew Sustain Energy Rev 2011;15(1):24–46.
[40] Antony Aroul Raj V, Velraj R. Review on free cooling of buildings using phase change materials. Renew Sustain Energy Rev 2010;14(9):2819–29.
[41] Feldman D, Shapiro MM, Fazio P. A heat storage module with a polymer structural matrix. Polym Eng Sci 1985;25(7):406–11.
[42] Inaba H, Tu P. Evaluation of thermophysical characteristics on shape-stabilized paraffin as a solid–liquid phase-change material. Heat Mass Transfer 1997;32:307–12.
[43] Ye H, Ge X. Preparation of polyethylene-paraffin compound as a form-stable solid-liquid phase change material. Sol Energy Mater Sol Cells 2000;64:37–44.
[44] Xiao M, Feng B, Gong K. Thermal performance of a high conductive shape-stabilized thermal storage material. Sol Energy Mater Sol Cells 2001;69:293–6.
[45] Xiao M, Feng B, Gong K. Preparation and performance of a shape stabilized phase change thermal storage materials with high thermal conductivity. Energy Convers Mgmt 2002;43:103–8.
[46] Wirtz RA, Peng S, Fuchs A. A polymer-based thermal energy storage composite for temperature control of sensors and electronics. In: Paper TED-AJ03-359 at the 6th ASME-JSME thermal engineering joint conference. 2003.
[47] Peng S, Fuchs A, Wirtz RA. Polymeric phase change composites for thermal energy storage. J Appl Polym Sci 2004;93(3):1240–51.
[48] Sarı A. Form-stable paraffin/high density polyethylene composites as solid–liquid phase change material for thermal energy storage: preparation and thermal properties. Energy Convers Mgmt 2004;45(13–14):2033–42.
[49] Zhang YP, Lin KP, Yang R, Di HF, Jiang Y. Preparation, thermal performance and application of shape-stabilized PCM in energy efficient buildings. Energy Build 2006;38(10):1262–9.
[50] Cai Y, Hu Y, Song L, Lu H, Chen Z, Fan W. Preparation and characterizations of HDPE-EVA alloy/OMT nanocomposites/paraffin compounds as a shape stabilized phase change thermal energy storage material. Thermochim Acta 2006;451:44–51.
[51] Cai Y, Hu Y, Song L, Tang Y, Yang R, Zhang Y, et al. Flammability and thermal properties of high density polyethylene/paraffin hybrid as a form-stable phase change material. J Appl Polym Sci 2006;99:1320–7.
[52] Cai Y, Hu Y, Song L, Kong Q, Yang R, Zhang Y, et al. Preparation and flammability of high density polyethylene/paraffin/organophilic montmorillonite hybrids as a form stable phase change material. Energy Convers Mgmt 2007;48:462–9.
[53] Krupa I, Mikova G, Luyt AS. Polypropylene as a potential matrix for the reation of shape stabilized phase change materials. Eur Polym J 2007;43: 895–907.
[54] Krupa I, Mikova G, Luyt AS. Phase change materials based on low-density polyethylene/paraffin wax blends. Eur Polym J 2007;43:4695–705.
[55] Kaygusuz K, Sarı A. High density polyethylene/paraffin composites as form-stable phase change material for thermal energy storage. Energy Sourc Recov Utiliz Environ Effects 2007;29(3):261–70.
[56] Cai Y, Wie Q, Huang F, Gao W. Preparation and properties studies of halogen-free flame retardant form-stable phase change materials based on paraffin/high density polyethylene composites. Appl Energy 2008;85:765–75.
[57] Cai Y, Wei Q, Huang F, Lin S, Chen F, Gao W. Thermal stability, latent heat and flame retardant properties of the thermal energy storage phase change materials based on paraffin/high density polyethylene composites. Renew Energy 2009;34:2117–23.
[58] Alkan C, Kaya K, Sarı A. Preparation, thermal properties and thermal reliability of form-stable paraffin/polypropylene composite for thermal energy storage. J Polym Environ 2009;17:254–8.
[59] Cai YB, Wei QF, Shao DF, Hu Y, Song L, Gao WD. Magnesium hydroxide and microencapsulated red phosphorus synergistic flame retardant form stable phase change materials based on HDPE/EVA/OMT nanocomposites/paraffin compounds. J Energy Inst 2009;82(1):28–36.
[60] Cheng W, Zhang R, Xie K, Liu N, Wang J. Heat conduction enhanced shape-stabilized paraffin/HDPE composite PCMs by graphite addition: preparation and thermal properties. Sol Energy Mater Sol Cells 2010;94:1636–42.
[61] Yan Q, Li L, Shen D. Thermal properties of shape-stabilized paraffin used for wallboard. Int J Sustain Energy 2010;29(2):87–95.
[62] Sarı A, Alkan C, Kolemen U, Uzun O, Eudragit S. (methyl methacrylate methacrylic acid copolymer)/fatty acid blends as form-stable phase change material for latent heat thermal energy storage. J Appl Polym Sci 2006;101:1401–6.
[63] Sarı A, Kaygusuz K. Studies on poly (vinyl chloride)/fatty acid blends as shape-stabilized phase change material for latent heat thermal energy storage. Indian J Eng Mater Sci 2006;13:253–8.
[64] Sarı A, Kaygusuz K. Poly (vinyl alcohol)/fatty acid blends for thermal energy storage. Energy Sourc Recov Utiliz Environ Effect 2007;29(10):873–83.
[65] Kaygusuz K, Alkan C, Sarı A, Uzun O. Encapsulated fatty acids in an acrylic resin as shape-stabilized phase change materials for latent heat thermal energy storage. Energy Sourc Recov Utiliz Environ Effect 2008;30:1050–9.
[66] Sarı A, Alkan C, Karaipekli A, Önal A. Preparation, characterization and thermal properties of styrene maleic anhydride copolymer (SMA)/fatty acid composites as form stable phase change materials. Energy Convers Mgmt 2008;49:373–80.
[67] Alkan C, Sarı A. Fatty acid/poly (methyl methacrylate) blends as form-stable phase change materials for latent heat storage. Sol Energy 2008;82:118–24.
[68] Wang L, Meng D. Fatty acid eutectic/polymethyl methacrylate composite as form-stable phase change material for thermal energy storage. Appl Energy 2010;87:2660–5.
[69] Jiang Y, Ding E. Study on transition characteristics of PEG/CDA solid–solid phase change materials. Polymer 2002;43(1):117–22.
[70] Su JC, Liu PS. A novel solid–solid phase change heat storage material with polyurethane block copolymer structure. Energy Convers Mgmt 2006;47:3185–91.
[71] Cao Q, Liu P. Hyperbranched polyurethane as novel solid-solid phase change material for thermal energy storage. Eur Polym J 2006;42:2931–9.
[72] Alkan C, Sarı A, Uzun O. Poly(ethylene glycol)/acrylic polymer blends for latent heat thermal energy storage. AIChE J 2006;52:3310–4.
[73] Sarı A, Alkan C, Karaipekli A, Uzun O. Poly(ethylene glycol)/poly(methyl methacrylate) blends as novel form-stable phase-change materials for thermal energy storage. J Appl Polym Sci 2010;116:929–33.
[74] Fang Y, Kang H, Wang W, Liu H, Gao X. Study on polyethylene glycol/epoxy resin composite as a form-stable phase change material. Energy Convers Mgmt 2010;51:2757–61.
[75] Wang W, Yang X, Fang Y, Ding J. Preparation and performance of form-stable polyethylene glycol/silicon dioxide composites as solid-liquid phase change materials. Appl Energy 2009;86:170–5.
[76] Wang W, Yang X, Fang Y, Ding J, Yan J. Enhanced thermal conductivity and thermal performance of form-stable composite phase change materials by using β-aluminum nitride. Appl Energy 2009;86:1196–200.
[77] Xi P, Gu X, Cheng B, Wang Y. Preparation and characterization of a novel polymeric based solid-solid phase change heat storage material. Energy Convers Mgmt 2009;50:1522–8.
[78] Li Y, Wu M, Liu R, Huang Y. Cellulose-based solid–solid phase change materials synthesized in ionic liquid. Sol Energy Mater Sol Cells 2009;93:1321–8.
[79] Zeng JL, Zhang J, Liu YY, Cao ZX, Zhang ZX, Xu F, et al. Polyaniline/1-tetradecanol composites form-stable PCMS and electrical conductive materials. J Therm Anal Calor 2008;91:455–61.
[80] Liao L, Cao Q, Liao H. Investigation of hyperbranched polyurethane as solid-solid phase chande material. J Mater Sci 2010;45(9):2436–41.
[81] Feng L, Zheng J, Yang H, Guo Y, Li W, Li X. Preparation and characterization of polyethylene glycol/active carbon composites as shape-stabilized phase change materials. Sol Energy Mater Sol Cells 2011;93(2):644–50.
[82] Murrell E, Bleed L. Solid-solid phase transition determined by differential scaning calorimetry, part I. Tetrahedral substances. Thermochim Acta 1970;1(3):239–46.

[83] Benson DK, Webb JD, Burrows RW, McFadden JDO, Christensen C. Materials research for passive solar systems: solid-state phase-change materials. Solar Energy Research Institute Report SERI/TR-255-1828. Golden, Colorado 80401; 1985.

[84] Benson DK, Burrows RW, Webb JD. Solid state phase transitions in pentaerythritol and related polyhydric alcohols. Sol Energy Mater 1986;13:133–52.

[85] Benson DK, Christensen C, Burrows RW, Shinton YD. New phase change thermal energy storage materials for building. In: Enerstock 85 – proceedings of the 3rd international conference on energy storage for building heating and Cooling. 1985. p. 416–20.

[86] Font J, Muntasell J, Navarro J, Tamarit JLl, Llovers J. Calorimetric study of the mixtures PE/NPG and PG/NPG. Sol Energy Mater 1987;15(4):299–310.

[87] Font J, Muntasell J, Navarro J, Tamarit JLl. Time and temperature dependence of the exchanged energy on solid-solid transition of pentaglycerine/neopentylglycol mixtures. Sol Energy Mater 1987;15(5):403–12.

[88] Barrio M, Font J, Muntasell J, Navarro J, Tamarit JLl. Applicability for heat storage of binary systems of neopentylglycol, pentaglycerine and pentaerythritol: a comparative analysis. Sol Energy Mater 1988;18:109–15.

[89] Barrio M, Font J, López JO, Muntasell J, Tamarit JLl, Chanh NB, et al. Binary system pentaerythritol/pentaglycerin. J Chim Phys 1990;87:255–70.

[90] Barrio M, Font J, López JO, Muntasell J, Tamarit JLl, Chanh NB, Haget Y. Binary system neopentylglycol/pentaglycerin. J Chim Phys 1990;87:1835–51.

[91] Barrio M, Font J, López JO, Muntasell J, Tamarit JLl, Haget Y. Plastic molecular alloys: the binary system tris(hydroximethyl)aminomethane/2-amino-2methyl-1,3-propanediol. J Chim Phys 1994;91:189–202.

[92] Zhang ZY, Yang ML. Heat capacity and phase transitions of mixtures of pentaerythritol and trimethylolpropane over the superambient temperature range. Thermochim Acta 1990;164:103–9.

[93] Suenaga K, Matsuo T, Suga H. Heat capacity and phase transition of trimethylolethane. Thermochim Acta 1990;163:263–70.

[94] Suga H. Calorimetric studies of some energy-related materials. Thermochim Acta 1999;328(1–2):9–17.

[95] Kamae R, Suenaga K, Matsuo T, Suga H. Low-temperature thermal properties of 2,2-dimethyl-1,3-propanediol and its deuterated analogues. J Chem Thermodyn 2001;33:471–84.

[96] Matsuo T, Suga H. Adiabatic microcalorimeters for heat capacity measurement at low temperature. Thermochim Acta 1985;88(1):149–58.

[97] Son CH, Morehouse JH. An experimental investigation of solid-state phase-change materials for solar thermal energy storage. J Sol Energy Eng 1991;113:244–9.

[98] Salud J, López DO, Barrio M, Tamarit JLl, Negrier P, Haget Y. Molecular interactions and packing in molecular alloys between nonisomorphous plastic phases. J Solid State Chem 1996;124(1):29–38.

[99] Salud J, López DO, Barrio M, Tamarit JLl. Two-component systems of isomorphous orientationally disordered crystals. Part 1. Packing of the mixed crystals. J Mater Chem 1999;9(4):909–16.

[100] Wang X, Lu E, Lin W, Liu T, Shi Z, Tang R, et al. Heat storage performance of the binary systems neopentyl glycol/pentaerythritol and neopentyl glycol/trihydroxy methyl-aminomethane as solid–solid phase change materials. Energy Convers Mgmt 2000;41:129–34.

[101] Wang X, Lu E, Lin W, Wang C. Micromechanism of heat storage in a binary system of two kinds of polyalcohols as a solid–solid phase change material. Energy Convers Mgmt 2000;41:135–44.

[102] Chandra D, Mandalia H, Chien WM, Lindle DW, Rudman R. Solid-solid phase transition in trimethylolpropane (TRMP). Z Phys Chem 2000;216(12):1389–400.

[103] Chandra D, Chien WM, Gandicotta V, Lindle DW. Heat capacities of "plastic crystal" solid state thermal energy storage materials. Z Phys Chem 2000;216(12):1433–44.

[104] Divi S, Chellappa R, Chandra D. Heat capacity measurement of organic thermal energy storage materials. J Chem Thermodyn 2006;38(11):1312–26.

[105] Witusiewicz VT, Sturz L, Hecht U, Rex S. Thermodynamic description and unidirectional solidification of eutectic organic alloys: II. $(CH_3)_2C(CH_2OH)_2$–$(NH_2)(CH_3)C(CH_2OH)_2$ system. Acta Mater 2004;52(17):5071–81.

[106] Gao W, Lin W, Liu T, Xia C. An experimental study on the heat storage performances of polyalcohols NPG, TAM, PE, and AMPD and their mixtures as solid-solid phase-change materials for solar energy applications. Int J Green Energy 2007;4:301–11.

[107] Tong ZC, Tan RB, Liu CG, Meng CC, Zhang JN. Thermodynamic investigation of a solid–solid phase change material: 2-amino-2-methyl-1,3-propanediol by calorimetric methods. Energy Convers Mgmt 2010;51:1905–10.

[108] Gally N, Glausch R, Heider U, Lotz N, Neuschutz M. Storage media for latent heat storage systems. US Patent Application 2002/0016505 A1; 2002.

[109] Steinert S, Voigt W, Glausch R, Neuschütz M. Thermal characteristics of solid–solid phase transitions in long-chain dialkyl ammonium salts. Thermochim Acta 2005;435:28–33.

[110] Addeo A, Nicolais L, Busico V, Migliaresi C. The development of thermal energy storage systems exploiting solid-solid phase transitions. Appl Energy 1980;6(5):353–62.

[111] Busico V, Corradini P, Vacatello M, Fittipaldi F, Nicolais L. Solid-solid phase transitions for thermal energy storage. In: Den Ouden C, editor. Thermal storage of solar energy. The Hague: Martinus Nijhoff Pub; 1981. p. 309.

[112] Busico V, Cernicchiaro P, Corradini P, Vacatello M. Polymorphism in anhydrous amphiphilic systems: long chain primary n-alkylammonium chlorides. J Phys Chem 1983;87:1631.

[113] Busico V, Cernicchiaro P, Scopa A, Vacatello M. Structural organization of polar-group-containing polymers in the molten state. Coll Polym Sci 1983;261:224.

[114] Busico V, Del Gaudio A, Vacatello M. Thermal behavior of some long chain alkylene diammonium tetrabromozincates. Gazz Chim Ital 1981;111:235.

[115] Busico V, Salerno V, Vacatello M. Conformational solid-solid phase transitions in long chain alkylammonium tetrachloromercurates (II). Gazz Chim Ital 1979;109:581.

[116] Busico V, Scopa A, Vacatello M. Melting behavior of hydrocarbon chain molecules with ionic end groups: primary n-alkylammonium F halides. Z Naturforsch 1982;37-A:1466.

[117] Busico V, Tartaglione T, Vacatello M. Thermal behavior of mixed long chain alkyl-ammonium tetrachlorozincates. Thermochim Acta 1983;62:77.

[118] Busico V, Vacatello M. Lipid bilayers in the "fluid" state: computer simulation and comparison with model compounds. Mol Cryst Liq Cryst 1983;97:195.

[119] Busico V, Vacatello M. Diffusion of long chain alkylammonium cations in layer compounds $(n\text{-}C_nH_{2n+1}NH_3)_2MCl_4$. Mol Cryst Liq Cryst 1983;95:251.

[120] Busico V, Carfagna C, Salerno V, Vacatello M, Fittipaldi F. The layer perovskites as thermal energy storage systems. Sol Energy 1980;24(6):575–9.

[121] Busico V, Carfagna C, Salerno V, Vacatello M. Thermal behaviour of complexes of general formula $(n\text{-}C_nH_{2n+1}NH_2)_2CuCl_2$. Thermochim Acta 1980;39(1): 1–5.

[122] Busico V, Corradini P, Vacatello M. Thermal behaviour and observation of a smectic mesophase in n-pentadecylammonium chloride. J Phys Chem 1982;86:1033.

[123] Busico V, Salerno V, Vacatello M. Solid state solubility of long chain alkylammonium tetrachloromanganates (II). Gazz Chim Ital 1979;109:577.

[124] Busico V, Vacatello M. DSC study of some long chain alkylene diammonium tetrachlorozincates. Gazz Chim Ital 1981;111(1):13.

[125] Carfagna C, Vacatello M, Corradini P. On the structure of the hydrocarbon layers in the high-temperature polymorphs of straight-chain n-alkylammonium tetrachlorometallates (II). Gazz Chim Ital 1977;107:131.

[126] Landi E, Salerno V, Vacatello M. Structural aspects of the solid state phase transitions in long chain alkylammonium tetrachlorometallates (II). Gazz Chim Ital 1977;107:27.

[127] Landi E, Vacatello M. Metal dependent thermal behaviour in $(n\text{-}C_nH_{2n+1}NH_3)_2MCl_4$. Thermochim Acta 1975;13:441–7.

[128] Landi E, Vacatello M. New disordered polymorphs in long chain alkylammonium tetrachlorocobaltates (II). Thermochim Acta 1975;12:141.

[129] Paraggio C, Salerno V, Busico V, Vacatello M. The thermal behavior of mixed long chain alkylammonium tetrachloromanganates (II). Thermochim Acta 1980;42:185.

[130] Salerno V, Landi E, Vacatello M. Transition metal complexes with long chain amines, Thermal behavior and crystal structure of $(n\text{-}C_nH_{2n+1}NH_2)_2ZnCl_2$. Thermochim Acta 1977;20:407–15.

[131] Salerno V, Grieco A, Vacatello M. Ordered and disordered phases in mixed dodecyl-ammonium and hexadecylammonium tetrachloromanganate (II). J Phys Chem 1976;80:2444.

[132] Vacatello M, Busico V, Corradini P. The conformation of hydrocarbon chains in disordered layer systems. J Chem Phys 1983;78:590.

[133] Vacatello M, Busico V. On the liquid crystalline behaviour of bis(n-pentadecylammo-nium) tetrabromozincate. Mol Cryst Liq Cryst Lett 1981;64:127.

[134] Vacatello M, Corradini P. Relationships between structure and properties of compounds of the type $(RNH_3)_2MX_4$. I. Compounds with M = Mn, X = Cl and R = n-$C_{10}H_{21}$, n-$C_{12}H_{25}$, n-$C_{14}H_{29}$ and n-$C_{16}H_{33}$. Gazz Chim Ital 1973;103:1027.

[135] Vacatello M, De Girolamo M, Busico V. Relationships between structure and properties in long chain bis(n-alkylammonium tetrabromocuprates (II) and bis(n-alkylammo-nium) tetrabromomanganates (II). J Chem Soc Faraday Trans 1981;177:2367.

[136] Vacatello M, Corradini P. Relationsphips between structure and properties of compounds f the type $(RNH_3)_2MX_4$. II. Compounds with M = Mn, X = Cl, and R = n-C_9H_{19}, n-$C_{11}H_{23}$, n-$C_{13}H_{27}$, n-$C_{15}H_{31}$ and n-$C_{17}H_{35}$. Gazz Chim Ital 1974;104:773.

[137] Li W, Zhang D, Zhang T, Wang T, Ruan D, Xing D, et al. Study of solid–solid phase change of $(n\text{-}C_nH_{2n+1}NH_3)_2MCl_4$ for thermal energy storage. Thermochim Acta 1999;326:183–6.

[138] Li WD, Ding EY. Preparation and characterization of cross-linking PEG/MDI/PE polymer as solid–solid phase change heat storage material. Sol Energy Mater Sol Cells 2007;91:764–8.

[139] Liu X, Liu H, Wang S, Zhang L, Cheng H. Preparation and thermal properties of form-stable paraffin phase change material encapsulation. Sol Energy 2006;80:1561–7.

[140] Liu X, Liu H, Wang S, Zhang L, Cheng H. Preparation and thermal properties of form stable paraffin phase change material encapsulation. Energy Convers Mgmt 2006;47:2515–22.

[141] Chen C, Wang L, Huang Y. Electrospinning of thermo-regulating ultra fine fibers based on polyethylene glycol/cellulose acetate composite. Polymer 2007;48(18):5202–7.

[142] Chen C, Wang L, Huang Y. Morphology and thermal properties of electro-spun fatty acids/polyethylene terephthalate composite fibers as novel form-stable phase change materials. Sol Energy Mater Sol Cells 2008;92:1382–7.

[143] Chen C, Wang L, Huang Y. A novel shape-stabilized PCM: electrospun ultrafine fibers based on lauric acid/polyethylene terephthalate composite. Mater Lett 2008;62:3515–7.

[144] Chen C, Wang L, Huang Y. Ultrafine electrospun fibers based on stearyl stearate/polyethylene terephthalate composite as form stable phase change materials. Chem Eng J 2009;150:269–74.
[145] Chen C, Wang L, Huang Y. Crosslinking of the electrospun polyethylene glycol l/cellulose acetate composite fibers as shape-stabilized phase change materials. Mater Lett 2009;63:569–71.
[146] Zhang D, Li Z, Zhou J, Wu K. Development of thermal energy storage concrete. Cement Concrete Res 2004;34(6):927–34.
[147] Zhang D, Zhou J, Wu K, Li Z. Granular phase change composites for thermal energy storage. Sol Energy 2005;78:471–80.
[148] Zhang D, Tian S, Xiao D. Experimental study on the phase change behavior of phase change material confined in pores. Sol Energy 2007;81(9):653–60.
[149] Khudhair AM, Farid M, Chen J, Bansal PK. Development and use of impregnated phase change materials in concrete for thermal comfort. In: Proceedings of the IIR – IRHACE international conference on "innovative equipment and systems for comfort and food preservation". 2006. p. 396–403.
[150] Li Z, Li X. Development of thermal insulation materials with granular phase change composite. In: Grosse Christian U, editor. Advances in construction materials. Berlin Heidelberg: Springer; 2007. p. 741–8. doi:10.1007/978-3-540-72448-3_75.
[151] Sarı A, Karaipekli A. Preparation, thermal properties and thermal reliability of capric acid/expanded perlite composite for thermal energy storage. Mater Chem Phys 2008;109(2–3):459–64.
[152] Sarı A, Karapekli A, Arkar J. Preparation, characterization and thermal properties of lauric acid/expanded perlite as novel form-stable composite phase change material. Chem Eng J 2009;155(3):899–904.
[153] Karapekli A, Sarı A. Capric–myristic acid/expanded perlite composite as form-stable phase change material for latent heat thermal energy storage. Renew Energy 2008;33(12):2599–605.
[154] Karapekli A, Sarı A, Kaygusuz K. Thermal characteristics of paraffin/expanded perlite composite for latent heat thermal energy storage. Energy Sourc Recov Utiliz Environ Effect 2009;31(10):814–23.
[155] Karapekli A, Sarı A. Capric–myristic acid/vermiculite composite as form-stable phase change material for thermal energy storage. Sol Energy 2009;83(3):323–32.
[156] Karapekli A, Sarı A. Preparation, thermal properties and thermal reliability of eutectic mixtures of fatty acids/expanded vermiculite as novel form-stable composites for energy storage. J Ind Eng Chem 2010;16(5):767–73.
[157] Nomura T, Okinaka N, Akiyama T. Impregnation of porous material with phase change material for thermal energy storage. Mater Chem Phys 2009;115(2–3):846–50.
[158] Barrio M, Font J, López JO, Muntasell J, Tamarit JLl. Floor radiant system with heat storage by a solid-solid phase transition material. Sol Energy Mater Sol Cells 1992;27(2):127–33.
[159] Font J, Muntasell J, Cardoner F. Preliminary study of a heat storage unit using a solid-solid transition. Sol Energy Mater Sol Cells 1994;33:169–76.
[160] Bauer CA, Wirtz RA. Thermal characteristics of a compact, passive thermal energy storage device. In: Paper 2-e-2-1 in: ASME international mechanical engineering conference and exposition. 2000.
[161] Zheng N, Wirtz RA. Methodology for designing a hybrid thermal energy storage heat sink. In: Paper presented at the ASME international mechanical engineering congress & exposition. 2000.
[162] Zheng N, Wirtz RA. A hybrid thermal energy storage device, Part 1: design methodology. J Electron Packag 2004;126(1):1–7.
[163] Lin K, Zhang Y, Xua X, Di H, Yang R, Qin P. Modeling and simulation of underfloor electric heating system with shape-stabilized PCM plates. Build Environ 2004;39:1427–34.
[164] Lin K, Zhang Y, Xu X, Di H, Yang R, Qin P. Experimental study of underfloor electric heating system with shape-stabilized PCM plates. Energy Build 2005;37:215–20.
[165] Lin K, Zhang Y, Xu X, Di H, Yang R. Study of an electrical heating system with ductless air supply and shape-stabilized PCM for thermal storage. Energy Convers Mgmt 2007;48:2016–24.
[166] Zhang YP, Xu X, Di HK, Lin KP, Yang R. Experimental study on the thermal performance of the shape-stabilized phase change material floor used in passive solar buildings. J Sol Energy Eng 2006;128(2):255–7.
[167] Zhou GB, Zhang YP, Wang X, Lin KP, Xiao W. An assessment of mixed type PCM–gypsum and shape-stabilized PCM plates in a building for passive solar heating. Sol Energy 2007;81:1351–60.
[168] Zhou GB, Zhang YP, Zhang QL, Lin KP, Di HF. Performance of a hybrid heating system with thermal storage using shape-stabilized phase-change material plates. Appl Energy 2007;84:1068–77.
[169] Zhou G, Zhang Y, Lin K, Xiao W. Thermal analysis of a direct-gain room with shape-stabilized PCM plates. Renew Energy 2008;33:1228–36.
[170] Zhou GB, Zhang YP, Wang X, Zhou SX. Numerical analysis of effect of shape stabilized phase change material plates in a building combined with night ventilation. Appl Energy 2009;86(1):52–9.
[171] Qin PH, Yang R, Zhang YP, Lin KP. Thermal performance of shape-stabilized phase-change materials. J Tsinghua Univ Ser Sci & Tech 2003;43(6):833–5 (in Chinese).
[172] Zhang Y, Zhou G, Yang R, Lin K. Our research on shape-stabilized PCM in energy-efficient buildings. In: Ecostock 2006 – proceedings of the 10th international conference on thermal energy storage. 2006.
[173] Yan Q, Li L, Liang C. Thermal performance of shape-stabilized phase change paraffin wallboard. Int J Sustain Energy 2010;29(4):185–90.
[174] Schröder J, Gawron K. Latent heat storage. Energy Res 1981;5:103–9.